Faculty of Natural Science and Technology
Department of Physics

MASTER'S THESIS FOR

STUD. TECHN. GURO KAHRS ROGNSVÅG

Thesis started:	02.06.2007
Thesis submitted:	07.03.2007

DISCIPLINE: PHYSICS

Norsk tittel: *Lineær sigma modell ved endelig temperatur*

English title: *Linear sigma model at finite temperature*

This work has been carried out at NTNU, under the supervision of Professor Jens O. Andersen.

Trondheim, 07.03.2007

Professor Jens O. Andersen

Responsible supervisor

ABSTRACT

This master thesis gives an introduction to finite temperature field theory and effective field theories. The need for resummation at finite temperature is discussed, and is used to find self-consistent equations for the sigma and pion masses in the $O(N)$ linear sigma model. Using the $O(4)$ linear sigma model as an effective model of two-flavor QCD, the chiral phase transition is studied. Both Hartree and large-N approximations are considered. The gap equations are renormalized using dimensional regularization and the MS scheme. It is shown that it is possible to renormalize the gap equations in the large-N approximation with temperature-independent counterterms. The order of the phase transition and the transition temperature depend on which approximation is used, and the results agree with results obtained by other authors.

ACKNOWLEDGMENT

I would like to thank my supervisor, professor Jens O. Andersen, for helpful guidance during the work of this master thesis, and for giving me the opportunity to write about what I find most interesting in physics. I also thank him for interesting discussions, not just on physics.

I also thank my fellow student Tormod Gjestland for his help and support. Many thanks also go to all the people who have made these years as a student worth remembering.

Finally, I would like to thank Marius Trebler for his patience and love, and for his support during a tough period.

Contents

ABSTRACT i

ACKOWLEDGMENT ii

LIST OF FIGURES 1

1 INTRODUCTION 4

2 IMAGINARY-TIME FORMALISM 6
- 2.1 The S-matrix and diagrammatic representation 7
- 2.2 Wick rotation 9
- 2.3 Imaginary-time Green's Functions 10

3 $\lambda\phi^4$ THEORY 13
- 3.1 Diagrammatic representation in the $\lambda\phi^4$-theory 13
- 3.2 Self-energy 17
  - 3.2.1 First-order correction 19
- 3.3 Thermodynamic potential 23
  - 3.3.1 First-order correction 25
- 3.4 The idea of renormalization 26
- 3.5 Regularization 26
  - 3.5.1 Momentum cutoff regularization 26
  - 3.5.2 Dimensional regularization 27
- 3.6 Counting of UV divergences 29
- 3.7 Counterterms 31
- 3.8 Minimal subtraction 32
- 3.9 First order correction in the massless case 35
- 3.10 Higher-order corrections and breakdown of perturbation theory 36

4 EFFECTIVE THEORIES 42
- 4.1 Resummation 42
- 4.2 Effective theories for QCD 42
- 4.3 The linear sigma model 44

5 PHASE TRANSITIONS AT FINITE TEMPERATURE 45
- 5.1 One scalar field 46
  - 5.1.1 Explicitly broken symmetry 52
- 5.2 N scalar fields 56
  - 5.2.1 Hartree approximation 57
  - 5.2.2 Large-N approximation 60
- 5.3 The $O(4)$ linear sigma model in the Hartree approximation . 60
  - 5.3.1 The chiral limit 60
  - 5.3.2 The physical point 67

5.4 The $O(4)$ linear sigma model in the large-N approximation . 70
5.4.1 The chiral limit 70
5.4.2 The physical point 74
5.5 Results and discussion of the Hartree and large-N approximations 76

6 SUMMARY **80**

BIBLIOGRAPHY **83**

List of Figures

2.1 Rotation of the k_0 contour to the imaginary axis. The rotation does not change the value of integral. 10
3.1 The numerator of the thermal two-point Green's function to first order in the coupling constant, given in Eq. (3.6). 14
3.2 The denominator of the thermal two-point Green's function to first order in the coupling constant, given in Eq. (3.7). . . 15
3.3 The thermal two-point Green's function to first order in the coupling constant. 15
3.4 The full propagator of a particle. Each circled 1PI is a sum of all 1PI diagrams. 18
3.5 One- and two-loop 1PI diagrams for $\lambda\phi^4$-theory. 18
3.6 First-order correction to the self-energy in $\lambda\phi^4$-theory. 19
3.7 Deformation of the contour in the evaluation of the Matsubara sum. (a) The sum of residues of the function $g(z)h(z)$ corresponds to an integration around a contour which encloses each pole individually. (b) The contour can be deformed to run along the imaginary axis a distance $+\epsilon$ to the right and a distance $-\epsilon$ to the left. (c) If $|g(z)h(z)|$ vanishes at infinity, the contour can be closed. 21
3.8 The first-order contribution to the thermodynamic potential. 25
3.9 Divergent diagrams in $\lambda\phi^4$-theory. 31
3.10 Diagrammatic contributions from the counterterms. 33
3.11 The first two infrared divergent diagrams in the infinite series of daisy diagrams in $\lambda\phi^4$-theory. 37
3.12 First-order contributions to the effective potential. 38
3.13 $\widetilde{M} = \frac{M}{T}$ as a function of λ. 41
3.14 $\overline{M} = \frac{M}{\sqrt{\lambda T^2/24}}$ as a function of λ. 41
5.1 One- and two-loop contributions to the effective potential of one scalar field. 48
5.2 $\widetilde{M}$ as a function of $\widetilde{T}$. The renormalized case (solid line) does not differ from the nonrenormalized case (dotted line). 53
5.3 $\widetilde{\phi}_0$ as a function of $\widetilde{T}$. The renormalized case (solid line) does not differ from the nonrenormalized case (dotted line). The order parameter indicates a first order phase transition. . . . 53
5.4 $\widetilde{M}$ as a function of $\widetilde{T}$ for $h = 0.01$. There is no difference between the case where $\widetilde{M}$ is renormalized (solid line) and the nonrenormalized case (dotted line). 55
5.5 $\widetilde{\phi}_0$ as a function of $\widetilde{T}$ for $\widetilde{h} = 0.01$. There is no phase transition, but rather a smooth crossover. The renormalized case (solid line) does not differ from the nonrenormalized case (dotted line). 55

5.6 One- and two-loop corrections to the effective potential for N scalar fields. Solid lines correspond to ϕ_σ and dashed lines correspond to ϕ_π. 57
5.7 The sigma mass M_σ, pion mass M_π and the mass in the symmetric phase, M, as functions of temperature in the Hartree approximation. The renormalized masses (solid lines) are qualitatively the same as the nonrenormalized masses (dotted lines). 66
5.8 ϕ_0 as a function of temperature in the renormalized (solid line) case and in the nonrenormalized (dotted line) case. The order parameter is qualitatively the same in the two cases. ϕ_0 indicates that a first-order phase transition takes place in the Hartree approximation. 66
5.9 M_σ and M_π as functions of temperature in the case of explicitly broken symmetry. The renormalized masses (solid lines) and the nonrenormalized masses (dotted lines) are not qualitatively different. 69
5.10 ϕ_0 as a function of temperature in the case of explicitly broken symmetry. The renormalized order parameter (solid line) is not qualitatively different from the nonrenormalized order parameter (dotted line). When the symmetry is explicitly broken, there is no phase transition, but rather a smooth crossover. 69
5.11 The sigma mass M_σ, pion mass M_π, and the mass, M, in the symmetric phase as functions of temperature. In the broken phase, there is no difference between the renormalized (solid line) and the nonrenormalized (dotted lines) cases. In the phase of restored symmetry, the renormalized mass depends on the choice of μ. 73
5.12 ϕ_0 as a function of temperature. There is no difference between the renormalized and the nonrenormalized cases. The order parameter indicates a second-order phase transition. . . 73
5.13 M_σ and M_π as functions of temperature in the case of explicitly broken symmetry. The renormalized masses (solid lines) does not differ qualitatively from the nonrenormalized masses (dotted lines). 75
5.14 ϕ_0 as a function of temperature. The order parameter is not qualitatively different in the renormalized (solid line) and nonrenormalized (dotted line) cases. There is no phase transition when the symmetry is explicitly broken, but rather a smooth crossover. 76

5.15 The order parameter in Hartree and large N approximation when $h \neq 0$. The first-order phase transition which is predicted in the Hartree approximation when $h = 0$ leaves the order parameter at $h \neq 0$ steeper than in the large-N approximation. 78

1 INTRODUCTION

Zero-temperature field theories are field theories which neglect temperature effects. At finite temperature, thermodynamic effects become important. At such temperatures, the particles interact in a thermal bath, and a merger of statistical mechanics and field theories is necessary. Field theories at finite temperature and density are called thermal field theories. Non-relativistic field theory at finite temperature and density was invented in the late 1950s [1] to give a description of condensed matter and non-relativistic nuclear matter. Fradkin first studied relativistic field theories at finite temperature in 1965 [1]. In the early 1970s, the interest in the problem of symmetry restoration at high temperature led to new developments. Kirzhnits (1972), Kirzhnits and Linde (1972), Dolan and Jackiw (1974), and Weinberg (1974) were the first to discuss restoration of spontaneously broken symmetry at high temperatures [2].

It is believed that a series of phase transitions occurred in the early Universe. The phase transition of QCD is one of them. There are two phenomena related to the QCD phase transition; the deconfinement of quarks and gluons, and the chiral symmetry restoration. It is believed that at some temperature, a phase transition from the hadronic phase to a deconfined phase of quark-gluon plasma takes place. A deconfinement also occurs at some critical density, when a phase transition between the hadronic phase and a phase of cold quark matter takes place. At about the same critical temperature and density at which the deconfinement phase transition takes place, the chiral phase transition takes place. Chiral symmetry mixes the flavors and flip the parity, which means that there should exist pairs of particles with opposite parity. Such pairs are not found in nature, so chiral symmetry must be broken at low temperatures. The symmetry is restored at high temperatures or high density. The relation between the chiral phase transition and the deconfinement phase transition is at present only partially understood, and it is not known if the phase transitions take place at the same critical temperature or density [3].

QCD is believed to give the correct description of strong interactions. Due to confinement at low temperatures, analytical calculations in QCD are impossible in this regime. Several effective models for QCD exist, which describes QCD at low temperatures. An example is the linear sigma model, which describes fermions interacting with mesons. This model is well suited for studying the chiral phase transition.

The purpose of this master thesis is to give an overview of thermal field theory, and to study the chiral phase transition using the linear sigma model as an effective theory. Thermal field theory can be described using two different formalisms; imaginary time formalism, or real time formalism. The real time formalism can be divided into closed time path formalism and

thermofield dynamics [4]. In this thesis the imaginary time, or Matsubara, formalism is used.

To study the chiral phase transition, two methods can be used; lattice gauge theories and the method of effective field theories [5]. The latter is considered in this thesis. The $O(4)$ linear sigma model is used as an effective model to study the chiral symmetry restoration.

The thesis is organized as follows. In chapter 2 the imaginary time formalism is introduced. The $\lambda\phi^4$-theory at finite temperature is studied in chapter 3. The first order corrections to the self-energy and thermodynamic potential are calculated, and the breakdown of perturbation theory is explained. An introduction to the idea of renormalization is given. Chapter 4 gives an introduction to effective theories. Resummation is reviewed, and QCD effective models are discussed. The linear sigma model is briefly presented. The chiral phase transition is studied in chapter 5. The phase transition in the case of one scalar field is presented as an example. The $O(4)$ linear sigma model is considered in both Hartree and large N approximation. Finally, a summary is given in chapter 6.

2 IMAGINARY-TIME FORMALISM

As mentioned in the introduction, thermal field theory can be described by using the imaginary time formalism or the real time formalism. In this section, the imaginary time formalism is presented. This formalism is also called the Matsubara formalism, after the person who first set up the diagrammatic perturbation theory of the partition function in a field-theoretic manner [6]. As will be seen, this formalism evaluates the partition function perturbatively using a diagrammatic method which is analogous to that of zero-temperature field theory.

In thermal equilibrium, the statistical behavior of a quantum system is studied through some appropriate statistical ensemble. The finite temperature behavior is given by the partition function

$$Z = \mathrm{Tr}\left[e^{-\beta\mathcal{H}}\right] \tag{2.1}$$

where $\rho(\beta) = e^{-\beta\mathcal{H}}$ is the density matrix, $\beta = \frac{1}{T}$ in natural units ($\hbar = k_B = c = 1$), and $\mathcal{H}$ is the Hamiltonian of the particular ensemble. The thermal expectation value of an observable A is given by

$$\langle A\rangle_\beta = \frac{1}{Z}\mathrm{Tr}\left[e^{-\beta\mathcal{H}}A\right] \tag{2.2}$$

The thermal average of the correlation function between two operators A and B is given by

$$\langle AB\rangle_\beta = \frac{1}{Z}\mathrm{Tr}\left[e^{-\beta\mathcal{H}}AB\right] \tag{2.3}$$

Given an ensemble and a set of operators in the Schrödinger picture, operators in a Heisenberg picture can be defined as [4]

$$A_H(t) = e^{i\mathcal{H}t}A_S e^{-i\mathcal{H}t}. \tag{2.4}$$

In Eq. (2.4), the subscript H indicates the Heisenberg picture and subscript S indicates the Schrödinger picture. The thermal average of the correlation function between two Heisenberg operators is thus written

$$\begin{aligned}\left\langle A_H(t)B_H(t')\right\rangle_\beta &= \frac{1}{Z}\mathrm{Tr}\left[e^{-\beta\mathcal{H}}A_H(t)B_H(t')\right]\\ &= \frac{1}{Z}\mathrm{Tr}\left[\left(e^{-\beta\mathcal{H}}A_H(t)e^{\beta\mathcal{H}}\right)e^{-\beta\mathcal{H}}B_H(t')\right]\\ &= \frac{1}{Z}\mathrm{Tr}\left[e^{-\beta\mathcal{H}}B_H(t')A_H(t+i\beta)\right]\\ &= \left\langle B_H(t')A_H(t+i\beta)\right\rangle_\beta.\end{aligned} \tag{2.5}$$

If the Hamiltonian of the system is separated into two parts, a free part and an interaction part, the density matrix can be written as follows [4]

$$\rho(\beta) = e^{-\beta(\mathcal{H}_0+\mathcal{H}_I)} = \rho_0(\beta)S(\beta), \tag{2.6}$$

where $\rho_0(\beta) \equiv e^{-\beta\mathcal{H}_0}$ is the density matrix in a noninteracting ensemble. $S(\beta)$ is given by

$$S(\beta) \equiv e^{-\beta\mathcal{H}_I} = \rho_0^{-1}(\beta)\rho(\beta). \tag{2.7}$$

The density matrix satisfies the following equations in the interval $0 \leq \tau \leq \beta$ [4]

$$\frac{\partial\rho_0(\tau)}{\partial\tau} = -\mathcal{H}_0\rho_0(\tau) \tag{2.8}$$

$$\frac{\partial\rho(\tau)}{\partial\tau} = -\mathcal{H}\rho(\tau) \tag{2.9}$$

$$= -\left(\mathcal{H}_0 + \mathcal{H}_I\right)\rho(\tau) \tag{2.10}$$

These equations can be thought of as the evolution equations of the density matrix with $0 \leq \tau \leq \beta$. The evolution equation of $S(\tau)$ is thus given by

$$\begin{aligned}\frac{\partial S(\tau)}{\partial\tau} &= \rho_0^{-1}(\tau)\left[\mathcal{H}_0 - \mathcal{H}\right]\rho(\tau) \\ &= -e^{\tau\mathcal{H}_0}\mathcal{H}_I e^{-\tau\mathcal{H}_0}S(\tau) \\ &= -\mathcal{H}_I(\tau)S(\tau)\end{aligned} \tag{2.11}$$

with the definition

$$\mathcal{H}_I(\tau) = e^{\tau\mathcal{H}_0}\mathcal{H}_I e^{-\tau\mathcal{H}_0}. \tag{2.12}$$

For imaginary values of τ, the transformation is unitary. Also, by writing $\tau = it$, the expression of $\mathcal{H}_I(\tau)$ coincides with the usual interaction picture $\mathcal{H}_I(t) = e^{it\mathcal{H}_0}\mathcal{H}_I e^{-it\mathcal{H}_0}$. Eq. (2.12) can be interpreted as an interaction picture in which the time has been rotated in the complex plane, $t \to -i\tau$. Rotations in the complex plane will be further discussed in section 2.2.

2.1 The S-matrix and diagrammatic representation

Consider a process where the particles are free at the beginning t_i and end t_f, but interact over a limited space-time region in the interim. The state vector at the beginning is denoted $\Phi(t_i)$ and that at the end $\Phi(t_f)$. The unitary operator $U(t_f, t_i)$ propagates the system from t_i to t_f [3],

$$\Phi(t_f) = U(t_f, t_i)\Phi(t_i). \tag{2.13}$$

In zero temperature field theory, the S-operator is the following limit of $U(t_f, t_i)$ [3]

$$S = \lim_{t_f \to \infty} \lim_{t_i \to -\infty} U(t_f, t_i). \tag{2.14}$$

In the interaction picture the evolution equation of $\Phi(t)$ is given by [3]

$$i\frac{\partial \Phi(t)}{\partial t} = H_I(t)\Phi(t), \tag{2.15}$$

which can be formally integrated to give

$$\begin{aligned} \Phi(t_f) &= U(t_f, t_i)\Phi(t_i) \\ &= e^{-i\int_{t_i}^{t_f} dt\, H_I(t)}\Phi(t_i). \end{aligned} \tag{2.16}$$

Since generally $[H_I(t), H_I(t')] \neq 0$, and two operators A and B which do not commute leads to $e^{A+B} \neq e^A e^B$, a time ordering operator is introduced [3]. The time ordering operator T_t has the property [7]

$$T_t\left\{A(t), B(t')\right\} = \Theta(t-t')A(t)B(t') \pm \Theta(t'-t)B(t')A(t), \tag{2.17}$$

where $+$ represents boson operators and $-$ represents fermion operators. The time ordering operator writes the operators A and B in chronological order. This gives

$$U(t_f, t_0) = T_t\left\{e^{-i\int_{t_i}^{t_f} dt\, H_I(t)}\right\}, \tag{2.18}$$

which leads to the time evolution operator

$$S = T_t\left\{e^{-i\int_{-\infty}^{\infty} dt\, H_I(t)}\right\}. \tag{2.19}$$

The evolution equation of $S(\tau)$ is given in Eq. (2.11). When integrated, remembering the need of a time ordering operator, $S(\beta)$ is given by

$$S(\beta) = T_\tau\left\{e^{-\int_0^\beta \mathcal{H}_I(\tau)d\tau}\right\}, \tag{2.20}$$

where T_τ is the ordering operator in τ. Similar to the expression for the usual time ordering, T_τ has the property

$$T_\tau\left\{A(\tau), B(\tau')\right\} = \Theta(\tau-\tau')A(\tau)B(\tau') \pm \Theta(\tau'-\tau)B(\tau')A(\tau), \tag{2.21}$$

where $+$ represents boson operators and $-$ represents fermion operators. Comparing Eqs. (2.19) and (2.20), $S(\beta)$ is interpreted as the time evolution operator at finite temperature. It is clear that the finite-temperature time evolution operator is analogous to the zero-temperature time evolution

operator. The difference is that in the finite-temperature case, the time integration is over a finite interval along the imaginary axis. In an expansion of the exponential in Eq. (2.20), each term would give rise to a Feynman diagram as in the zero-temperature case. Thermal quantities also have a diagrammatic representation [4].

2.2 Wick rotation

A Wick rotation is a rotation in the complex plane turning a real variable into an imaginary variable. Wick rotation makes it possible to find a solution to a problem in Minkowski space by finding a solution to a related problem in Euclidean space. The Minkowski metric in four dimensions is

$$ds^2 = dt^2 - dx^2 - dy^2 - dz^2, \tag{2.22}$$

or $ds^2 = -dt^2+dx^2+dy^2+dz^2$. Here, we will use Eq. (2.22). The Minkowski metric and that of four-dimensional Euclidean space

$$ds_E^2 = dt^2 + dx^2 + dy^2 + dz^2 \tag{2.23}$$

are not distinct if t takes complex values. If $w = it$, the Minkowski metric reads

$$\begin{aligned} ds^2 &= (-idw)^2 - dx^2 - dy^2 - dz^2 \\ &= -dw^2 - dx^2 - dy^2 - dz^2 \\ &= -ds_E^2, \end{aligned} \tag{2.24}$$

where ds_E^2 is the Euclidean metric in real coordinates x, y, z and w.

The operator $e^{-it\mathcal{H}}$ propagates a quantum state through a real time interval t [3]. As seen above, the operator that propagates a state through an imaginary time interval is given by $e^{-\tau\mathcal{H}}$, where $\tau = it$. This is not a physical propagation, but the operator is well-defined mathematically. It can be used to find the eigenvalues $e^{-E\tau}$ of $e^{-\tau\mathcal{H}}$, given by $E = -\frac{1}{\tau}\ln\left(e^{-\tau\mathcal{H}}\right)$ [3]. Finding eigenvalues and eigenvectors of $e^{-\tau\mathcal{H}}$ is equivalent to finding eigenvalues of $\mathcal{H}$. Thus no information is lost when rotating to Euclidean time. The eigenvalues and eigenvectors of $e^{-\tau\mathcal{H}}$ can be used to find the eigenvalues and eigenvectors of $e^{-it\mathcal{H}}$.

Integrals of the following form can be evaluated by using the routing of the contour past the poles to perform a Wick rotation into Euclidean space [8]:

$$\begin{aligned} I &= \int \frac{d^dk}{(2\pi)^d} \frac{1}{\left[k^2 - m^2 + i\epsilon\right]^l} \\ &= \int d\Omega_d \int \frac{k^{d-1}dk}{(2\pi)^d} \frac{1}{\left[k^2 - m^2 + i\epsilon\right]^l}. \end{aligned} \tag{2.25}$$

Rotating the k_0 contour 90^o in the complex plane does not change the value of the integral. The rotation is shown in Fig. 2.1. By letting $k^0 \to ik_E^0$, the

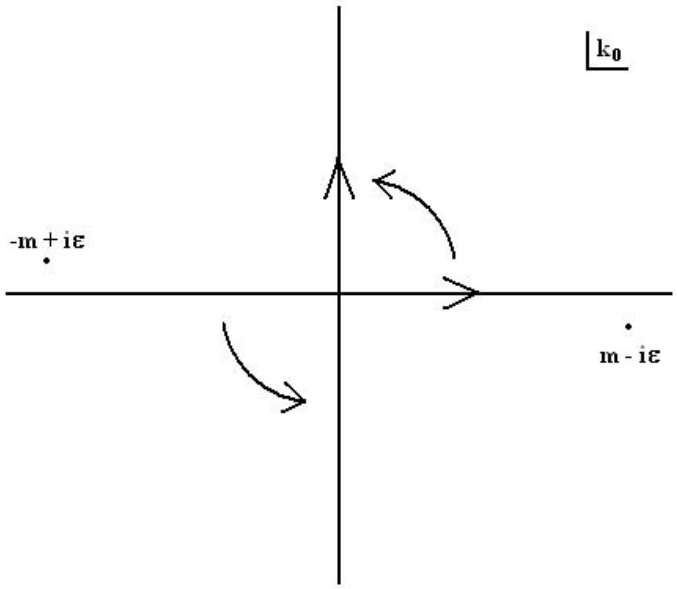

Figure 2.1: Rotation of the k_0 contour to the imaginary axis. The rotation does not change the value of integral.

integral in Eq. (2.25) can be written

$$\begin{aligned} I &= i(-1)^l \frac{\Omega_d}{(2\pi)^d} \int_0^\infty dk_E \frac{k_E^{d-1}}{\left[k_E^2 + m^2\right]^l} \\ &= i(-1)^l \int \frac{d^d k_E}{(2\pi)^d} \frac{1}{\left[k_E^2 + m^2\right]^l}, \end{aligned} \tag{2.26}$$

where the subscript E indicates Euclidean space. After the rotation the $i\epsilon$-term in the denominator is not included. The integral is divergent if $d > 2l$.

2.3 Imaginary-time Green's Functions

In field theory, Green's functions are the vacuum expectation values of time-ordered products of Heisenberg operators [8]

$$G^{(n)}(x_1, \ldots, x_n) = \langle 0 | \, T \left\{ \phi_H(x_1) \ldots \phi_H(x_n) \right\} | 0 \rangle \, . \tag{2.27}$$

For finite temperature field theories, the vacuum is replaced by a thermal bath. The two-point thermal Green function can be defined as [4]

$$\begin{aligned} G_\beta(\tau,\tau') &= \left\langle T_\tau \left\{ \phi_H(\tau)\phi_H^\dagger(\tau') \right\} \right\rangle_\beta \\ &= \frac{1}{Z}\mathrm{Tr}\left[e^{-\beta\mathcal{H}} T_\tau \left\{ \phi_H(\tau)\phi_H^\dagger(\tau') \right\} \right], \end{aligned} \tag{2.28}$$

where $\tau = it$. In Eq. (2.28), the spatial coordinates have been suppressed since they are not relevant for the following discussion. Evaluating $G_\beta(0,\tau)$ for $\tau > 0$ gives

$$\begin{aligned} G_\beta(0,\tau) &= \left\langle \Theta(0-\tau)\phi_H(0)\phi_H^\dagger(\tau) \pm \Theta(\tau-0)\phi_H^\dagger(\tau)\phi_H(0) \right\rangle_\beta \\ &= \pm \left\langle \phi_H^\dagger(\tau)\phi_H(0) \right\rangle_\beta \end{aligned} \tag{2.29}$$

By using Eq. (2.5) and keeping in mind that the time is rotated to imaginary time, the following is obtained

$$\left\langle \phi_H^\dagger(\tau)\phi_H(0) \right\rangle_\beta = \left\langle \phi_H(\beta)\phi_H^\dagger(\tau) \right\rangle_\beta = G_\beta(\beta,\tau). \tag{2.30}$$

Thus,

$$G_\beta(0,\tau) = \pm G_\beta(\beta,\tau). \tag{2.31}$$

The two-point thermal Green's functions are anti-periodic for fermionic fields and periodic for bosonic fields in the imaginary-time formalism.

The thermal Green's functions are defined on a finite time interval with period β. This means that the Fourier transforms involve discrete frequencies [4]

$$G_\beta(\tau) = \frac{1}{\beta}\sum_n e^{-i\omega_n'\tau} G_\beta(\omega_n'), \tag{2.32}$$

$$G_\beta(\omega_n') = \frac{1}{2}\int_{-\beta}^{\beta} d\tau e^{i\omega_n'\tau} G_\beta(\tau), \tag{2.33}$$

where $\omega_n' = \frac{n'\pi}{\beta}$ for $n' = 0, \pm 1, \pm 2, \ldots$. Eq. (2.33) can be written as [4]

$$\begin{aligned} G_\beta(\omega_n') &= \frac{1}{2}\int_{-\beta}^{0} d\tau e^{i\omega_n'\tau} G_\beta(\tau) + \frac{1}{2}\int_0^\beta d\tau e^{i\omega_n'\tau} G_\beta(\tau) \\ &= \pm\frac{1}{2}\int_{-\beta}^{0} d\tau e^{i\omega_n'\tau} G_\beta(\tau+\beta) + \frac{1}{2}\int_0^\beta d\tau e^{i\omega_n'\tau} G_\beta(\tau) \\ &= \frac{1}{2}\left(1 \pm e^{-i\omega_n'\beta}\right)\int_0^\beta d\tau e^{i\omega_n'\tau} G_\beta(\tau) \\ &= \frac{1}{2}\left(1 \pm e^{-i\pi n'}\right)\int_0^\beta d\tau e^{i\omega_n'\tau} G_\beta(\tau), \end{aligned} \tag{2.34}$$

where the upper sign is for bosons and lower sign is for fermions. When n' is odd, $G_\beta(\omega_n')$ vanishes for bosons, and when n' is even, $G_\beta(\omega_n')$ vanishes for fermions. Thus for nonzero values of $G_\beta(\omega_n')$, even numbers of n' are needed for bosons, written as $n' = 2n$ where $n = 0, \pm 1, \pm 2, \ldots$. Odd numbers of n' are needed for fermions, written as $n' = 2n+1$ where $n = 0, \pm 1, \pm 2, \ldots$. The anti-periodicity/periodicity for fermions/bosons thus gives

$$\omega_n = \left\{ \begin{array}{ll} \frac{2n\pi}{\beta} & \text{bosons} \\ \frac{(2n+1)\pi}{\beta} & \text{fermions} \end{array} \right\}, \tag{2.35}$$

where $n \in Z$. The frequencies ω_n are called Matsubara frequencies [4].

Including the spatial coordinates in the two-point Green's function gives the following expressions

$$G_\beta(\tau, \vec{x}) = \frac{1}{\beta} \sum_n \int \frac{d^3k}{(2\pi)^3} e^{-i(\omega_n \tau - \vec{k}\cdot\vec{x})} G_\beta(\omega_n, \vec{k}), \tag{2.36}$$

$$G_\beta(\omega_n, \vec{k}) = \int_0^\beta d\tau \int d^3x \, e^{i(\omega_n \tau - \vec{k}\cdot\vec{x})} G_\beta(\tau, \vec{x}), \tag{2.37}$$

since the spatial coordinates are continuous as in the zero-temperature case. For a free scalar field, the zero-temperature Green's function satisfies

$$\left(\partial_\mu \partial^\mu + m^2\right) G(x) = -\delta^4(x). \tag{2.38}$$

Performing Wick rotations $t \to -i\tau$ and $k^0 \to i k_E^0$ leads to $G(x) \to -G_\beta(\tau, \vec{x})$ [4], and Eq. (2.38) reads

$$\left(\frac{\partial^2}{\partial \tau^2} + \nabla^2 - m^2\right) G_\beta(\tau, \vec{x}) = -\delta^3(x)\delta(\tau). \tag{2.39}$$

Inserting Eq. (2.36) into Eq. (2.39), and using the usual expression of $\delta^3(x)$ as well as the representation of $\delta(\tau)$

$$\delta(\tau) = \frac{1}{\beta} \sum_n e^{-i\omega_n \tau}, \tag{2.40}$$

the two-point Green's function in momentum space at finite temperature is

$$\begin{aligned} G_\beta(\omega_n, \vec{k}) &= \frac{1}{\omega_n^2 + \vec{k}^2 + m^2} \\ &= \frac{1}{\omega_n^2 + \omega_k^2}, \end{aligned} \tag{2.41}$$

where $\omega_k^2 = \vec{k}^2 + m^2$.

3 $\lambda\phi^4$ THEORY

The Lagrangian for a $\lambda\phi^4$-theory in Minkowski space is given by

$$\mathcal{L} = \frac{1}{2}(\partial_\mu \phi_B)(\partial^\mu \phi_B) - \frac{1}{2}m_B^2\phi_B^2 - \frac{\lambda_B}{4!}\phi_B^4, \tag{3.1}$$

where the last term is a self-interaction. The abbreviation $\phi_B(x) \equiv \phi_B$, where $x = (t, \vec{x})$, is used. The subscript B indicates that the field, mass and coupling constant are bare parameters. Bare and renormalized parameters will be discussed in sections 3.5-3.8. When rotating to Euclidean time, $t \to -i\tau$, we obtain for the Lagrangian in Eq. (3.1)

$$\begin{aligned} \mathcal{L} &\to -\left(\frac{1}{2}(\partial_\mu \phi_B)^2 + \frac{1}{2}m_B^2\phi_B^2 + \frac{\lambda_B}{4!}\phi_B^4\right) \\ &= -\mathcal{L}_E. \end{aligned} \tag{3.2}$$

In Eq. (3.2), we have used that in Euclidean space $\partial_\mu = \partial^\mu$, and $\partial_0 = \frac{\partial}{\partial\tau}$. The abbreviation $\phi_B(x) \equiv \phi_B$ is used, where now $x = (\tau, \vec{x})$.

3.1 Diagrammatic representation in the $\lambda\phi^4$-theory

A typical diagram consists of pieces connected to external points and pieces which are not connected to external points [9]. To see how these different pieces contribute to the correlation functions, consider the thermal two-point Green's function for the $\lambda\phi^4$-theory,

$$\begin{aligned} G_\beta(x, x') &= \left\langle T_\tau \left\{\phi_H(x)\phi_H(x')\right\}\right\rangle_\beta \\ &= \frac{\mathrm{Tr}\left[e^{-\beta\mathcal{H}_0}S(\beta)T_\tau\left\{\frac{1}{S(\tau)}\phi_I(x)S(\tau)\frac{1}{S(\tau')}\phi_I(x)S(\tau')\right\}\right]}{\mathrm{Tr}\left[e^{-\beta\mathcal{H}_0}S(\beta)\right]}, \end{aligned} \tag{3.3}$$

where the relation between operators in the Heisenberg and interaction pictures $A_H(\tau) = e^{\tau\mathcal{H}_I}A_I(\tau)e^{-\tau\mathcal{H}_I}$ has been used [4] and $x = (\tau, \vec{x})$. Since β is the largest value of τ, $S(\beta)$ can be written inside the τ-ordering in the numerator of Eq. (3.3). Furthermore, the order of the factors inside the τ-ordering does not matter. Thus, Eq. (3.3) can be written as

$$\begin{aligned} G_\beta(x, x') &= \frac{\mathrm{Tr}\left[e^{-\beta\mathcal{H}_0}T_\tau\left\{\phi_I(x)\phi_I(x')S(\beta)\right\}\right]}{\mathrm{Tr}\left[e^{-\beta\mathcal{H}_0}S(\beta)\right]} \\ &= \frac{\left\langle T_\tau\left\{\phi_I(x)\phi_I(x')S(\beta)\right\}\right\rangle_{\beta,0}}{\left\langle S(\beta)\right\rangle_{\beta,0}}, \end{aligned} \tag{3.4}$$

where $\langle\ \rangle_{\beta,0}$ denotes the thermal average in a non-interacting ensemble. First, consider the numerator of Eq. (3.4), which we call $G^1_\beta(x,x')$. Expanding the exponential of $S(\beta)$ to first order in the coupling constant, it can be written as

$$\begin{aligned} G^1_\beta(x,x') &= \left\langle T_\tau \left\{ \phi(x)\phi(x') e^{-\int_0^\beta d\tau'' \int d^3x'' \frac{\lambda_B}{4!}\phi^4(x'')} \right\} \right\rangle_{\beta,0} \\ &= \left\langle T_\tau \left\{ \phi(x)\phi(x') \left(1 + \frac{-\lambda_B}{4!} \int_0^\beta d\tau'' \int d^3x'' \phi^4(x'') \right) \right\} \right\rangle_{\beta,0}, \end{aligned} \tag{3.5}$$

where the subscript I has been dropped. The first term in Eq. (3.5) is the free field propagator, $G_0(x,x') = \langle T_\tau \{\phi(x)\phi(x')\}\rangle_{\beta,0}$. Eq. (3.5) can be written as

$$\begin{aligned} G^1_\beta(x,x') &= G_0(x,x') \\ &\quad + 3\left(\frac{-\lambda_B}{4!}\right) G_0(x,x') \int_0^\beta d\tau'' \int d^3x'' G_0(x'',x'') G_0(x'',x'') \\ &\quad + 12\left(\frac{-\lambda_B}{4!}\right) \int_0^\beta d\tau'' \int d^3x'' G_0(x,x'') G_0(x',x'') G_0(x'',x''). \end{aligned} \tag{3.6}$$

Eq. (3.6) is shown diagrammatically in Fig. (3.1). In the second line in Eq.

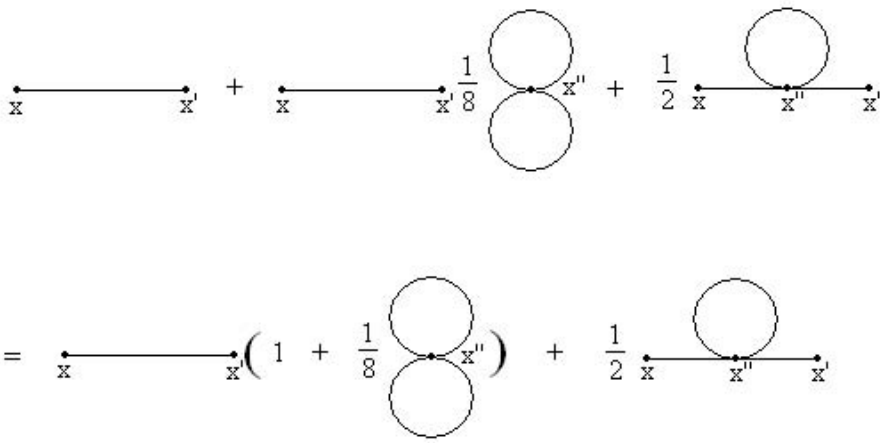

Figure 3.1: The numerator of the thermal two-point Green's function to first order in the coupling constant, given in Eq. (3.6).

(3.6), the points x and x' are not connected with the point x''. This term leads to the disconnected diagram which is the second diagram in the first

line of Fig. 3.1. The last term in Eq. (3.6) connects the points x and x' with the point x'' and leads to the third diagram in the first line of Fig. 3.1. This is a connected diagram [9].

Expanding the denominator of Eq. (3.4) to first order in the coupling constant gives

$$\langle S(\beta)\rangle_{\beta,0} = \left\langle T_\tau \left\{ 1 + \frac{-\lambda_B}{4!} \int_0^\beta d\tau \int d^3x \phi^4(x) \right\} \right\rangle_{\beta,0} . \tag{3.7}$$

Eq. (3.7) is shown diagrammatically in Fig. 3.2. The diagrams in the

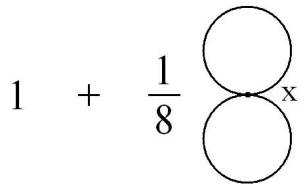

Figure 3.2: The denominator of the thermal two-point Green's function to first order in the coupling constant, given in Eq. (3.7).

denominator cancel the disconnected diagrams in the numerator, and the following is obtained for the two-point Green's function to first order in the coupling constant

$$\begin{aligned} G_\beta(x,x') &= \left\langle T_\tau \left\{ \phi(x)\phi(x') \right\} \right\rangle_\beta \\ &= \text{sum of connected pieces with two external lines.} \end{aligned} \tag{3.8}$$

$G_\beta(x,x')$ to first order is shown diagrammatically in Fig. 3.3.

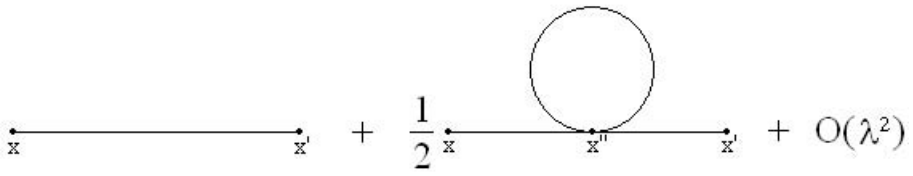

Figure 3.3: The thermal two-point Green's function to first order in the coupling constant.

To show that Eq. (3.8) applies to all orders in the coupling constant, consider the following expression for the diconnected diagrams in the numerator of Eq. (3.4) to order n [10]:

$$\begin{aligned}
&\left\langle T_\tau \left\{ \phi(x)\phi(x') \frac{(-1)^n}{n!} \int_0^\beta d\tau_1 \cdots \int_0^\beta d\tau_n \mathcal{H}_I(x_1) \cdots \mathcal{H}_I(x_n) \right\} \right\rangle_{\beta,0} \\
&= \frac{(-1)^n}{n!} \int_0^\beta d\tau_1 \cdots \int_0^\beta d\tau_m \left\langle T_\tau \left\{ \phi(x)\phi(x') \mathcal{H}_I(x_1) \cdots \mathcal{H}_I(x_m) \right\} \right\rangle_c \\
&\cdot \int_0^\beta d\tau_{m+1} \cdots \int_0^\beta d\tau_n \left\langle T_\tau \left\{ \mathcal{H}_I(x_{m+1}) \cdots \mathcal{H}_I(x_n) \right\} \right\rangle_{\beta,0},
\end{aligned} \tag{3.9}$$

where $\mathcal{H}_I(x)$ is the interaction Hamiltonian. The $\langle \ldots \rangle_c$ connects x and x' to some of the points x_i and the $\langle \ldots \rangle_{\beta,0}$ gives the parts which have no external lines. Redistribution of the x_i's where $i = 1, \ldots, n$ among the $H_I(x)$'s in $\langle \ldots \rangle_c$ and among the $H_I(x)$'s in $\langle \ldots \rangle_{\beta,0}$, gives an overall factor of $\frac{n!}{m!(n-m)!}$. Thus, Eq. (3.9) can be written as

$$\begin{aligned}
&\frac{(-1)^m}{m!} \int_0^\beta d\tau_1 \cdots \int_0^\beta d\tau_m \left\langle T_\tau \left\{ \phi(x)\phi(x') \mathcal{H}_I(x_1) \cdots \mathcal{H}_I(x_m) \right\} \right\rangle_c \\
&\times \frac{(-1)^{n-m}}{(n-m)!} \int_0^\beta d\tau_{m+1} \cdots \int_0^\beta d\tau_n \left\langle T_\tau \left\{ \mathcal{H}_I(x_{m+1}) \cdots \mathcal{H}_I(x_n) \right\} \right\rangle_{\beta,0}.
\end{aligned} \tag{3.10}$$

Summing the contribution from the diagrams of all orders which consist of a particular connected part and an arbitrary disconnected part gives [10]

$$\begin{aligned}
&\frac{(-1)^m}{m!} \int_0^\beta d\tau_1 \cdots \int_0^\beta d\tau_m \left\langle T_\tau \left\{ \phi(x)\phi(x') \mathcal{H}_I(x_1) \cdots \mathcal{H}_I(x_m) \right\} \right\rangle_c \\
&\cdot \left\langle 1 - \int_0^\beta d\tau_{m+1} T_\tau \left\{ \mathcal{H}_I(x_{m+1}) \right\} + \cdots \right\rangle_{\beta,0}.
\end{aligned} \tag{3.11}$$

Thus, all connected parts in the numerator are multiplied with a factor $\langle S(\beta) \rangle_{\beta,0}$, which cancels against the $\langle S(\beta) \rangle_{\beta,0}$ in the denominator. The result we obtained above for first order in the coupling constant is general, and Eq. (3.8) applies to all orders.

Eq. (3.8) can be generalized to n-point Green's functions [9]

$$\begin{aligned}
G_\beta(x, \ldots, x_n) &= \left\langle T_\tau \left\{ \phi(x_1) \cdots \phi(x_n) \right\} \right\rangle_\beta \\
&= \text{sum of connected pieces with } n \text{ external lines.}
\end{aligned} \tag{3.12}$$

$\langle S(\beta) \rangle_{\beta,0}$ contains no external points, so the diagrams in the expansion of $\langle S(\beta) \rangle_{\beta,0}$ have no external lines. In general, the contribution from order n can be written as a sum of disconnected parts, each of which is a product of connected pieces [2]. Assume that each contribution in the expansion consists of k_i diagrams of type V_i. The total expansion gives [9]

$$\sum_{\{k_i\}} \prod_i \frac{1}{k_i!} (V_i)^{k_i} = e^{\sum_i V_i}, \tag{3.13}$$

where $\{k_i\}$ is all ordered sets $\{k_1, k_2, k_3 \ldots\}$ of nonnegative integers, and the factor $\frac{1}{k_i}$ comes from interchanging the k_i V_i's. Thus, only the connected diagrams are left, and $\langle S(\beta)\rangle_{\beta,0}$ is the exponential of the sum of all connected diagrams with no external lines. These diagrams are called vacuum diagrams, and contribute to the thermodynamic potential as seen in the following. From Eq. (2.7), the denominator of the two-point Green's function reads

$$\begin{aligned} \langle S(\beta)\rangle_{\beta,0} &= \left\langle e^{-\beta \mathcal{H}_I} \right\rangle_{\beta,0} \\ &= \frac{\mathrm{Tr}\left[e^{-\beta\mathcal{H}_0} e^{-\beta\mathcal{H}_I}\right]}{\mathrm{Tr}\left[e^{-\beta\mathcal{H}_0}\right]} \\ &= \frac{\mathrm{Tr}\left[e^{-\beta\mathcal{H}}\right]}{Z_0} = \frac{Z}{Z_0}. \end{aligned} \tag{3.14}$$

Using Eq. (3.14), the thermodynamic potential is given by

$$\begin{aligned} \Phi &= -T \ln Z \\ &= -T \ln Z_0 - T \ln \langle S(\beta)\rangle_{\beta,0} \\ &= \Phi_0 + \Phi'. \end{aligned} \tag{3.15}$$

where Φ_0 is the potential for the non-interacting ensemble and Φ' are the corrections to the potential from the interactions. It was found above that

$$\langle S(\beta)\rangle_{\beta,0} = e^{\sum_i V_i}. \tag{3.16}$$

Thus, $\Phi' = -T \sum_i \mathcal{V}_i$ is the sum of the connected diagrams with no external lines.

3.2 Self-energy

At zero temperature, the self-energy is the contribution to a propagating particle from vacuum fluctuations. At finite temperature, thermal contributions must be included as well. Each contribution to the propagating particle consists of free propagators separated by different scattering processes. The full propagator is shown in Fig. (3.4), where 1PI represents one-particle irreducible diagrams. A 1PI diagram is a diagram which does not fall apart when cutting a line [9]. Each circled 1PI in Fig. (3.4) is a sum of all 1PI diagrams. Fig. (3.5) shows the 1PI diagrams for the $\lambda\phi^4$-theory,

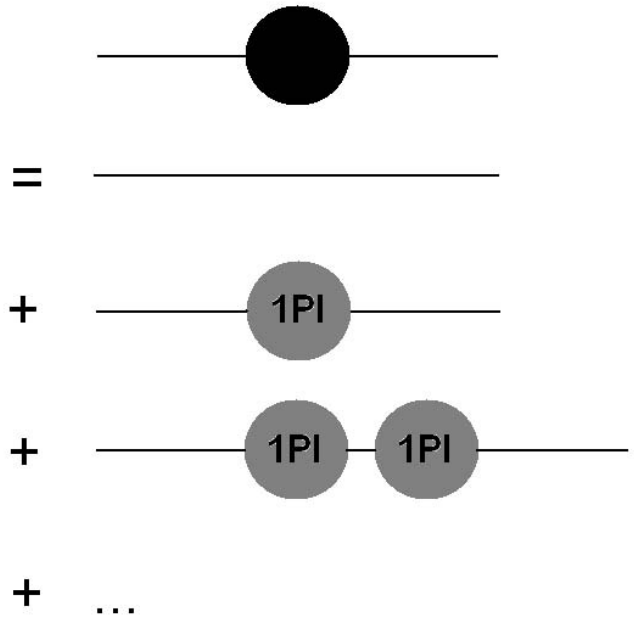

Figure 3.4: The full propagator of a particle. Each circled 1PI is a sum of all 1PI diagrams.

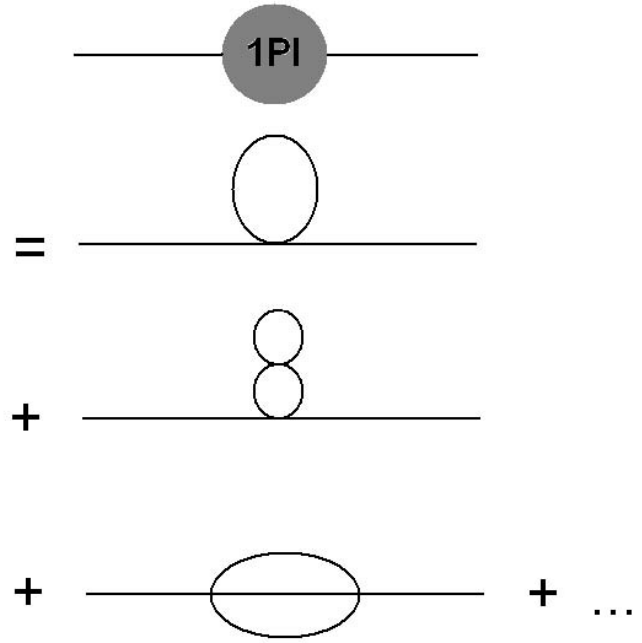

Figure 3.5: One- and two-loop 1PI diagrams for $\lambda\phi^4$-theory.

from perturbative expansion of the S-matrix. In momentum space, the full propagator $\mathcal{G}_\beta(\omega_n, \vec{k})$ can be written as

$$\begin{aligned}\mathcal{G}_\beta(\omega_n, \vec{k}) &= G_\beta + G_\beta(-\Sigma(k))G_\beta + G_\beta(-\Sigma(k))G_\beta(-\Sigma(k))G_\beta + \dots \\ &= G_\beta \sum_{n=1}^{\infty}(-\Sigma(k)G_\beta)^{n-1} = \frac{1}{(G_\beta)^{-1} + \Sigma(k)},\end{aligned} \tag{3.17}$$

where G_β is the propagator found in Eq. (2.41). $\Sigma(k)$ is the self-energy of the $\lambda\phi^4$-theory, and $-\Sigma(k)$ represents the sum of all 1PI diagrams. Using the expression for the free thermal propagator of the $\lambda\phi^4$-theory, Eq. (3.17) reads

$$\mathcal{G}_\beta(\omega_n, \vec{k}) = \frac{1}{\omega_n^2 + \omega_k^2 + \Sigma(k)}. \tag{3.18}$$

3.2.1 First-order correction

Consider the first-order correction shown in Fig. (3.6). The self-energy is

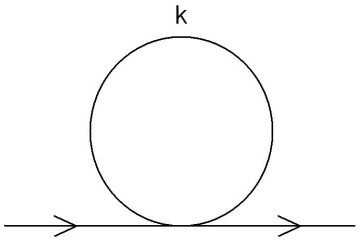

Figure 3.6: First-order correction to the self-energy in $\lambda\phi^4$-theory.

given by

$$\Sigma = \frac{\lambda_B}{2}\sum\!\!\!\!\!\!\int_k \frac{1}{\omega_n^2 + \omega_k^2}. \tag{3.19}$$

where $\sum\!\!\!\!\!\!\int_k = T\sum_n \int \frac{d^3k}{(2\pi)^3}$ and $\omega_k^2 = \vec{k}^2 + m_B^2$. To first order, the self-energy is independent of external momenta.

To evaluate the sum in Eq. (3.19) it can be rewritten as a sum of residues of a suitable function. The residue theorem states that for a function $f(z)$ which is analytic inside a simple closed path C, except for finitely many singularities in $z_1, z_2, \dots, z_k$, the integral of $f(z)$ taken counterclockwise around C is given by [11]

$$\oint_C f(z)dz = 2\pi i \sum_{j=1}^{k} Res_{z=z_j} f(z). \tag{3.20}$$

The residues at simple poles are given by [11]

$$\mathrm{Res}_{z=z_j} f(z) = \lim_{z\to z_j} (z - z_j) f(z). \tag{3.21}$$

The frequency sum can written as

$$\sum_n \frac{1}{\omega_n^2 + \omega_k^2} = \sum_n \frac{1}{(\omega_k - i\omega_n)(\omega_k + i\omega_n)} \equiv \sum_n h(i\omega_n). \tag{3.22}$$

The idea behind the evaluation of the frequency sum, is to introduce a function $g(z)$ which has simple poles at $z = i\omega_n$. For bosons the Matsubara frequency is given by $\omega_n = 2\pi nT$. The function $g(z) = \coth\left(\frac{z}{2T}\right)$ can be used to evaluate the frequency sum in the case of bosons, as it generates poles at $z = i2\pi Tn = i\omega_n$. The function $h(z)$ has no poles on the imaginary axis. The contour integral of the product $g(z)h(z)$ is given by

$$\begin{aligned}
\oint_C \frac{dz}{2\pi i} g(z)h(z) &= \sum_n \mathrm{Res}_{z=i\omega_n} g(z)h(z) \\
&= \sum_n \lim_{z\to i\omega_n} (z - i\omega_n) g(z)h(z) \\
&= \sum_n \lim_{z\to i\omega_n} (z - i\omega_n) h(z) \frac{e^{\frac{z}{2T}} + e^{-\frac{z}{2T}}}{e^{\frac{z}{2T}} - e^{-\frac{z}{2T}}} \\
&= \sum_n \lim_{z\to i\omega_n} (z - i\omega_n) h(z) \frac{e^{\frac{z}{T}} + 1}{e^{\frac{z-i\omega_n}{T}} - 1} \\
&\approx \sum_n \lim_{z\to i\omega_n} (z - i\omega_n) h(z) T \frac{e^{\frac{z}{T}} + 1}{z - i\omega_n} \\
&= 2T \sum_n h(i\omega_n),
\end{aligned} \tag{3.23}$$

where C is given in Fig. 3.7(a). The contour can be deformed into that shown in Fig. 3.7(b). Thus, we can write

$$\begin{aligned}
2T \sum_n h(i\omega_n) = &\int_{i\infty-\epsilon}^{-i\infty-\epsilon} \frac{dz}{2\pi i} g(z)h(z) \\
&+ \int_{-i\infty+\epsilon}^{i\infty+\epsilon} \frac{dz}{2\pi i} g(z)h(z).
\end{aligned} \tag{3.24}$$

Doing the substitution $z \to -z$ in the first integral, Eq. (3.24) can be written as

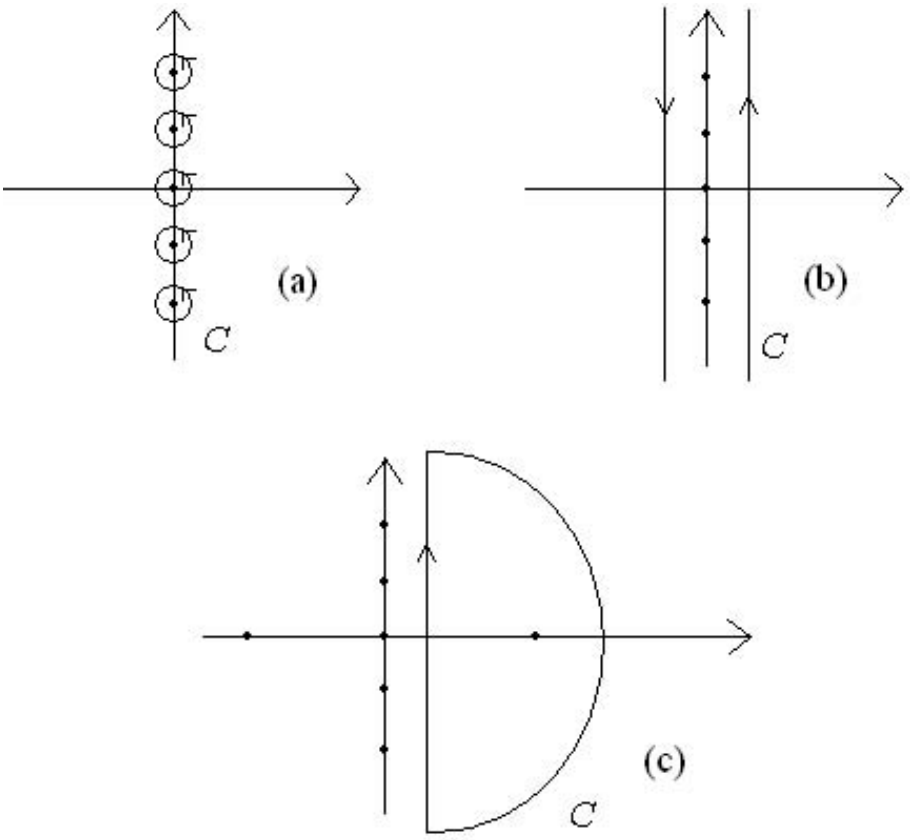

Figure 3.7: Deformation of the contour in the evaluation of the Matsubara sum. (a) The sum of residues of the function $g(z)h(z)$ corresponds to an integration around a contour which encloses each pole individually. (b) The contour can be deformed to run along the imaginary axis a distance $+\epsilon$ to the right and a distance $-\epsilon$ to the left. (c) If $|g(z)h(z)|$ vanishes at infinity, the contour can be closed.

$$2T\sum_n h(i\omega_n) = \int_{-i\infty+\epsilon}^{i\infty+\epsilon} \frac{dz}{2\pi i}\left[-g(-z)h(-z) + g(z)h(z)\right]. \tag{3.25}$$

By using that $g(-z) = -g(z)$ and $h(-z) = h(z)$, we obtain

$$2T\sum_n h(i\omega_n) = 2\int_{-i\infty+\epsilon}^{i\infty+\epsilon} \frac{dz}{2\pi i} g(z)h(z). \tag{3.26}$$

$g(z)$ can be written as $g(z) = 1 + 2\frac{1}{e^{\beta z}-1}$, which gives the following

$$2T\sum_n h(i\omega_n) = 2\int_{-i\infty+\epsilon}^{i\infty+\epsilon} \frac{dz}{2\pi i} h(z)\left[1 + 2\frac{1}{e^{\beta z}-1}\right]. \tag{3.27}$$

$h(z)$ has no poles on the imaginary axis. Thus, Eq. (3.27) can be written as

$$\begin{aligned} 2T\sum_n h(i\omega_n) = {} & 2\int_{-i\infty}^{i\infty} \frac{dz}{2\pi i} h(z) \\ & + 4\int_{-i\infty+\epsilon}^{i\infty+\epsilon} \frac{dz}{2\pi i} h(z)\frac{1}{e^{\beta z}-1}. \end{aligned} \tag{3.28}$$

The frequency sum splits into a temperature-independent part and a temperature-dependent part. The temperature-independent part can be calculated directly and gives $2\int_{-i\infty}^{i\infty}\frac{dz}{2\pi i}h(z) = \frac{1}{\omega_k}$. To calculate the temperature-dependent part, we can close the contour in the right half plane as shown in Fig. 3.7(c). When the radius goes to infinity, the function $g(z)h(z)$ goes to zero, so the contribution from the semicircle vanishes at infinity. $h(z)$ has a pole inside C located at $z = \omega_k$. The temperature-dependent part is given by

$$\begin{aligned} 4\oint_C \frac{dz}{2\pi i}\frac{1}{e^{\beta z}-1} &= -4\mathrm{Res}_{z=\omega_k} h(z)\frac{1}{e^{\beta z}-1} \\ &= -4\lim_{z\to\omega_k}(z-\omega_k)h(z)\frac{1}{e^{\beta z}-1} \\ &= \frac{2}{\omega_k}\frac{1}{e^{\beta\omega_k}-1} \end{aligned} \tag{3.29}$$

Thus, the frequency sum can be written as

$$T\sum_n h(i\omega_n) = \frac{1}{2\omega_k}\left[1 + 2\frac{1}{e^{\beta\omega_k}-1}\right]. \tag{3.30}$$

Inserting the expression for the Matsubara sum, the self-energy Σ is given by

$$\Sigma = \frac{\lambda_B}{2} \int \frac{d^3k}{(2\pi)^3} \left[\frac{1}{2\omega_k} + \frac{n_B(\omega_k)}{\omega_k} \right], \tag{3.31}$$

where $n_B(\omega_k) = \frac{1}{e^{\beta\omega_k}-1}$ is the distribution function for bosons. Eq. (3.31) has a term which is temperature-independent, corresponding to zero temperature, and a term which is explicitly temperature-dependent. The zero-temperature term is divergent when $|\vec{k}| \to \infty$. Sections 3.5-3.8 give a short introduction to renormalization, and how to get rid of this divergence.

3.3 Thermodynamic potential

As seen from Eq. (3.31) the first-order correction to the self-energy is given by

$$\begin{aligned} \Sigma &= \frac{\lambda_B}{2} \sum\!\!\!\!\!\!\int_k \frac{1}{\omega_n^2 + \omega_k^2} \\ &= \frac{\lambda_B}{4} \int \frac{d^3k}{(2\pi)^3} \frac{1}{\omega_k} + \frac{\lambda_B}{2} \int \frac{d^3k}{(2\pi)^3} \frac{1}{\omega_k} \frac{1}{e^{\beta\omega_k} - 1} \\ &\equiv \Sigma_0 + \Sigma_T \end{aligned} \tag{3.32}$$

By multiplying Eq. (3.32) by $2m_B$ and integrating over m_B, the temperature-independent term gives

$$\begin{aligned} \int dm_B \, 2m_B \Sigma_0 &= \frac{\lambda_B}{4} \int \frac{d^3k}{(2\pi)^3} \int \frac{dm_B \, 2m_B}{\sqrt{\vec{k}^2 + m_B^2}} \\ &= \frac{\lambda_B}{2} \int \frac{d^3k}{(2\pi)^3} \sqrt{\vec{k}^2 + m_B^2}, \end{aligned} \tag{3.33}$$

where a constant independent of mass and momentum has been omitted. The temperature-dependent term gives

$$\begin{aligned} \int dm_B \, 2m_B \Sigma_T &= \frac{\lambda_B}{2} \int \frac{d^3k}{(2\pi)^3} \int \frac{dm_B \, 2m_B}{\sqrt{\vec{k}^2 + m_B^2}} \frac{1}{e^{\beta\sqrt{\vec{k}^2+m_B^2}} - 1} \\ &= \frac{\lambda_B}{2} \int \frac{d^3k}{(2\pi)^3} \, 2T \int dx \frac{1}{e^x - 1} \end{aligned} \tag{3.34}$$

where in the last equality the substitution $x = \beta\sqrt{\vec{k}^2 + m_B^2}$ has been used. Using

$$\sum_{k=0}^{n} q^k = \frac{1-q^n}{1-q} \tag{3.35}$$

Eq. (3.34) can be written as

$$\begin{aligned}\int dm_B\, 2m_B\Sigma_T &= \frac{\lambda_B}{2}\int \frac{d^3k}{(2\pi)^3}\, 2T \int dx \sum_{n=0}^{\infty} e^{-(n+1)x} \\ &= \frac{\lambda_B}{2}\int \frac{d^3k}{(2\pi)^3}\, 2T \sum_{n=1}^{\infty} \frac{-1}{n}\left(e^{-\beta\sqrt{\vec{k}^2+m_B^2}}\right)^n \\ &= \frac{\lambda_B}{2}\int \frac{d^3k}{(2\pi)^3}\, 2T \sum_{n=1}^{\infty} \frac{-1}{n}\,(1-w)^n\,,\end{aligned} \tag{3.36}$$

where $w = 1-e^{-\beta\sqrt{\vec{k}^2+m_B^2}}$. A constant independent of mass and momentum is omitted. Expressing the sum in Eq. (3.36) using

$$\ln(x) = \sum_{n=1}^{\infty}(-1)^{n+1}\frac{(x-1)^n}{n} = \sum_{n=1}^{\infty}\frac{-1}{n}\,(1-x)^n \qquad 0 \le x \le 2, \tag{3.37}$$

the equation can be written as

$$\int dm_B\, 2m_B\Sigma_T = \lambda_B T \int \frac{d^3k}{(2\pi)^3}\ln\left(1-e^{-\frac{1}{T}\sqrt{\vec{k}^2+m_B^2}}\right). \tag{3.38}$$

Thus,

$$\int dm_B\, 2m_B\Sigma = \lambda_B \int \frac{d^3k}{(2\pi)^3}\left[\frac{1}{2}\omega_k + T\ln\left(1-e^{-\frac{\omega_k}{T}}\right)\right], \tag{3.39}$$

up to a mass- and momentum-independent constant. Inserting $\Sigma = \frac{\lambda_B}{2}\sum\!\!\!\!\!\!\int_k \frac{1}{\omega_n^2+\omega_k^2}$ on the left-hand side of Eq. (3.39) and performing the integration, the following is obtained

$$\frac{1}{2}\sum\!\!\!\!\!\!\int_k \ln\left[\omega_n^2+\omega_k^2\right] = \int \frac{d^3k}{(2\pi)^3}\left[\frac{1}{2}\omega_k + T\ln\left(1-e^{-\beta\omega_k}\right)\right]. \tag{3.40}$$

The right-hand side of Eq. (3.40) can be recognized as the sum of the zero-point vacuum energy and the grand canonical potential Φ of a massive ideal bose gas, divided by the volume.

The thermodynamic potential can be expressed as a power series of the coupling constant [12]:

$$\Phi = \Phi_0 + \Phi_1 + \Phi_2 + \ldots, \tag{3.41}$$

where Φ_0 is the thermodynamic potential for the free field given in Eq. (3.40), Φ_1 is the correction to first order in the coupling constant, and so on. As shown above, the corrections to the grand potential come from vacuum diagrams.

3.3.1 First-order correction

The first-order correction to the thermodynamic potential is from the double-bubble in Fig. (3.8). This bubble diagram yields the correction

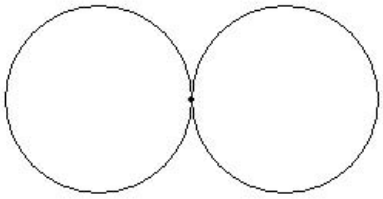

Figure 3.8: The first-order contribution to the thermodynamic potential.

$$\frac{\Phi_1}{V} = \frac{\lambda_B}{8}\left(\sum\!\!\!\!\!\!\int_k \frac{1}{\omega_n^2 + \omega_k^2}\right)^2 \tag{3.42}$$

Using the expression for the Matsubara sum found in section 3.2.1, Eq. (3.42) can be written as

$$\begin{aligned}\frac{\Phi_1}{V} &= \frac{\lambda_B}{8}\left(\int \frac{d^3k}{(2\pi)^3}\frac{1}{2\omega_k}\left[1 + 2n_B(\vec{k})\right]\right)^2 \\ &= \frac{\lambda_B}{8}\left(\int \frac{d^3k}{(2\pi)^3}\frac{1}{2\omega_k}\right)^2 + \frac{\lambda_B}{8}\left(\int \frac{d^3k}{(2\pi)^3}\frac{n_B(\vec{k})}{\omega_k}\right)^2 \\ &+ \frac{\lambda_B}{8}\left(\int \frac{d^3k}{(2\pi)^3}\frac{1}{\omega_k}\right)\left(\int \frac{d^3k}{(2\pi)^3}\frac{n_B(\vec{k})}{\omega_k}\right).\end{aligned} \tag{3.43}$$

The first term in Eq. (3.43) is temperature-independent and divergent when $|\vec{k}| \to \infty$, the second term is temperature-dependent and finite, and the third term is temperature-dependent and divergent when $|\vec{k}| \to \infty$. As mentioned above, sections 3.5-3.8 show how to get rid of the divergences.

3.4 The idea of renormalization

Higher-order diagrams without loops are called tree diagrams, and generally for weakly interacting theories the tree level diagrams give accurate results. For stronger interactions, or for very precise results, higher-order diagrams containing closed loops must be included. However, most loop diagrams are divergent [3]. The idea of renormalization appeared due to the understanding of the limited nature of the idealization of a free particle in quantum theory [13]. Particles interact with vacuum. The result of such interactions are the change of charge and mass of the particles. The observed charges and masses are the sum of these interactions. Renormalization was introduced to eliminate the divergences of higher-order diagrams. It is based on a simple idea. Consider an electron. The parameters m_B and e_B representing the mass and charge of the non-interacting, bare electron has no physical meaning. Observable magnitudes, m and e, characterizing electrons are the result of interactions between the electrons and the vacuum. The observable magnitudes are thought of as the sums $m = m_B + \Delta m$ and $e = e_B + \Delta e$ [13], where Δm and Δe absorb the infinities occuring in calculations involving m_B and e_B. Infinities may be systematically eliminated by relating bare quantities to physical quantities [3].

3.5 Regularization

For dimensions close to $d = 4$, many higher-order Feynman integrals diverge when the momentum goes to infinity, or for very short wavelengths [14]. These divergences are called ultraviolet (UV) divergences and are the only divergences for massive fields. For dimension d, integrals of the two-point function as shown in Eq. (2.26) diverge for large momenta when $2l < d$. This is a UV divergence.

For massless fields, another type of divergences occur at small momenta or long wavelengths - infrared (IR) divergences. Considering Eq. (2.41) these divergences can easily be seen. For the zeroth Matsubara mode for bosons, $\omega_n = 0$. If the mass is also zero, integrals of the two-point function are divergent when the momentum goes to zero. This is an IR divergence.

The divergences can be contolled by some regularization procedure. Regularization is essentially a mathematical trick to make divergent integrals well-defined. There are several regularization procedures [14]. Only two of them are mentioned here, momentum cutoff and dimensional regularization. The latter will be used throughout this thesis.

3.5.1 Momentum cutoff regularization

In this regularization procedure, a cutoff Λ represents a particular energy scale. The integral

$$I = \int_0^\infty dk\, F(k), \tag{3.44}$$

which is UV divergent, is written as

$$I_\Lambda = \int_0^\Lambda dk\, F(k), \tag{3.45}$$

which is finite. All momenta are limited to $|\vec{k}| < \Lambda$, and no UV divergences occur in I_Λ. The integral in Eq. (3.45) can in general be calculated as [14]

$$I_\Lambda = f(\Lambda) + g\left(\frac{1}{\Lambda}\right) + C, \tag{3.46}$$

which is divergent when $\Lambda \to \infty$. This divergence reflects the divergence of the integral in Eq. (3.44). The regularization procedure makes it possible to carry out the integral and writing an expression depending on the cut-off Λ. However, in the limit $\Lambda \to \infty$,the expression is still divergent, and renormalization is needed to get rid of the divergences.

An undesirable feature of the momentum cutoff procedure is that the translation invariance is destroyed. Problems may also arise if the symmetries of a theory correspond to local transformations, like in gauge theories [14].

3.5.2 Dimensional regularization

From Eq. (2.26) it is seen that the integral converges for small enough d. Computing the Feynman integral in terms of the dimension d, and assuming it being convergent for any value of d, the integration should be well-defined when $d = 4 - \epsilon$ for infinitesimal ϵ [3]. The integral

$$I = \int d^4k\, F(k) \to I_d = \int d^dk\, F(k), \tag{3.47}$$

and can be written as

$$I_d = f(\mathcal{O}(\epsilon)) + g\left(\frac{1}{\epsilon}\right) + C. \tag{3.48}$$

Analytically continuing back to $d = 4$, i.e. $\epsilon \to 0$, the original logarithmic divergences occur as poles in ϵ, and power divergences disappear. This will be shown in the end of this section.

To take a closer look at dimensional regularization, consider the temperature-independent term in the first-order correction to the self-energy

$$\Sigma_0 = \frac{\lambda_B}{2}\int \frac{d^3k}{(2\pi)^3}\frac{1}{2\omega_k}. \tag{3.49}$$

To find an expression of the integral in Eq. (3.49), dimensional regularization can be used. The integral in Eq. (3.49) is written as

$$\begin{aligned} I &= \mu^{4-d}\int \frac{d^{d-1}k}{(2\pi)^{d-1}}\frac{1}{2\sqrt{k^2+m_B^2}} \\ &= \mu^{4-d}\frac{\Omega_{d-1}}{2(2\pi)^{d-1}}\int_0^\infty dk\,\frac{k^{d-2}}{\sqrt{k^2+m_B^2}}, \end{aligned} \tag{3.50}$$

where $k^2 = \vec{k}^2$. μ is an arbitrary mass parameter introduced to make the final expression have correct dimensions [9]. If d is small enough, the integral converges. The d-dimensional angular integral can be found in the following way [9]

$$\begin{aligned} \int d^dx\, e^{-x^2} &= \Omega_d\int_0^\infty dx\, x^{d-1}e^{-x^2} \\ &= \Omega_d\frac{1}{2}\int_0^\infty du\, u^{\frac{u}{2}-1}e^{-u} = \frac{1}{2}\Omega_d\Gamma\left(\frac{d}{2}\right). \end{aligned} \tag{3.51}$$

In the last line we have made the substitution $x^2 = u$. By writing

$$\begin{aligned} \int d^dx\, e^{-x^2} &= \int_{-\infty}^\infty dx_1\int_{-\infty}^\infty dx_2\cdots\int_{-\infty}^\infty dx_d\, e^{-(x_1^2+x_2^2\cdots+x_d^2)} \\ &= \left(\int_{-\infty}^\infty dx\, e^{-x^2}\right)^d = (\sqrt{\pi})^d, \end{aligned} \tag{3.52}$$

the d-dimensional angular integral reads

$$\Omega_d = \frac{2\pi^{\frac{d}{2}}}{\Gamma(\frac{d}{2})}. \tag{3.53}$$

Inserting this result into Eq. (3.50), we obtain

$$\begin{aligned} I &= \frac{\mu^\epsilon}{2(2\pi)^{3-\epsilon}}\pi^{\frac{3-\epsilon}{2}}(m_B^2)^{1-\frac{\epsilon}{2}}\frac{\Gamma\left(\frac{1}{2}-\frac{3-\epsilon}{2}\right)}{\Gamma\left(\frac{1}{2}\right)} \\ &= \frac{m_B^2}{16\pi^2}2^\epsilon\mu^\epsilon\pi^{\frac{\epsilon}{2}}(m_B^2)^{-\frac{\epsilon}{2}}\Gamma\left(-1+\frac{\epsilon}{2}\right), \end{aligned} \tag{3.54}$$

where we have used $\epsilon = 4 - d$. Using $x^\epsilon = 1 + \epsilon \ln(x) + \mathcal{O}(\epsilon^2)$ and expanding the gamma-function around $\epsilon = 0$, the integral reads

$$I = \frac{m_B^2}{(4\pi)^2}\left[-\frac{2}{\epsilon} - 1 + \gamma_E + \ln\left(\frac{m_B^2}{4\pi\mu^2}\right)\right] \tag{3.55}$$

in the limit $\epsilon \to 0$. Thus, the divergent part of the first-order correction to the self-energy reads

$$\Sigma_0 = \frac{\lambda_B}{2}\frac{m_B^2}{(4\pi)^2}\left[-\frac{2}{\epsilon} - 1 + \gamma_E + \ln\left(\frac{m_B^2}{4\pi\mu^2}\right)\right] \tag{3.56}$$

in the limit $\epsilon \to 0$. The integral diverges and the $\frac{1}{\epsilon}$-term must be canceled by renormalization.

The integral in Eq. (3.49) goes as

$$I \sim \int_0^\Lambda dk \frac{k^2}{\sqrt{k^2 + m_B^2}}, \tag{3.57}$$

where Λ is a momentum cutoff. Expanding the integrand around $m_B^2 = 0$, the integration will lead to terms $\sim \Lambda^2$ and $\sim m_B^2 \ln \Lambda$ which are divergent in the $\Lambda \to \infty$ limit. Compared to Eq. (3.55), only the logarithmic divergence occurs after using dimensional regularization, and the power divergence has disappeared, as claimed above.

Considering the temperature-independent term of the thermodynamic potential given in Eq. (3.40), the following is obtained by using dimensional regularization

$$\begin{aligned}
\int \frac{d^3k}{(2\pi)^3}\frac{1}{2}\omega_k &\to \mu^{4-d}\int \frac{d^{d-1}k}{(2\pi)^{d-1}}\frac{1}{2}\sqrt{k^2 + m_B^2} \\
&= \frac{\mu^\epsilon}{2(2\pi)^{3-\epsilon}}\pi^{\frac{3-\epsilon}{2}}(m_B^2)^{2-\frac{\epsilon}{2}}\frac{\Gamma\left(-\frac{1}{2} - \frac{3-\epsilon}{2}\right)}{\Gamma\left(-\frac{1}{2}\right)} \\
&= -\frac{m_B^4}{32\pi^2}2^\epsilon\mu^\epsilon\pi^{\frac{\epsilon}{2}}(m_B^2)^{-\frac{\epsilon}{2}}\Gamma\left(-2 + \frac{\epsilon}{2}\right) \\
&= \frac{m_B^4}{64\pi^2}\left[-\frac{2}{\epsilon} - \frac{3}{2} + \gamma_E + \ln\left(\frac{m_B^2}{4\pi\mu^2}\right)\right]
\end{aligned} \tag{3.58}$$

in the limit $\epsilon \to 0$.

3.6 Counting of UV divergences

To localize the UV divergences, naive counting of momentum power is used. Roughly speaking, a diagram diverges if the powers of momentum in the

numerator is larger than or equal to the powers of the momentum in the denominator. The superficial degree of divergence is defined as follows [9]

$$D = \text{ power of } k \text{ in numerator } - \text{ power of } k \text{ in denominator.} \tag{3.59}$$

Naively, it would be expected that a diagram diverges as $\sim \Lambda^D$ if $D > 0$ and as $\sim \ln\Lambda$ if $D = 0$. If $D < 0$ no divergence occurs. However, these naive expectations are often wrong [9].

In a scalar theory with a ϕ^n interaction term, the Euclidean Lagrangian in d dimensions reads

$$\mathcal{L} = \frac{1}{2}\left(\partial_\mu \phi_B\right)^2 + \frac{1}{2} m_B^2 \phi_B^2 + \frac{\lambda_B}{n!}\phi_B^n. \tag{3.60}$$

From dimensional analysis, the action $S = \int d^d x\, \mathcal{L}$ is dimensionless, since $\hbar = 1$. In terms of mass dimension, S has dimension $[S] = 0$. The mass dimension of $d^d x$ is $\left[d^d x\right] = -d$, which leads to the mass dimension $[\mathcal{L}] = d$ of the Lagrangian. From Eq. (3.60) it can be found that ϕ_B has mass dimension $[\phi_B] = \frac{d-2}{2}$, and λ_B has mass dimension $[\lambda_B] = d - n\frac{d-2}{2}$. Consider a diagram with N external lines, which could originate from the interaction term $\alpha\phi^N$. From the mass dimension for λ_B found above, the parameter α has mass dimension $[\alpha] = d - N\frac{d-2}{2}$. If a diagram in the $\lambda\phi^n$-theory has V vertices, its divergent part is proportional to $\lambda_B^V \Lambda^D$ [9], where Λ is some cutoff with mass dimension $[\Lambda] = 1$ and D is the superficial degree of divergence. Thus, the following is obtained

$$d - N\frac{d-2}{2} = V\left[d - n\frac{d-2}{2}\right] + D. \tag{3.61}$$

The class of theories in which the divergences can be systematically eliminated from observable quantities are called renormalizable [3]. The degree of renormalization can be characterized as follows [9]

- If the coupling constant has positive mass dimension, the theory is super-renormalizable.
- If the coupling constant is dimensionless, the theory is renormalizable.
- If the coupling constant has negative mass dimension, the theory is non-renormalizable.

In super-renormalizable theories only a finite number of Feynman diagrams superficially diverge. The same is true in renormalizable theories, but the divergences occur at all orders in perturbation theory. All amplitudes are divergent at a sufficiently high order in perturbation theory in non-renormalizable theories [9].

For $d = 4$ and $n = 4$, the superficial degree of divergence is

$$D = 4 - N, \tag{3.62}$$

where N is the number of external legs in a diagram. As mentioned above, divergences occur when $D \geq 0$. In order for this to be true $N \leq 4$. For the $\lambda\phi^4$-theory, the diagrams which are divergent are shown in Fig. 3.9. In

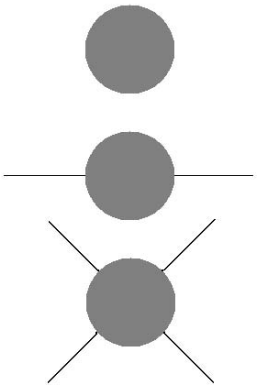

Figure 3.9: Divergent diagrams in $\lambda\phi^4$-theory.

the $\lambda\phi^4$-theory in four dimensions the coupling constant is dimensionless. Thus, this theory is renormalizable. The amplitudes in Fig. 3.9 contain three infinite constants [9], which could be absorbed in the bare mass, bare coupling and bare field. In the next section, the Lagrangian is reformulated in order for the bare quantities to not appear explicitly in the Lagrangian.

3.7 Counterterms

By adding so-called counterterms to the Lagrangian, it can be written as [14]

$$\begin{aligned}\mathcal{L} &= \frac{1}{2}\left(\partial_\mu\phi\right)^2 + \frac{1}{2}m^2\phi^2 + \frac{\lambda}{4!}\phi^4 \\ &+ c_\phi\frac{1}{2}\left(\partial_\mu\phi\right)^2 + c_m\frac{1}{2}m^2\phi^2 + c_\lambda\frac{\lambda}{4!}\phi^4 \\ &= \frac{1}{2}(1+c_\phi)\left(\partial_\mu\phi\right)^2 + \frac{1}{2}(1+c_m)m^2\phi^2 \\ &+ \frac{1}{4!}(1+c_\lambda)\lambda\phi^4\end{aligned} \tag{3.63}$$

in Euclidean space. In Eq. (3.63) ϕ, m and λ represents the renormalized quantities. The renormalized parameters are finite and are defined by a set of renormalization conditions [14]. Defining $Z_\phi = 1 + c_\phi$, $Z_m = 1 + c_m$ and $Z_\lambda = 1 + c_\lambda$ the Lagrangian reads

$$\mathcal{L} = \frac{1}{2} Z_\phi \left(\partial_\mu \phi\right)^2 + \frac{1}{2} Z_m m^2 \phi^2 + \frac{1}{4!} Z_\lambda \lambda \phi^4. \tag{3.64}$$

The Z's convert the bare parameters into the renormalized parameters. To obtain the initial bare Euclidean Lagrangian in Eq. (3.2) the following is defined

$$\phi_B = Z_\phi^{\frac{1}{2}} \phi, \tag{3.65}$$

$$m_B^2 = \frac{Z_m}{Z_\phi} m^2 \tag{3.66}$$

and

$$\lambda_B = \frac{Z_\lambda}{Z_\phi^2} \lambda. \tag{3.67}$$

After using dimensional regularization to write the integral in Eq. (3.49) as the expression given in Eq. (3.55), the integral diverge in a certain way when $\epsilon \to 0$. If the number of loops N increases, the Feynman integrals contain singularities of the type $\frac{1}{\epsilon^i}$, where $i = 1, \ldots, N$ [14]. In this regularization procedure, it should be possible to write the Z's in the form [14]

$$Z = 1 + \sum_{k=1}^{N} \lambda^k \sum_{i=0}^{k} \frac{c_i^k}{\epsilon^i}. \tag{3.68}$$

The coefficients c_i^k are chosen to cancel the divergences $\frac{1}{\epsilon^i}$, order by order in λ.

The counterterms contributes to the diagrammatic expansion. The contributions are shown in Fig. 3.10 [9]. The first contribution is the mass and field counterterms c_m and c_ϕ. The second contribution is the coupling constant counterterm c_λ. The counterterms are introduced to absorb the infinite shift between the bare parameters and the physical parameters, and are chosen so that all divergences are subtracted.

3.8 Minimal subtraction

After employing dimensional regularization, the Feynman integral can be written as an expression containing poles in ϵ. The expression can be renormalized by subtracting the terms containg ϵ-poles. The minimal subtraction (MS) scheme was invented by G. t'Hooft to renormalize nonabelian gauge theories of weak and electromagnetic interactions [15]. In the MS scheme, the counterterms acquire the form in Eq. (3.68) [14]. The counterterms

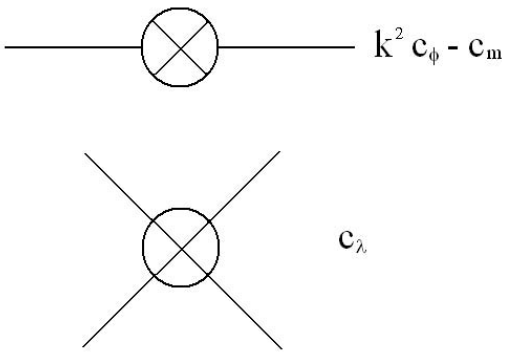

Figure 3.10: Diagrammatic contributions from the counterterms.

are independent of the mass m (except for an overall factor m^2 in the mass counterterm) and the renormalization parameter μ. In the MS scheme, the following is obtained

$$\begin{aligned}&\frac{m_B^2}{(4\pi)^2}\left[-\frac{2}{\epsilon}-1+\gamma_E+\ln\left(\frac{m_B^2}{4\pi\mu^2}\right)\right]\rightarrow\\&\frac{m^2}{(4\pi)^2}\left[-1+\gamma_E+\ln\left(\frac{m^2}{4\pi\mu^2}\right)\right].\end{aligned}\tag{3.69}$$

The first term in Eq. (3.69) is obtained from the use of dimensional regularization of the bare Lagrangian. The last term is obtained from the use of dimensional regularization of the Lagrangian with counterterms in the MS scheme. To see how this is obtained, consider the first-order correction to the self-energy. From the bare Lagrangian this correction reads

$$\Sigma=\frac{\lambda_B}{2}\int\frac{d^3k}{(2\pi)^3}\left[\frac{1}{2\omega_k}+\frac{n_B(\omega_k)}{\omega_k}\right],\tag{3.70}$$

where $\omega_k^2=\vec{k}^2+m_B^2$. λ_B and m_B are the bare coupling constant and bare mass, respectively. The first term is UV divergent. Using dimensional regularization, we start with writing Eq. (3.70) as

$$\begin{aligned}&\frac{\lambda_B}{2}\int\frac{d^3k}{(2\pi)^2}\left[\frac{1}{2\omega_k}+\frac{n_B(\omega_k)}{\omega_k}\right]\\&\rightarrow\frac{\lambda_B}{2}\mu^{4-d}\int\frac{d^{d-1}k}{(2\pi)^{d-1}}\left[\frac{1}{2\omega_k}+\frac{n_B(\omega_k)}{\omega_k}\right]\\&=I_1+I_2.\end{aligned}\tag{3.71}$$

The first integral is the zero-temperature integral calculated in section 3.5.2, and gives

$$I_1 = \frac{\lambda_B}{2}\frac{m_B^2}{(4\pi)^2}\left[-\frac{2}{\epsilon} - 1 + \gamma_E + \ln\left(\frac{m_B^2}{4\pi\mu^2}\right)\right], \tag{3.72}$$

where $\epsilon = 4 - d$. The second integral in Eq. (3.71) is

$$I_2 = \frac{\lambda_B}{2}\mu^\epsilon \int \frac{d^{3-\epsilon}k}{(2\pi)^{3-\epsilon}}\frac{n_B(\omega_k)}{\omega_k}. \tag{3.73}$$

The temperature-dependent term in Eq. (3.70) is UV finite, and I_2 contains no poles in ϵ. However, evaluating I_2 would give $\mathcal{O}(\epsilon)$-terms. In cases where the temperature-independent term is multiplied with the temperature-dependent term, such as in the double-bubble contribution to the thermodynamic potential, the $\mathcal{O}(\epsilon)$-terms in the temperature-dependent term could cancel the ϵ-poles in the temperature-dependent term. We will not encounter calculations of such terms in the rest of this thesis, so in the following we let $\epsilon \to 0$ and write

$$I_2 = \frac{\lambda_B}{2}\int \frac{d^3k}{(2\pi)^3}\frac{n_B(\omega_k)}{\omega_k}. \tag{3.74}$$

In general, one should be careful when doing this.

Eq. (3.70) is thus written as

$$\begin{aligned}\Sigma = &\frac{\lambda_B}{2}\frac{m_B^2}{(4\pi)^2}\left[-\frac{2}{\epsilon} - 1 + \gamma_E + \ln\left(\frac{m_B^2}{4\pi\mu^2}\right)\right] \\ &+ \frac{\lambda_B}{2}\int \frac{d^3k}{(2\pi)^3}\frac{n_B(\omega_k)}{\omega_k}.\end{aligned} \tag{3.75}$$

Starting from the Lagrangian with counterterms, the counterterm contribution to first order in λ is the first contribution in Fig. 3.10 [14]. This leads to

$$\begin{aligned}\Sigma = &\frac{\lambda}{2}\frac{m^2}{(4\pi)^2}\left[-\frac{2}{\epsilon} - 1 + \gamma_E + \ln\left(\frac{m^2}{4\pi\mu^2}\right)\right] \\ &+ \frac{\lambda}{2}\int \frac{d^3k}{(2\pi)^3}\frac{n_B(\omega_k)}{\omega_k} + \text{counterterms},\end{aligned} \tag{3.76}$$

where $\omega_k^2 = \vec{k}^2 + m^2$. λ and m are the renormalized parameters. There is no term proportional to k^2 in Eq. (3.70), so $c_\phi = 0$. c_m is fixed to cancel the ϵ-pole, leading to a mass counterterm equal to $\frac{\lambda}{2}\frac{m^2}{(4\pi)^2}\frac{2}{\epsilon}$. This gives

$$\begin{aligned}\Sigma = &\frac{\lambda}{2}\frac{m^2}{(4\pi)^2}\left[-1+\gamma_E+\ln\left(\frac{m^2}{4\pi\mu^2}\right)\right]\\ &+\frac{\lambda}{2}\int\frac{d^3k}{(2\pi)^3}\frac{n_B(\omega_k)}{\omega_k}.\end{aligned} \tag{3.77}$$

3.9 First order correction in the massless case

In the massless case, the temperature-independent term of the self-energy is zero by use of dimensional regularization. Considering the temperature-dependent term and inserting $m = 0$, the self-energy reads

$$\Sigma = \frac{\lambda}{(2\pi)^2}\int_0^\infty \frac{dk\ k}{e^{\beta k}-1}, \tag{3.78}$$

where $k = |\vec{k}|$. By use of the substitution $u = \beta k$, Eq. (3.78) reads

$$\Sigma = \frac{\lambda}{(2\pi)^2}T^2\int_0^\infty \frac{du\ u}{e^u}\frac{1}{1-e^{-u}}. \tag{3.79}$$

From Eq. (3.35) the integral in Eq. (3.79) can be expressed as

$$\begin{aligned}\Sigma &= \frac{\lambda}{(2\pi)^2}T^2\sum_{n=0}^\infty\int_0^\infty du\ u\ e^{-(1+n)u}\\ &= \frac{\lambda}{(2\pi)^2}T^2\sum_{n=1}^\infty\frac{1}{n^2}.\end{aligned} \tag{3.80}$$

The sum in Eq. (3.80) is the Riemann-Zeta function of two, and is given by

$$\sum_{n=1}^\infty\frac{1}{n^2} = \frac{\pi^2}{6}. \tag{3.81}$$

Thus, the first-order correction to the self-energy in the massless case is

$$\Sigma = \frac{\lambda T^2}{24}. \tag{3.82}$$

Using dimensional regularization, the temperature-independent term of the thermodynamic potential given in Eq. (3.40) is zero in the massless case. The pressure to zeroth order in λ in the massless case thus reads

$$\begin{aligned}P = -\frac{\Phi}{V} &= -T\frac{2}{(2\pi)^2}\int_0^\infty dk\ k^2\ln\left[1-e^{-\beta k}\right]\\ &= T^4\frac{4}{(2\pi)^2}\sum_{n=1}^\infty\frac{1}{n^4} = \frac{\pi^2T^4}{90},\end{aligned} \tag{3.83}$$

where the sum is recognized as the Riemann-Zeta function of four, which equals $\frac{\pi^4}{90}$. Eq. (3.83) is the pressure of an non-interacting massless bose gas.

In Eq. (3.43), a term where the temperature-independent contribution is multiplied with the temperature-dependent contribution occurs. As mentioned above, in such terms the temperature-dependent integral should not simply be written as in Eq. (3.74). The integral should be evaluated before taking the limit $\epsilon \to 0$. However, since the temperature-independent integral is zero in the massless case when using dimensional regularization, the first and the third term in Eq. (3.43) vanish in the massless case. Inserting $m = 0$ into the second term of Eq. (3.43) gives

$$\frac{\Phi_1}{V} = \frac{\lambda}{8}\left[\frac{2}{(2\pi)^2}\int_0^\infty dk\, k \frac{1}{e^{\beta k}-1}\right]^2. \tag{3.84}$$

By making the substitution $u = \beta k$ as above, Eq. (3.84) reads

$$\begin{aligned}
\frac{\Phi_1}{V} &= \frac{\lambda}{8}\frac{4}{(2\pi)^4}T^4\left[\int_0^\infty dx\, x\frac{e^{-x}}{1-e^{-x}}\right]^2 \\
&= \frac{\lambda}{8}\frac{4}{(2\pi)^4}T^4\left[\int_0^\infty dx\, x\sum_{n=0}^\infty e^{-x(1+n)}\right]^2 \\
&= \frac{\lambda}{8}\frac{4}{(2\pi)^4}T^4\left[\sum_{n=1}^\infty \frac{1}{n^2}\right]^2 \\
&= \frac{\lambda T^4}{1152}.
\end{aligned} \tag{3.85}$$

The pressure in the massless case to first order in λ is given by

$$P = -\frac{\Phi}{V} = T^4\left(\frac{\pi^2}{90} - \frac{\lambda}{1152}\right). \tag{3.86}$$

3.10 Higher-order corrections and breakdown of perturbation theory

In ordinary perturbation theory the next contribution to the self-energy is expected to go as λ^2, from the second and third diagrams in Fig. 3.5. This is not correct, as will be shown in the following discussion.

When $m = 0$, the second diagram in Fig. 3.5 is infrared divergent for the $n = 0$ mode, as it goes as $\sim \int_0^\infty \frac{dk}{k^2}$, where $k = |\vec{k}|$. It is the first diagram of an infinite series of daisy diagrams [12], each of which is increasingly infrared divergent. The daisy diagrams are shown in Fig. 3.11

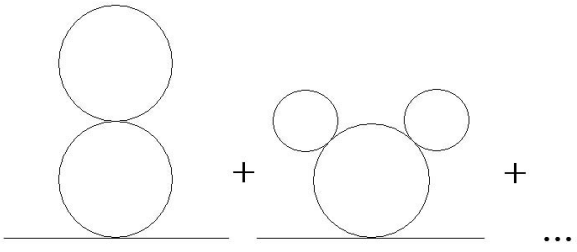

Figure 3.11: The first two infrared divergent diagrams in the infinite series of daisy diagrams in $\lambda\phi^4$-theory.

The one-loop correction to the self-energy is a thermal mass generated by the interactions with the thermal bath. In the massless case it is given by $\frac{\lambda T^2}{24}$. The problem of infrared divergences arises because the bosons acquire thermal mass, and the free, massless propagator $\frac{1}{\omega_n^2+\vec{k}^2}$ should be replaced by the effective propagator $\frac{1}{\omega_n^2+\vec{k}^2+M^2}$ where M^2 is a thermal mass. The thermal fluctuations change the propagator into that of a massive particle.

As will be seen in the following, the effective propagator resums the daisy diagrams. The effective propagator would correspond to a free Lagrangian given by

$$\mathcal{L}_{free} = \frac{1}{2}\left(\partial_\mu\phi\right)^2 + \frac{1}{2}M^2\phi^2. \tag{3.87}$$

The subscript B is omitted for the field, since $Z_\phi = 1$ in first-order corrections which are considered here. In the massless $\lambda\phi^4$-theory, the Lagrangian reads

$$\mathcal{L} = \frac{1}{2}\left(\partial_\mu\phi\right)^2 + \frac{\lambda_B}{4!}\phi^4. \tag{3.88}$$

To obtain the free Lagrangian in Eq. (3.87), we add and subtract a term $\frac{1}{2}M^2\phi^2$, giving an effective Lagrangian which is written as

$$\begin{aligned}\mathcal{L}_{eff} &= \left(\partial_\mu\phi\right)\left(\partial^\mu\phi\right) + \frac{1}{2}M^2\phi^2 - \frac{1}{2}M^2\phi^2 + \frac{\lambda_B}{4!}\phi^4 \\ &= \mathcal{L}_{free} + \mathcal{L}_{int}.\end{aligned} \tag{3.89}$$

$\mathcal{L}_{free}$ is given by Eq. (3.87) and

$$\mathcal{L}_{int} = -\frac{1}{2}M^2\phi^2 + \frac{\lambda_B}{4!}\phi^4. \tag{3.90}$$

The term $-\frac{1}{2}M^2\phi^2$ is treated as an interaction term. To first order, the contributions to the effective potential are shown in Fig. 3.12. The effective potential reads

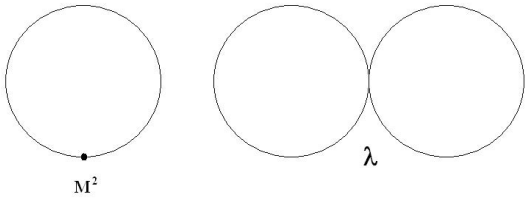

Figure 3.12: First-order contributions to the effective potential.

$$V_{eff} = \frac{1}{2}\sum\!\!\!\!\!\!\int_k \ln\left(\omega_n^2 + \omega_{kM}^2\right) - \frac{M^2}{2}\sum\!\!\!\!\!\!\int_k \frac{1}{\omega_n^2 + \omega_{kM}^2} + \frac{\lambda_B}{8}\left(\sum\!\!\!\!\!\!\int_k \frac{1}{\omega_n^2 + \omega_{kM}^2}\right)^2, \tag{3.91}$$

where $\omega_{kM}^2 = \vec{k}^2 + M^2$. The effective potential is minimized with respect to M^2. The following is obtained

$$\begin{aligned}\frac{V_{eff}}{\partial M^2} = &\frac{1}{2}\sum\!\!\!\!\!\!\int_k \frac{1}{\omega_n^2 + \omega_{kM}^2} \\ &- \frac{1}{2}\sum\!\!\!\!\!\!\int_k \frac{1}{\omega_n^2 + \omega_{kM}^2} - \frac{M^2}{2}\sum\!\!\!\!\!\!\int_k \frac{-1}{\left(\omega_n^2 + \omega_{kM}^2\right)^2} \\ &+ \frac{\lambda_B}{4}\sum\!\!\!\!\!\!\int_k \frac{1}{\omega_n^2 + \omega_{kM}^2}\sum\!\!\!\!\!\!\int_k \frac{-1}{\left(\omega_n^2 + \omega_{kM}^2\right)^2} = 0,\end{aligned} \tag{3.92}$$

which gives

$$M^2 = \frac{\lambda_B}{2}\sum\!\!\!\!\!\!\int_k \frac{1}{\omega_n^2 + \omega_{kM}^2} = \frac{\lambda_B}{2}\sum\!\!\!\!\!\!\int_k \frac{1}{\omega_n^2 + \vec{k}^2 + M^2}. \tag{3.93}$$

Expanding the right-hand side of Eq. (3.93) around $M^2 = 0$, we obtain

$$\begin{aligned}M^2 = &\frac{\lambda_B}{2}\sum\!\!\!\!\!\!\int_k \frac{1}{\omega_n^2 + \vec{k}^2} - M^2\frac{\lambda_B}{2}\sum\!\!\!\!\!\!\int_k \frac{1}{\left(\omega_n^2 + \vec{k}^2\right)^2} \\ &+ M^4\frac{\lambda_B}{2}\sum\!\!\!\!\!\!\int_k \frac{1}{\left(\omega_n^2 + \vec{k}^2\right)^3} - \ldots.\end{aligned} \tag{3.94}$$

Eq. (3.94) shows that the thermal mass which the bosons acquire, leads to a resummation of daisy diagrams with a massless propagator. Except for the

first diagram which is the tadpole, the diagrams are infrared divergent, but the sum of the diagrams is infrared finite.

Eq. (3.93) can be written as

$$M^2 = \frac{\lambda_B}{2}\int \frac{d^3k}{(2\pi)^3}\left(\frac{1}{2\omega_{kM}} - \frac{n_B(\omega_{kM})}{\omega_{kM}}\right). \tag{3.95}$$

The first term is UV divergent. Using dimensional regularization, Eq. (3.95) can be written as

$$\begin{aligned} M^2 = &\frac{\lambda_B}{2}\frac{M^2}{(4\pi)^2}\left[-\frac{2}{\epsilon} - 1 + \gamma_E + \ln\left(\frac{M^2}{4\pi\mu^2}\right)\right] \\ &+ \frac{\lambda_B}{2}\int \frac{d^3k}{(2\pi)^3}\frac{n_B(\omega_k)}{\omega_k}. \end{aligned} \tag{3.96}$$

In the limit $\epsilon \to 0$, the expression is divergent, and the term $\frac{1}{\epsilon}$ should be removed by renormalization.

How will the MS scheme work for the resummation? Compared to the cases above, the divergent term is now $-\frac{\lambda_B M^2}{16\pi^2\epsilon}$, where M^2 is temperature dependent. This requires a temperature-dependent mass counterterm. In general, resummation and renormalization can be in conflict. Resummation rearranges the perturbation series and reorganizes the diagrams by their IR relevance. The IR relevance is not necessarily the same as the UV relevance, and the counterterms may be separated from the diagrams in the resummation [16]. The UV divergences are not removed, leading to a UV inconsistent theory. For a UV consistent theory, it is also necessary to resum the counterterm diagrams.

Eq. (3.96) can actually be renormalized using temperature-independent counterterms. This is done by defining the renormalized coupling constant as

$$\frac{1}{\lambda} = \frac{1}{\lambda_B} + \frac{1}{16\pi^2\epsilon}. \tag{3.97}$$

The above definition of the renormalized coupling constant is discussed for the more general case in section 5.1. Using Eq. (3.97), the renormalized expression for M^2 reads

$$\begin{aligned} M^2 = &\frac{\lambda}{2}\frac{M^2}{(4\pi)^2}\left[-1 + \gamma_E + \ln\left(\frac{M^2}{4\pi\mu^2}\right)\right] \\ &+ \frac{\lambda}{2}\int \frac{d^3k}{(2\pi)^3}\frac{n_B(\omega_{kM})}{\omega_{kM}}, \end{aligned} \tag{3.98}$$

By doing the coupling constant renormalization in Eq. (3.97), the mass counterterm in this case is zero. Thus, Eq. (3.96) has been renormalized using counterterms which are independent of temperature.

Consider the integral in Eq. (3.98). It can be written as

$$M_T^2 = \frac{\lambda}{4\pi^2} M^2 \int_1^\infty du\, \sqrt{u^2-1} \frac{1}{e^{\beta M u} - 1} \tag{3.99}$$

by doing the substitution $u = \sqrt{\frac{\vec{k}^2}{M^2} + 1}$. Using [1]

$$\int_1^\infty du\, \sqrt{u^2-1} \frac{1}{e^{au}-1} = \frac{2\pi^2}{a^2}\left[\frac{1}{12} - \frac{a}{4\pi} + \mathcal{O}(a^2 \ln a)\right], \tag{3.100}$$

M_T^2 can be written as

$$M_T^2 = \frac{\lambda}{2} T^2 \left[\frac{1}{12} - \frac{1}{4\pi}\frac{M}{T} + \ldots\right]. \tag{3.101}$$

The leading order term goes as $\sim \lambda T^2$. Next to leading order goes as $\sim \lambda^{3/2} T^2$, not $\sim \lambda^2 T^2$ as would be expected from naive perturbation theory. This reflects the breakdown of perturbation theory due to IR divergences.

Eq. (3.98) can be solved numerically. Dividing Eq. (3.98) by T^2, we obtain the following equation for $\widetilde{M}^2 = \frac{M^2}{T^2}$

$$\begin{aligned} \widetilde{M}^2 = {} & \frac{\lambda}{2} \frac{\widetilde{M}^2}{(4\pi)^2}\left[-1 + \gamma_E + \ln\left(\widetilde{M}^2 \frac{T^2}{4\pi\mu^2}\right)\right] \\ & + \frac{\lambda}{2}\frac{1}{2\pi^2}\int_0^\infty dx \frac{x^2}{\sqrt{x^2+\widetilde{M}^2}} \frac{1}{e^{\sqrt{x^2+\widetilde{M}^2}} - 1}, \end{aligned} \tag{3.102}$$

where we have used the substitution $x = \frac{k}{T}$. $\widetilde{M}^2$ as a function of λ is shown in Fig. 3.13. Normalizing M to its weak-coupling value $\frac{\lambda T^2}{24}$ the following is obtained

$$\begin{aligned} \overline{M}^2 = {} & \frac{\lambda}{2} \frac{\overline{M}^2}{(4\pi)^2}\left[-1 + \gamma_E + \ln\left(\frac{\lambda \overline{M}^2}{24} \frac{T^2}{4\pi\mu^2}\right)\right] \\ & + \frac{6}{\pi^2}\int_0^\infty dx \frac{x^2}{\sqrt{x^2 + \frac{\lambda\overline{M}^2}{24}}} \frac{1}{e^{\sqrt{x^2+\frac{\lambda\overline{M}^2}{24}}} - 1}, \end{aligned} \tag{3.103}$$

where $\overline{M}^2 = \frac{M^2}{\lambda T^2/24}$. Fig. 3.14 shows $\overline{M}^2$ as a function of λ. At some given temperature, $\frac{T^2}{4\pi\mu^2}$ is just a constant. Since we are interested in the qualitative behavior of $\widetilde{M}$ and $\overline{M}$ as a function of λ, $\frac{T^2}{4\pi\mu^2}$ is given the value $\frac{T^2}{4\pi\mu^2} = 1$ here.

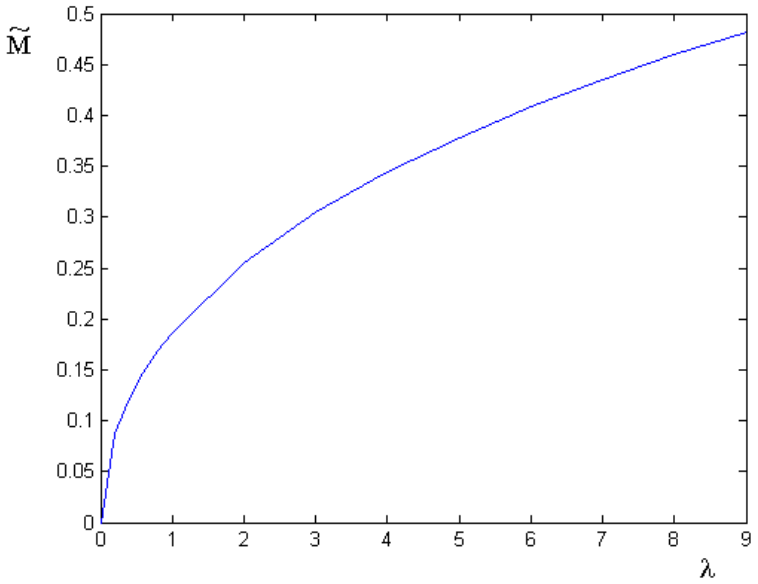

Figure 3.13: $\widetilde{M} = \frac{M}{T}$ as a function of λ.

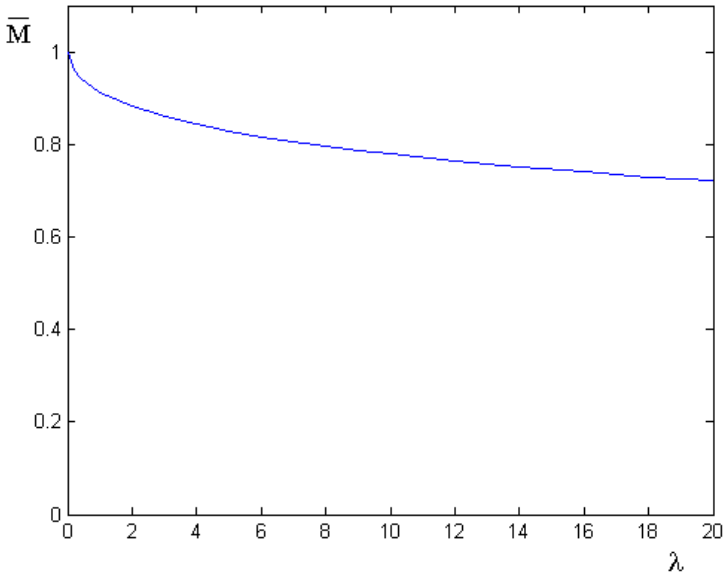

Figure 3.14: $\overline{M} = \frac{M}{\sqrt{\lambda T^2/24}}$ as a function of λ.

4 EFFECTIVE THEORIES

An effective theory is a theory which describes the physics at a given length scale or energy scale. For lengths smaller than or energies larger than this scale, one can no longer focus only on the degrees of freedom relevant at this scale. For example, describing the Earths motion around the sun, the correct effective theory is classical mechanics, although quantum mechanics is a more fundamental theory. Only when the lengths become small enough, classical mechanics cannot describe the system, and quantum mechanics is the correct theory.

An effective theory is thus a theory where the degrees of freedom which are relevant at higher energies, do not explicitly appear. An example is that of a heavy particle; at energies smaller than the mass of the particle, the particle cannot be created. The Lagrangian valid at such small energies does not contain this degree of freedom. The advantage of constructing effective theories is that it simplifies many calculations considerably [17].

4.1 Resummation

The free propagator in the imaginary time formalism reads $\frac{1}{\omega_n^2+\omega_k^2}$, where $\omega_n^2 = (2\pi nT)^2$ is the Matsubara frequency for bosons and $\omega_k^2 = \vec{k}^2 + m^2$. When $m = 0$, the free propagator is $\frac{1}{\vec{k}^2}$ for the $n = 0$ mode. For the $n \neq 0$ modes, the Matsubara frequency acts as an IR cutoff mass $m^2 \sim T^2$. As shown in the previous section, the first-order correction to the self-energy is a thermal mass generated by thermal fluctuations and goes as $\sim \sqrt{\lambda}T$ in the massless case. For $T >> \sqrt{\lambda}T$, the thermal mass is just a small perturbation to the $n \neq 0$ modes, and can be neglected for these modes. For the $n = 0$ mode, the thermal mass is not negligible for momenta of order $\sqrt{\lambda}T$ or smaller, and perturbation theory breaks down. This requires resummation of daisy diagrams.

As explained above, there are two separated energy scales, which go as $\sim \sqrt{\lambda}T$ and $\sim T$. $\mathcal{L}_{eff}$ given in Eq. (3.89) is the Lagrangian of an effective theory which includes energies smaller than or equal to $\sqrt{\lambda}T$. The effective theory is appropriate for calculations for such low energies, while the high-energy effects enter through the parameters of $\mathcal{L}_{eff}$. For example, the one-loop correction to the self-energy, $\Sigma = \frac{\lambda T^2}{24}$, is determined by the $n \neq 0$ modes [12].

4.2 Effective theories for QCD

There are several effective theories for QCD. The goal for these theories are to describe QCD at low temperatures to a desired accuracy. Some basic assumptions must be made. The QCD effective theory at low temperatures should confine the quarks and gluons; only colorless states exist. This is

due to asymptotic freedom in QCD; the coupling constant increases as the distance decreases or as the energy decreases. The coupling constant becomes too large at low energies for the interaction between quarks and gluons to be described as a small perturbation, and an effective theory is needed.

A second assumtion is that the effective theory describes a spontaneous breaking of chiral symmetry. Consider QCD with two massless quarks, u and d. The field is written as

$$\psi = \begin{pmatrix} u \\ d \end{pmatrix}, \tag{4.1}$$

and the Dirac Lagrangian reads

$$\mathcal{L} = \overline{\psi}\left(i\gamma^{\mu}\partial_{\mu}\right)\psi. \tag{4.2}$$

ψ can be decomposed into a right-handed field, $\psi_R = \frac{1}{2}\left(1+\gamma_5\right)\psi$, and a left-handed field, $\psi_L = \frac{1}{2}\left(1-\gamma_5\right)\psi$, giving

$$\psi = \begin{pmatrix} u_L \\ d_L \end{pmatrix} + \begin{pmatrix} u_R \\ d_R \end{pmatrix} = \psi_L + \psi_R. \tag{4.3}$$

This leads to the Lagrangian

$$\mathcal{L} = \overline{\psi}_L\left(i\gamma^{\mu}\partial_{\mu}\right)\psi_L + \overline{\psi}_R\left(i\gamma^{\mu}\partial_{\mu}\right)\psi_R. \tag{4.4}$$

$\mathcal{L}$ is invariant under independent $U(2)$ transformations, $U_L(2)$ and $U_R(2)$. The symmetry $U_L(2)\times U_R(2)$ can be written as $SU_L(2)\times SU_R(2)\times U_A(1)\times U_V(1)$ [3], where the subscript A represents the axial symmetry and V represents the vector symmetry. $U_V(1)$ is related to the conservation of baryon number, while $U_A(1)$ is broken by axial anomaly [9]. The symmetry which is left, $SU_L(2)\times SU_R(2)$, must be spontaneously broken down to $SU_V(2)$ for low temperatures, due to the fact that pairs of particles with opposite parity are not found in nature. For example, there is no parity partner of the proton. The three broken generators correspond to three massless Goldstone bosons.

In QCD, the quarks do have nonzero masses. The nonzero masses of the quarks explicitly breaks the $SU_A(2)\times SU_V(2)$ symmetry. However, the masses of u and d quarks are small, so the axial symmetry can be considered as approximate. Three pseudo-Goldstonde bosons with small, but nonzero masses, should appear. All hadrons have masses ≥ 0.5 GeV [18], except the pions. Pions have much smaller masses than other hadrons, and are interpreted as pseudo-Goldstone bosons.

4.3 The linear sigma model

The linear sigma model has been widely used as an effective QCD model at low temperatures. The model is a theory of fermions (quarks and nucleons) interacting with mesons [5], and is an effective theory well-suited for describing both the physics of mesons and the chiral phase transition. The mesonic part of the model contains four scalar fields, the sigma field and three pion fields. They form the chiral field $(\sigma, \vec{\pi})^T$ [5]. The order parameter of the chiral phase transition is the quark condensate $\langle \overline{\psi}\psi \rangle$ where ψ is the quark field [1]. In the $O(4)$ linear sigma model, the sigma field can be used to represent the quark condensate since both behave in the same manner under chiral phase transition [5]. The symmetry of QCD with two massless flavors is $SU_R(2) \times SU_L(2)$, which is isomorphic to $O(4)$. The mesonic part of the linear sigma model is invariant under $O(4)$ symmetry, and considering mesons only, the $O(4)$ linear sigma model can be used as an effective theory. By studying the phase transition when $O(4)$ is broken down to $O(3)$, one might gain insight into the chiral symmetry breaking of QCD. The phase transition in the $O(4)$ linear sigma model will be closer examined in section 5.

5 PHASE TRANSITIONS AT FINITE TEMPERATURE

Spontaneous symmetry breaking and phase transitions induced by temperature are important ingredients of the early Universe. The period from the Planck time $t_{pl} \approx 10^{-43}$ s corresponding to the temperature $T_{pl} \approx 10^{19}$ GeV, to the time $t_{QCD} \approx 10^{-5}$ s corresponding to $T_{QCD} \approx 200 - 300$ MeV can be divided into intervals separated by the phase transitions which characterize them, as follows [19]

- $T_{pl} > T > T_{GUT} \approx 10^{15}$ GeV

  In this period, the physics is described by a grand unified theory (GUT), which unifies the strong and electroweak interactions. At $T = T_{GUT}$ corresponding to $t = t_{GUT} \approx 10^{-37}$ s, there is a spontaneous breaking of the GUT symmetry and a phase transition takes place.

- $T_{GUT} > T > T_{EW} \approx 100$ GeV

  In this period the strong and electroweak interactions are no longer unified. Due to the large temperature range of this period, it is possible that other phase transitions occur for temperatures between T_{GUT} and T_{EW}. At $T = T_{EW}$ corresponding to $t = t_{EW} \approx 10^{-11}$ s, the electroweak phase transition takes place. Leptons acquire masses, and the intermediate vector bosons give rise to photons and the massive W^+, W^- and Z bosons.

- $T_{EW} > T > T_{QCD}$

  Electromagnetic and weak interactions are no longer unified. W^+, W^- and Z bosons disappears rapidly through decay and annihilation when the temperature falls below 90 GeV. Quarks and gluons occur as quark-gluon plasma, and the chiral symmetry applies. At $T = T_{QCD}$ corresponding to $t = t_{QCD}$, the QCD phase transition takes place. The quarks and gluons are confined and the chiral symmetry is broken. As mentioned in the introduction, the relation between the chiral phase transition and confinement is only partially understood. It is not known if $T_{confinement} = T_{chiral}$. Compared to the large temperature ranges between the various phase transitions mentioned above, it is sufficient to assume that the chiral phase transition and confinement takes place at the same temperature $T = T_{QCD}$ in this rough description of the early Universe.

In this section the $O(4)$ linear sigma model will be studied. This model is an effective model of QCD, and by studying the phase transition when $O(4)$ symmetry is broken down to $O(3)$ symmetry, one might gain some insight

into the chiral phase transition of QCD. We start with the $\lambda\phi^4$-theory for one scalar field as a simple example. Then the $O(4)$ linear sigma model will be studied in the Hartree and large-N approximations.

The finite-temperature terms do not introduce any new UV divergences in ordinary perturbation, so renormalization of zero-temperature UV divergences is sufficient to make the theory finite. As discussed in section 3.10, resummation leads to a breakdown of perturbation theory, and temperature-dependent counterterms seem necessary to renormalize the theory. It was shown that defining the renormalized coupling constant $\frac{1}{\lambda} = \frac{1}{\lambda_B} + \frac{1}{16\pi^2\epsilon}$ and the renormalized mass $m^2 = \frac{\lambda}{\lambda_B} m_B^2$, the gap equation Eq. (3.93) could be renormalized with temperature-independent counterterms. Andersen uses this approach in [20] to renormalize the gap equations for the two-particle irreducible (2PI) $\frac{1}{N}$ expansion. The 2PI formalism, also called the Cornwall-Jackiw-Tomboulis (CJT) formalism, only takes into account 2PI diagrams. The 2PI formalism will not be further discussed here, and the reader is referred to e.g. [21]. The renormalized coupling constant and mass defined above are used to renormalize the large-N approximation, but it does not work in the Hartree approximation. To renormalize the Hartree approximation, temperature-dependent counterterms are used. In [22], Lenaghan and Rischke study the $O(N)$ model using the 2PI formalism. They renormalize the gap equations by using temperature-dependent counterterms, both for the Hartree and the large-N approximations.

The results of the renormalized thermal masses for the sigma and pion fields are compared to the case where the the zero temperature contributions have been discarded, referred to as the nonrenormalized case.

5.1 One scalar field

The Lagrangian density of $\lambda\phi^4$-theory at zero temperature is given in Eq. (3.1) and reads

$$\mathcal{L} = \frac{1}{2}\left(\partial_\mu\phi\right)\left(\partial^\mu\phi\right) - \frac{1}{2}m_B^2\phi^2 - \frac{\lambda_B}{4!}\phi^4, \tag{5.1}$$

where the abbreviation $\phi(x) \equiv \phi$ is used. The subscript B on the field is omitted since to first order $Z_\phi = 1$, and we will only consider first-order corrections here. The Lagrangian density in Eq. (5.1) is invariant when $\phi \to -\phi$. The potential is

$$V(\phi) = \frac{1}{2}m_B^2\phi^2 + \frac{\lambda_B}{4!}\phi^4. \tag{5.2}$$

The potential has a minimum at $\phi_0 = \langle 0|\phi|0\rangle = 0$ if $m_B^2 > 0$, and two minima at $\phi_0 = \langle 0|\phi|0\rangle = \pm\sqrt{-\frac{6m_B^2}{\lambda_B}}$ if $m_B^2 < 0$. In the latter case, invariance under the symmetry operation $\phi \to -\phi$ no longer applies when the system is in the vacuum state. The symmetry is spontaneously broken. At finite

temperature, interactions with the thermal bath contributes to the mass proportional to T. At some temperature T_c the vacuum expectation value of the field changes from nonzero to zero due to the thermal fluctuations.

To evaluate the symmetry breaking at finite temperature, the Euclidean Lagrangian density for a single scalar field is considered

$$\mathcal{L}_E = \frac{1}{2}\left(\partial_\mu \phi\right)^2 + \frac{1}{2} m_B^2 \phi^2 + \frac{\lambda_B}{4!}\phi^4. \tag{5.3}$$

As in section 3.10, a term $\frac{1}{2}M^2\phi^2$ is added and subtracted,

$$\mathcal{L}_E = \frac{1}{2}\left(\partial_\mu \phi\right)\left(\partial^\mu \phi\right) + \frac{1}{2} m_B^2 \phi^2 + \frac{1}{2}M^2\phi^2 - \frac{1}{2}M^2\phi^2 + \frac{\lambda_B}{4!}\phi^4. \tag{5.4}$$

Assuming $m_B^2 < 0$, the Lagrangian density in Eq. (5.4) has (at least at low temperatures) a nonzero value ϕ_0 of the vacuum expectation value. By making the shift $\phi \to \phi_0 + \phi$, where ϕ are fluctuations about the classical vacuum ϕ_0 with zero vacuum expectation value such that $\langle 0|\phi_0 + \phi|0\rangle = \phi_0$, the Lagrangian can be separated into the free part

$$\mathcal{L}_0 = \frac{1}{2}\left(\partial_\mu \phi\right)\left(\partial^\mu \phi\right) + \frac{1}{2}M^2\phi^2, \tag{5.5}$$

and the interaction part

$$\begin{aligned}\mathcal{L}_{int} = V_0 &- \frac{1}{2}\left(M^2 - m_B^2 - \frac{\lambda_B}{2}\phi_0^2\right)\phi^2 \\ &+ \frac{\lambda_B}{6}\phi_0\phi^3 + \frac{\lambda_B}{4!}\phi^4,\end{aligned} \tag{5.6}$$

where $V_0 = \frac{1}{2}m_B^2\phi_0^2 + \frac{\lambda_B}{4!}\phi_0^4$. In Eq. (5.6) the terms linear in ϕ have been omitted since they only enter as a constant in the minimum of the potential. Up to two loops, the contribution to the potential is shown in Fig. 5.1. In the Hartree approximation, the contributions to the potential come from the diagrams on the first line in Fig. 5.1. The potential reads

$$\begin{aligned}V_{eff} = V_0 &+ \frac{1}{2}\sum\!\!\!\!\!\!\int_k \ln\left(\omega_n^2 + \omega_{kM}^2\right) \\ &- \frac{1}{2}\left(M^2 - m_B^2 - \frac{\lambda_B}{2}\phi_0^2\right)\sum\!\!\!\!\!\!\int_k \frac{1}{\omega_n^2 + \omega_{kM}^2} \\ &+ \frac{\lambda_B}{8}\left(\sum\!\!\!\!\!\!\int_k \frac{1}{\omega_n^2 + \omega_{kM}^2}\right)^2,\end{aligned} \tag{5.7}$$

where $\omega_{kM}^2 = \vec{k}^2 + M^2$. Minimizing V_{eff} with respect to ϕ_0 and M^2 gives the following equations

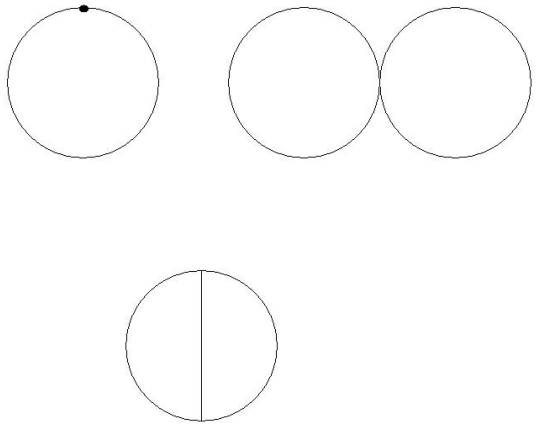

Figure 5.1: One- and two-loop contributions to the effective potential of one scalar field.

$$\phi_0 \left(m_B^2 + \frac{\lambda_B}{6}\phi_0^2 + \frac{\lambda_B}{2} \sum\!\!\!\!\!\!\int_k \frac{1}{\omega_n^2 + \omega_{kM}^2} \right) = 0 \tag{5.8}$$

$$M^2 = m_B^2 + \frac{\lambda_B}{2}\phi_0^2 + \frac{\lambda_B}{2} \sum\!\!\!\!\!\!\int_k \frac{1}{\omega_n^2 + \omega_{kM}^2}, \tag{5.9}$$

respectively. The first two terms in Eq. (5.9) are the tree-level mass, and the third term is the tadpole correction. Eq. (5.9) is the general case of Eq. (3.93), where the tree level mass was zero. To see that Eq. (5.9) can be renormalized with temperature-independent counterterms, we start with writing the equation as

$$\Sigma = \frac{\lambda_B}{2} \sum\!\!\!\!\!\!\int_k \frac{1}{\omega_n^2 + \vec{k}^2 + m_B^2 + \frac{\lambda_B}{2}\phi_0^2 + \Sigma}. \tag{5.10}$$

In Eq. (5.10) we have used that $M^2 = m_B^2 + \frac{\lambda_B}{2}\phi_0^2 + \Sigma$, where Σ is the self-energy. Eq. (5.10) can be expanded around $\Sigma = 0$ to give

$$\begin{aligned}\Sigma = &\frac{\lambda_B}{2}\sum\!\!\!\!\!\!\int_k \frac{1}{\omega_n^2+\vec{k}^2+m_B^2+\frac{\lambda_B}{2}\phi_0^2} \\ &-\Sigma\frac{\lambda_B}{2}\sum\!\!\!\!\!\!\int_k \frac{1}{\left(\omega_n^2+\vec{k}^2+m_B^2+\frac{\lambda_B}{2}\phi_0^2\right)^2} \\ &+\Sigma^2\frac{\lambda_B}{2}\sum\!\!\!\!\!\!\int_k \frac{1}{\left(\omega_n^2+\vec{k}^2+m_B^2+\frac{\lambda_B}{2}\phi_0^2\right)^3}-\cdots .\end{aligned} \tag{5.11}$$

Eq. (5.11) is a series of daisy diagrams with a massive propagator. The self-energy is written as a power series in the coupling constant

$$\Sigma = \Sigma_1 + \Sigma_2 + \cdots , \tag{5.12}$$

where $\Sigma_1 \sim \lambda_B$, $\Sigma_2 \sim \lambda_B^2$, and so on. The bare parameters can be written as [20]

$$m_B^2 = m^2 + \sum_{n=1}^{\infty}\delta m_n^2 \tag{5.13}$$

$$\lambda_B = \lambda + \sum_{n=1}^{\infty}\delta\lambda_n. \tag{5.14}$$

Inserting Eqs. (5.12), (5.13) and (5.14) into Eq. (5.11), we can find Σ_n, δm_n^2 and $\delta\lambda_n$ by iteration. The first iteration gives

$$\begin{aligned}\Sigma_1 = &\frac{\lambda}{2}\sum\!\!\!\!\!\!\int_k \frac{1}{\omega_n^2+\vec{k}^2+m^2+\frac{\lambda}{2}\phi_0^2} \\ &+\delta m_1^2+\frac{\delta\lambda_1}{2}\phi_0^2.\end{aligned} \tag{5.15}$$

Using dimensional regularization, Eq. (5.15) can be written as

$$\begin{aligned}\Sigma_1 = &\frac{\lambda}{2}\frac{m^2+\frac{\lambda}{2}\phi_0^2}{(4\pi)^2}\left[-\frac{2}{\epsilon}-1+\gamma_E+\ln\left(\frac{m^2+\frac{\lambda}{2}\phi_0^2}{4\pi\mu^2}\right)\right] \\ &+\frac{\lambda}{2}\int\frac{d^3k}{(2\pi)^3}\frac{1}{\sqrt{\vec{k}^2+m^2+\frac{\lambda}{2}\phi_0^2}}\frac{1}{e^{\beta\sqrt{\vec{k}^2+m^2+\frac{\lambda}{2}\phi_0^2}}-1} \\ &+\delta m_1^2+\frac{\delta\lambda_1}{2}\phi_0^2.\end{aligned} \tag{5.16}$$

Thus, the counterterms in the first iteration is chosen as $\delta m_1^2 = \frac{\lambda m^2}{16\pi^2\epsilon}$ and $\delta\lambda_1 = \frac{\lambda^2}{16\pi^2\epsilon}$ in order to cancel the divergent terms. The renormalization procedure can be carried out iteratively to all orders. The n'th counterterms are given by [20]

$$\delta m_n^2 = \frac{\lambda^n m^2}{(16\pi^2\epsilon)^n}, \tag{5.17}$$

$$\delta\lambda_n = \frac{\lambda^{n+1}}{(16\pi^2\epsilon)^n}. \tag{5.18}$$

Summing the counterterms to all orders gives

$$m_B^2 = m^2 + \sum_{n=1}^{\infty} \frac{\lambda^n m^2}{(16\pi^2\epsilon)^n} = m^2 \sum_{n=0}^{\infty} \frac{\lambda^n}{(16\pi^2\epsilon)^n} = \frac{m^2}{1 - \frac{\lambda}{16\pi^2\epsilon}}, \tag{5.19}$$

$$\lambda_B = \lambda + \sum_{n=1}^{\infty} \frac{\lambda^{n+1}}{(16\pi^2\epsilon)^n} = \lambda \sum_{n=0}^{\infty} \frac{\lambda^n}{(16\pi^2\epsilon)^n} = \frac{\lambda}{1 - \frac{\lambda}{16\pi^2\epsilon}}. \tag{5.20}$$

Eqs. (5.19) and (5.20) give the following relation between the renormalized and bare parameters

$$\frac{m_B^2}{\lambda_B} = \frac{m^2}{\lambda}. \tag{5.21}$$

Returning to Eq. (5.9), we get

$$\begin{aligned} M^2 = m_B^2 + \frac{\lambda_B}{2}\phi_0^2 + \frac{\lambda_B}{2}\frac{M^2}{(4\pi)^2}\left[-\frac{2}{\epsilon} - 1 + \gamma_E + \ln\left(\frac{M^2}{4\pi\mu^2}\right)\right] \\ + \frac{\lambda_B}{2}\int \frac{d^3k}{(2\pi)^3}\frac{n_B(\omega_{kM})}{\omega_{kM}}, \end{aligned} \tag{5.22}$$

when using dimensional regularization. Dividing the equation by λ_B and inserting Eqs. (5.20) and (5.21), the following renormalized expression for M^2 is obtained

$$\begin{aligned} M^2 = m^2 + \frac{\lambda}{2}\phi_0^2 + \frac{\lambda}{2}\frac{M^2}{(4\pi)^2}\left[-1 + \gamma_E + \ln\left(\frac{M^2}{4\pi\mu^2}\right)\right] \\ + \frac{\lambda}{2}\int \frac{d^3k}{(2\pi)^3}\frac{n_B(\omega_{kM})}{\omega_{kM}}. \end{aligned} \tag{5.23}$$

Eq. (5.8) has the trivial solution $\phi_0 = 0$ and the solution

$$\frac{\lambda_B}{2}\phi_0^2 = -3m_B^2 - \frac{3\lambda_B}{2}\sum\!\!\!\!\!\!\int_k \frac{1}{\omega_n^2 + \omega_{kM}^2}. \tag{5.24}$$

From Eqs. (5.9) and (5.24), it is found that $\frac{\lambda_B}{2}\phi_0^2 = \frac{3}{2}M^2$ before renormalization, and

$$\frac{\lambda}{2}\phi_0^2 = \frac{3}{2}M^2 \tag{5.25}$$

after renormalization. Inserting Eq. (5.25) into Eq. (5.23), the expression for M^2 reads

$$\begin{aligned} M^2 = -2m^2 &- \lambda\frac{M^2}{(4\pi)^2}\left[-1 + \gamma_E + \ln\left(\frac{M^2}{4\pi\mu^2}\right)\right] \\ &- \lambda\int\frac{d^3k}{(2\pi)^3}\frac{n_B(\omega_{kM})}{\omega_{kM}} \end{aligned} \tag{5.26}$$

when $T < T_c$. $\lambda\phi^4$-theory is not a physical model, so there is no particular value to assign to m. Instead, defining $\widetilde{M}^2 \equiv \frac{M^2}{-m^2}$ and $\widetilde{T}^2 \equiv \frac{T^2}{-m^2}$ makes it possible to write

$$\begin{aligned} \widetilde{M}^2 = 2 &- \lambda\frac{\widetilde{M}^2}{(4\pi)^2}\left[-1 + \gamma_E + \ln\left(\frac{\widetilde{M}^2(-m_r^2)}{4\pi\mu^2}\right)\right] \\ &- \lambda\frac{\widetilde{T}^2}{2\pi^2}\int_0^\infty du\frac{u^2}{\sqrt{u^2 - \frac{\widetilde{M}^2}{\widetilde{T}^2}}}\frac{1}{e^{\sqrt{u^2 - \frac{\widetilde{M}^2}{\widetilde{T}^2}}} - 1}, \end{aligned} \tag{5.27}$$

by making the substitution $u = \frac{k}{T}$ in the integral in Eq. (5.26).

When $T = 0$ the last term in Eq. (5.27) vanishes and

$$\widetilde{M}^2 = \widetilde{M}_0^2 = 2 - \lambda\frac{\widetilde{M}_0^2}{(4\pi)^2}\left[-1 + \gamma_E + \ln\left(\frac{\widetilde{M}_0^2(-m^2)}{4\pi\mu^2}\right)\right] \tag{5.28}$$

Choosing $\widetilde{M}_0^2 = 2$ gives $4\pi\mu^2 = e^{\gamma_E - 1}\left(-m^2\widetilde{M}_0^2\right)$. With this value inserted in Eq. (5.27), the following expression for $\widetilde{M}^2$ at finite temperature is obtained

$$\begin{aligned} \widetilde{M}^2 = 2 &- \lambda\frac{\widetilde{M}^2}{(4\pi)^2}\left[-1 + \gamma_E + \ln\left(\frac{\widetilde{M}^2}{2e^{\gamma_E - 1}}\right)\right] \\ &- \lambda\frac{\widetilde{T}^2}{2\pi^2}\int_0^\infty du\frac{u^2}{\sqrt{u^2 - \frac{\widetilde{M}^2}{\widetilde{T}^2}}}\frac{1}{e^{\sqrt{u^2 - \frac{\widetilde{M}^2}{\widetilde{T}^2}}} - 1}, \end{aligned} \tag{5.29}$$

From Eq. (5.25) the expression $\frac{\lambda}{2}\widetilde{\phi}_0^2 = \frac{3}{2}\widetilde{M}^2$ is derived, where $\widetilde{\phi}_0^2 \equiv \frac{\phi_0^2}{-m^2}$.

When $\phi_0 = 0$ the symmetry is restored. In this case the expression for M^2 reads

$$\begin{aligned} M^2 = m^2 + \frac{\lambda}{2}\frac{M^2}{(4\pi)^2}\left[-1 + \gamma_E + \ln\left(\frac{M^2}{4\pi\mu^2}\right)\right] \\ + \frac{\lambda}{2}\int \frac{d^3k}{(2\pi)^3}\frac{n_B(\omega_{kM})}{\omega_{kM}}. \end{aligned} \tag{5.30}$$

By using the definition of $\widetilde{M}$ and $\widetilde{T}$ above, the following is obtained

$$\begin{aligned} \widetilde{M}^2 = -1 + \frac{\lambda}{2}\frac{\widetilde{M}^2}{(4\pi)^2}\left[-1 + \gamma_E + \ln\left(\frac{\widetilde{M}^2}{2e^{\gamma_E - 1}}\right)\right] \\ + \frac{\lambda}{2}\frac{\widetilde{T}^2}{2\pi^2}\int_0^\infty du \frac{u^2}{\sqrt{u^2 - \frac{\widetilde{M}^2}{\widetilde{T}^2}}}\frac{1}{e^{\sqrt{u^2 - \frac{\widetilde{M}^2}{\widetilde{T}^2}}} - 1}. \end{aligned} \tag{5.31}$$

Eqs. (5.29) and (5.31) can be solved numerically. A plot of $\widetilde{M}$ as a function of $\widetilde{T}$ is shown in Fig. 5.2, and a plot of $\widetilde{\phi}_0$ as a function of $\widetilde{T}$ is shown in Fig. 5.3. The coupling constant has been given the value $\lambda = 3$. The results are compared with the case where the zero temperature integrals have been discarded. Renormalization does not affect the mass or order parameter. For a small interval of $\widetilde{T}$, both solutions $\widetilde{\phi}_0 = 0$ and $\widetilde{\phi}_0 \neq 0$ exist. This means that there are two local minima. At the start of the interval, $\widetilde{\phi}_0 \neq 0$ is the global minimum of the potential, and at the end of the interval $\widetilde{\phi}_0 = 0$ is the global minimum. At some point in the interval, the global minimum goes from $\widetilde{\phi}_0 \neq 0$ to $\widetilde{\phi}_0 = 0$ and a phase transition occurs. The phase transition is of first order.

5.1.1 Explicitly broken symmetry

By subtracting a term $h\phi$ from the Lagrangian in Eq. (5.3), the symmetry $\phi \to -\phi$ is explicitly broken. The result of this is that the solution $\phi_0 = 0$ no longer exists, and instead of Eq. (5.8) the following is obtained

$$\begin{aligned} h &= \phi_0\left[m_B^2 + \frac{\lambda_B}{6}\phi_0^2 + \frac{\lambda_B}{2}\sum\!\!\!\!\!\!\int_k \frac{1}{\omega_n^2 + \omega_{kM}^2}\right] \\ &= \phi_0\left[M^2 - \frac{\lambda_B}{3}\phi_0^2\right]. \end{aligned} \tag{5.32}$$

M^2 is given by Eq. (5.9), as before. After renormalization, M^2 is given by Eq. (5.23). Eq. (5.32) can be rewritten to give

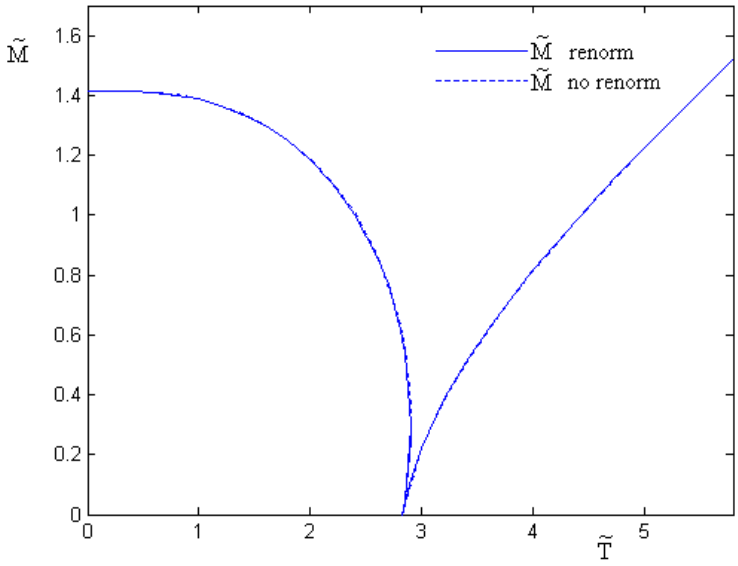

Figure 5.2: $\widetilde{M}$ as a function of $\widetilde{T}$. The renormalized case (solid line) does not differ from the nonrenormalized case (dotted line).

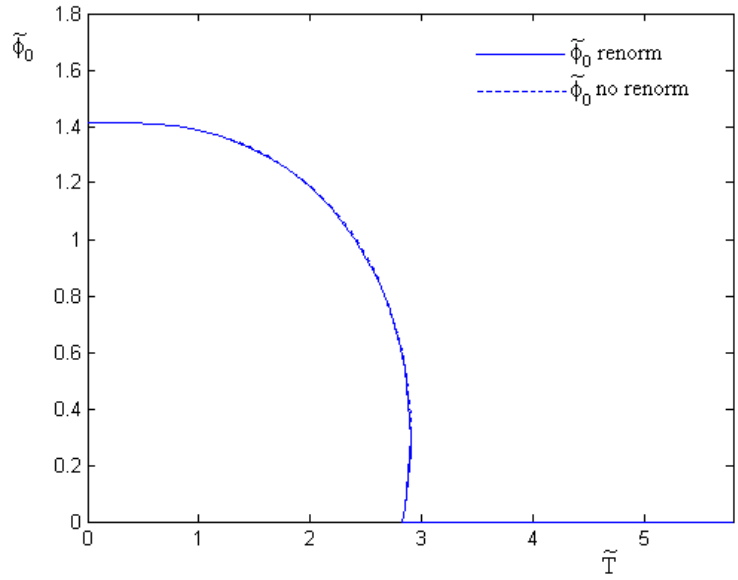

Figure 5.3: $\widetilde{\phi}_0$ as a function of $\widetilde{T}$. The renormalized case (solid line) does not differ from the nonrenormalized case (dotted line). The order parameter indicates a first order phase transition.

$$\phi_0^2 = \frac{3}{\lambda}\left[M^2 - \frac{h}{\phi_0}\right] \tag{5.33}$$

after renormalization. With the above definitions of $\widetilde{M}$, $\widetilde{T}$ and $\widetilde{\phi}_0$, Eq. (5.23) can be written as

$$\begin{aligned}\widetilde{M}^2 = -1 + \frac{\lambda}{2}\widetilde{\phi}_0^2 + \frac{\lambda}{2}\frac{\widetilde{M}^2}{(4\pi)^2}\left[-1 + \gamma_E + \ln\left(\frac{\widetilde{M}^2(-m^2)}{4\pi\mu^2}\right)\right] \\ + \frac{\lambda}{2}\frac{\widetilde{T}^2}{2\pi^2}\int_0^\infty du \frac{u^2}{\sqrt{u^2 - \frac{\widetilde{M}^2}{\widetilde{T}^2}}}\frac{1}{e^{\sqrt{u^2-\frac{\widetilde{M}^2}{\widetilde{T}^2}}} - 1}.\end{aligned} \tag{5.34}$$

When $T = 0$, $\widetilde{M}^2 = \widetilde{M}_0^2$ and $\widetilde{\phi}_0 = \widetilde{\overline{\phi}}_0$. $\overline{\phi}_0$ can be found from the minimum of the classical potential V_0 and is given by

$$\overline{\phi}_0^2 = \frac{6}{\lambda}(-m^2). \tag{5.35}$$

Thus $\widetilde{\overline{\phi}}_0^2 = \frac{6}{\lambda}$, and inserting this into Eq. (5.34) at zero temperature gives

$$\widetilde{M}_0^2 = 2 + \frac{\lambda}{2}\frac{\widetilde{M}_0^2}{(4\pi)^2}\left[-1 + \gamma_E + \ln\left(\frac{\widetilde{M}_0^2(-m^2)}{4\pi\mu^2}\right)\right]. \tag{5.36}$$

Again, choosing $\widetilde{M}_0^2 = 2$ gives $4\pi\mu^2 = e^{\gamma_E - 1}\left(-m^2\widetilde{M}_0^2\right)$. The expressions for nonzero temperature thus read

$$\begin{aligned}\widetilde{M}^2 = -1 + \frac{\lambda}{2}\widetilde{\phi}_0^2 + \frac{\lambda}{2}\frac{\widetilde{M}^2}{(4\pi)^2}\left[-1 + \gamma_E + \ln\left(\frac{\widetilde{M}^2}{2e^{\gamma_E - 1}}\right)\right] \\ + \frac{\lambda}{2}\frac{\widetilde{T}^2}{2\pi^2}\int_0^\infty du \frac{u^2}{\sqrt{u^2 - \frac{\widetilde{M}^2}{\widetilde{T}^2}}}\frac{1}{e^{\sqrt{u^2-\frac{\widetilde{M}^2}{\widetilde{T}^2}}} - 1},\end{aligned} \tag{5.37}$$

and

$$\widetilde{\phi}_0^2 = \frac{3}{\lambda}\left[\widetilde{M}^2 - \frac{\widetilde{h}}{\widetilde{\overline{\phi}}}\right], \tag{5.38}$$

where $\widetilde{h} \equiv \frac{h}{(-m^2)^{\frac{3}{2}}}$. Eqs. (5.37) and (5.38) can be solved numerically. A plot of $\widetilde{M}$ as a function of $\widetilde{T}$ is shown in Fig. 5.4, and a plot of $\widetilde{\phi}_0$ as a function $\widetilde{T}$ is shown in Fig. 5.5. As above, the coupling constant has the value $\lambda = 3$, and $\widetilde{h}$ is given the value $\widetilde{h} = 0.01$. There is no phase transition for $h \neq 0$, but rather a smooth crossover. Again, renormalization does not affect the results.

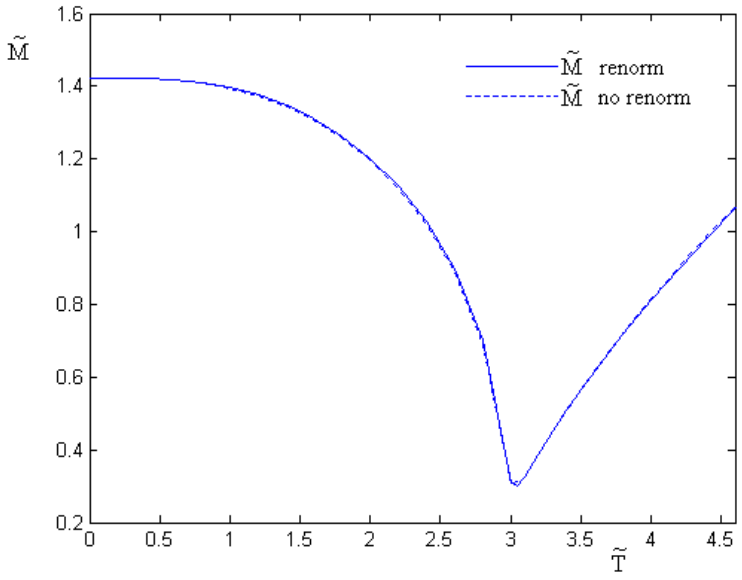

Figure 5.4: $\widetilde{M}$ as a function of $\widetilde{T}$ for $h = 0.01$. There is no difference between the case where $\widetilde{M}$ is renormalized (solid line) and the nonrenormalized case (dotted line).

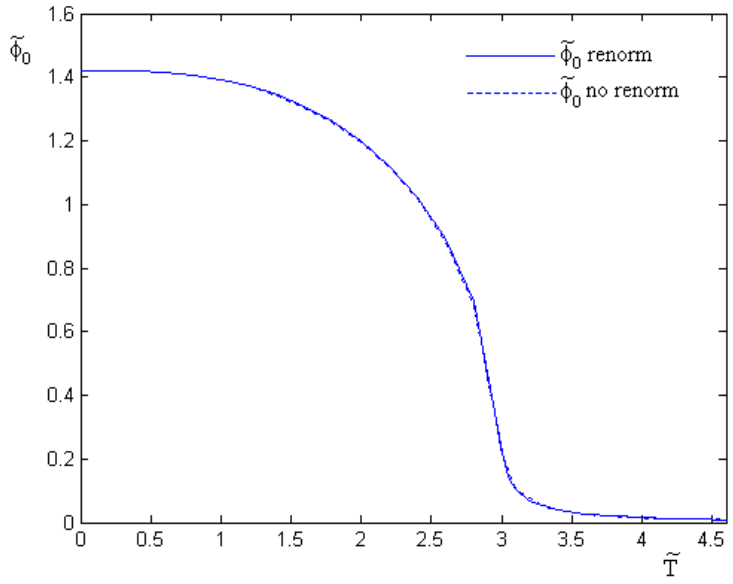

Figure 5.5: $\widetilde{\phi}_0$ as a function of $\widetilde{T}$ for $\widetilde{h} = 0.01$. There is no phase transition, but rather a smooth crossover. The renormalized case (solid line) does not differ from the nonrenormalized case (dotted line).

5.2 N scalar fields

The Euclidean Lagrangian density of an N-component scalar field $\vec{\phi} = (\phi_\sigma, \vec{\phi}_\pi)^T$ is

$$\mathcal{L}_E = \frac{1}{2}(\partial_\mu \phi_i)^2 + \frac{1}{2} m_B^2 \vec{\phi}^2 + \frac{\lambda_B}{2N}(\vec{\phi}^2)^2, \tag{5.39}$$

where repeated indices indicates summation and $\vec{\phi}^2 = \sum_{i=1}^N \phi_i^2$. Expanding around the classical field $\vec{\phi_0} = (\phi_0, 0, \ldots, 0)^T$, the Lagrangian density reads

$$\begin{aligned} \mathcal{L}_E = & \frac{1}{2}(\partial_\mu \phi_i)^2 + \frac{1}{2} m_B^2 \phi_0^2 + \frac{1}{2} m_B^2 \vec{\phi}^2 \\ & + \frac{\lambda_B}{2N}\left(4\phi_0^2\phi_\sigma^2 + \phi_0^4 + (\vec{\phi}^2)^2 + 4\phi_0\phi_\sigma\vec{\phi}^2 + 2\phi_0^2\vec{\phi}^2\right). \end{aligned} \tag{5.40}$$

In Eq. (5.40) the terms $C\phi_\sigma$, where C is some constant, has been omitted. Adding and subtracting the terms $\frac{1}{2}M_\sigma^2\phi_\sigma^2$ and $\frac{1}{2}M_\pi^2\phi_\pi^2$, the Lagrangian density can be separated into the free parts

$$\mathcal{L}_0^\sigma = \frac{1}{2}(\partial_\mu \phi_i)^2 + \frac{1}{2} M_\sigma^2 \phi_\sigma^2 \tag{5.41}$$

and

$$\mathcal{L}_0^\pi = \frac{1}{2}(\partial_\mu \phi_i)^2 + \frac{1}{2} M_\pi^2 \vec{\phi}_\pi^2, \tag{5.42}$$

and the interaction part

$$\begin{aligned} \mathcal{L}_{int} &= V_0 - \frac{1}{2}\left(M_\pi^2 - m_B^2 - \frac{2\lambda_B}{N}\phi_0^2\right)\vec{\phi}_\pi^2 - \frac{1}{2}\left(M_\sigma^2 - m_B^2 - \frac{6\lambda_B}{N}\phi_0^2\right)\phi_\sigma^2 \\ &\quad + \frac{2\lambda_B}{N}\phi_0\phi_\sigma^3 + \frac{2\lambda_B}{N}\phi_0\phi_\sigma\vec{\phi}_\pi^2 + \frac{\lambda_B}{2N}(\phi_\sigma^2 + \vec{\phi}_\pi^2)^2 \\ &= V_0 - \frac{1}{2}\overline{M}_\sigma^2\phi_\sigma^2 - \frac{1}{2}\overline{M}_\pi^2\vec{\phi}_\pi^2 \\ &\quad + \frac{2\lambda_B}{N}\phi_0\phi_\sigma^3 + \frac{2\lambda_B}{N}\phi_0\phi_\sigma\vec{\phi}_\pi^2 + \frac{\lambda_B}{2N}(\phi_\sigma^2 + \vec{\phi}_\pi^2)^2, \end{aligned} \tag{5.43}$$

where $V_0 = \frac{1}{2}m_B^2\phi_0^2 + \frac{\lambda_B}{2N}\phi_0^4$, $\overline{M}_\sigma^2 = M_\sigma^2 - m_B^2 - \frac{6\lambda_B}{N}\phi_0^2$ and $\overline{M}_\pi^2 = M_\pi^2 - m_B^2 - \frac{2\lambda_B}{N}\phi_0^2$. The one- and two-loop corrections to the potential are shown in Fig. 5.6. Solid lines correspond to ϕ_σ and dashed lines correspond to ϕ_π.

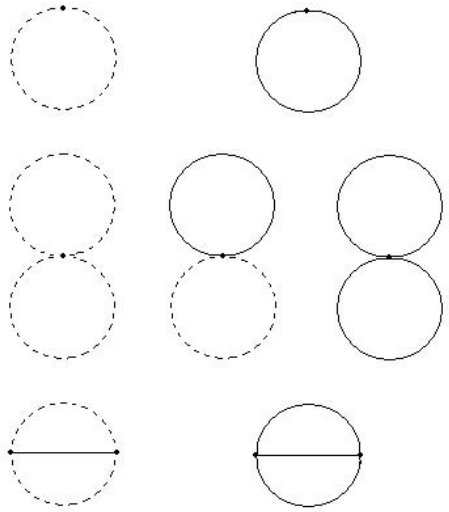

Figure 5.6: One- and two-loop corrections to the effective potential for N scalar fields. Solid lines correspond to ϕ_σ and dashed lines correspond to ϕ_π.

5.2.1 Hartree approximation

The contributions in the Hartree approximation are the diagrams in the first two lines of Fig. 5.6. This gives the following expression of the effective potential

$$\begin{aligned} V_{eff} = V_0 &+ \frac{1}{2}\sum\!\!\!\!\!\!\int_k \ln\left(\omega_n^2+\omega_{k\sigma}^2\right) + \frac{N-1}{2}\sum\!\!\!\!\!\!\int_k \ln\left(\omega_n^2+\omega_{k\pi}^2\right) \\ &- \frac{1}{2}\overline{M}_\sigma^2\sum\!\!\!\!\!\!\int_k \frac{1}{\omega_n^2+\omega_{k\sigma}^2} - \frac{N-1}{2}\overline{M}_\pi^2\sum\!\!\!\!\!\!\int_k \frac{1}{\omega_n^2+\omega_{k\pi}^2} \\ &+ \frac{3\lambda_B}{2N}\left(\sum\!\!\!\!\!\!\int_k \frac{1}{\omega_n^2+\omega_{k\sigma}^2}\right)^2 + 2(N-1)\frac{\lambda_B}{2N}\sum\!\!\!\!\!\!\int_k \frac{1}{\omega_n^2+\omega_{k\sigma}^2}\sum\!\!\!\!\!\!\int_k \frac{1}{\omega_n^2+\omega_{k\pi}^2} \\ &+ (N-1)(3+N-2)\frac{\lambda_B}{2N}\left(\sum\!\!\!\!\!\!\int_k \frac{1}{\omega_n^2+\omega_{k\pi}^2}\right)^2, \end{aligned} \tag{5.44}$$

where $\omega_{k\sigma}^2 = \vec{k}^2 + M_\sigma^2$ and $\omega_{k\pi}^2 = \vec{k}^2 + M_\pi^2$. Minimizing the effective potential with respect to ϕ_0 gives

$$\begin{aligned} \frac{\partial V_{eff}}{\partial \phi_0} = m_B^2\phi_0 &+ \frac{2\lambda_B}{N}\phi_0^3 + \frac{6\lambda_B}{N}\phi_0\sum\!\!\!\!\!\!\int_k \frac{1}{\omega_n^2+\omega_{k\sigma}^2} \\ &+ (N-1)\frac{2\lambda_B}{N}\phi_0\sum\!\!\!\!\!\!\int_k \frac{1}{\omega_n^2+\omega_{k\pi}^2} = 0. \end{aligned} \tag{5.45}$$

Eq. (5.45) has the trivial solution $\phi_0 = 0$ and the solution

$$\begin{aligned}\frac{2\lambda_B}{N}\phi_0^2 = -m_B^2 &- \frac{6\lambda_B}{N}\sum\!\!\!\!\!\!\int_k \frac{1}{\omega_n^2+\omega_{k\sigma}^2} \\ &- (N-1)\frac{2\lambda_B}{N}\sum\!\!\!\!\!\!\int_k \frac{1}{\omega_n^2+\omega_{k\pi}^2}.\end{aligned} \tag{5.46}$$

Minimizing the effective potential with respect to M_σ^2 and M_π^2 gives

$$\begin{aligned}\frac{\partial V_{eff}}{\partial M_\sigma^2} &= -\frac{1}{2}\overline{M}_\sigma^2\sum\!\!\!\!\!\!\int_k \frac{-1}{\left(\omega_n^2+\omega_{k\sigma}^2\right)^2} \\ &+ \frac{3\lambda_B}{N}\sum\!\!\!\!\!\!\int_k \frac{1}{\omega_n^2+\omega_{k\sigma}^2}\sum\!\!\!\!\!\!\int_k \frac{-1}{\left(\omega_n^2+\omega_{k\sigma}^2\right)^2} \\ &+ \frac{(N-1)\lambda_B}{N}\sum\!\!\!\!\!\!\int_k \frac{1}{\omega_n^2+\omega_{k\pi}^2}\sum\!\!\!\!\!\!\int_k \frac{-1}{\left(\omega_n^2+\omega_{k\sigma}^2\right)^2} \\ &= 0\end{aligned} \tag{5.47}$$

and

$$\begin{aligned}\frac{\partial V_{eff}}{\partial M_\pi^2} &= -\frac{N-1}{2}\overline{M}_\pi^2\sum\!\!\!\!\!\!\int_k \frac{-1}{\left(\omega_n^2+\omega_{k\pi}^2\right)^2} \\ &+ \frac{(N-1)(N+1)\lambda_B}{N}\sum\!\!\!\!\!\!\int_k \frac{1}{\omega_n^2+\omega_{k\pi}^2}\sum\!\!\!\!\!\!\int_k \frac{-1}{\left(\omega_n^2+\omega_{k\pi}^2\right)^2} \\ &+ \frac{(N-1)\lambda_B}{N}\sum\!\!\!\!\!\!\int_k \frac{1}{\omega_n^2+\omega_{k\sigma}^2}\sum\!\!\!\!\!\!\int_k \frac{-1}{\left(\omega_n^2+\omega_{k\pi}^2\right)^2} \\ &= 0.\end{aligned} \tag{5.48}$$

Eq. (5.47) gives the following expression for M_σ^2

$$\begin{aligned}M_\sigma^2 = m_B^2 + \frac{6\lambda_B}{N}\phi_0^2 &+ \frac{6\lambda_B}{N}\sum\!\!\!\!\!\!\int_k \frac{1}{\omega_n^2+\omega_{k\sigma}^2} \\ &+ \frac{2(N-1)\lambda_B}{N}\sum\!\!\!\!\!\!\int_k \frac{1}{\omega_n^2+\omega_{k\pi}^2},\end{aligned} \tag{5.49}$$

and Eq. (5.48) gives the following expression for M_π^2

$$\begin{aligned}M_\pi^2 = m_B^2 + \frac{2\lambda_B}{N}\phi_0^2 &+ \frac{2\lambda_B}{N}\sum\!\!\!\!\!\!\int_k \frac{1}{\omega_n^2+\omega_{k\sigma}^2} \\ &+ \frac{2(N+1)\lambda_B}{N}\sum\!\!\!\!\!\!\int_k \frac{1}{\omega_n^2+\omega_{k\pi}^2}.\end{aligned} \tag{5.50}$$

For temperatures $T < T_c$, ϕ_0 is given by Eq. (5.46) and the $O(N)$ symmetry of the Lagrangian density is broken down to $O(N-1)$. $N-1$ massless bosons should occur according to Goldstone's theorem; M_π^2 should be zero. Inserting Eq. (5.46) into Eq. (5.50), M_π^2 can be written as

$$M_\pi^2 = \frac{4\lambda_B}{N}\left(\sum\!\!\!\!\!\!\int_k \frac{1}{\omega_n^2+\omega_{k\pi}^2} - \sum\!\!\!\!\!\!\int_k \frac{1}{\omega_n^2+\omega_{k\sigma}^2}\right). \tag{5.51}$$

If $M_\pi^2 = 0$, then $\sum\!\!\!\!\!\!\int_k \frac{1}{\omega_n^2+\omega_{k\pi}^2} = \sum\!\!\!\!\!\!\int_k \frac{1}{\omega_n^2+\omega_{k\sigma}^2}$, which implies $M_\pi^2 = M_\sigma^2$. First, this is undesirable since the masses should not be equal in the broken phase. We know this from the zero temperature values of M_σ and M_π, which are not equal. In the real world, pions are interpreted as pseudo-Goldstone bosons with small masses $m_\pi = 139.6$ MeV [18]. The zero temperature value of the sigma mass is in the range $m_\sigma = 400 - 1200$ MeV [18]. Second, M_σ^2 is given by

$$M_\sigma^2 = \frac{6\lambda_B}{N}\phi_0^2 - \frac{2\lambda_B}{N}\phi_0^2 = \frac{4\lambda_B}{N}\phi_0^2 \neq 0, \tag{5.52}$$

and thus $M_\pi^2 = 0$ is not a solution. Goldstone's theorem is not satiesfied at all temperatures in the Hartree approximation. As will be shown in section 5.3, after proper renormalization M_π can be chosen to be zero at zero temperature, but it will become nonzero at nonzero temperatures in the broken phase [22].

For $N >> 1$ in the Hartree approximation, the following expression is obtained for ϕ_0^2 in the broken phase

$$\frac{2\lambda}{N}\phi_0^2 = -m_B^2 - 2\lambda_B \sum\!\!\!\!\!\!\int_k \frac{1}{\omega_n^2+\omega_{k\pi}^2}. \tag{5.53}$$

The expressions for M_σ^2 and M_π^2 are given by

$$M_\sigma^2 = m_B^2 + \frac{6\lambda_B}{N}\phi_0^2 + 2\lambda_B \sum\!\!\!\!\!\!\int_k \frac{1}{\omega_n^2+\omega_{k\pi}^2} \tag{5.54}$$

$$M_\pi^2 = m_B^2 + \frac{2\lambda_B}{N}\phi_0^2 + 2\lambda_B \sum\!\!\!\!\!\!\int_k \frac{1}{\omega_n^2+\omega_{k\pi}^2}. \tag{5.55}$$

Inserting Eq. (5.53) into Eq. (5.55) we see that $M_\pi^2 = 0$ in the broken phase. Goldstone's theorem is satisfied when $N >> 1$ in the Hartree approximation. Subtracting Eq. (5.55) from Eq. (5.54) gives

$$M_\sigma^2 - M_\pi^2 = \frac{4\lambda_B}{N}\phi_0^2. \tag{5.56}$$

$\phi_0 = 0$ in the phase where the $O(N)$ symmetry is restored, which implies $M_\sigma^2 = M_\pi^2$. The masses become degenerate in this phase.

5.2.2 Large-N approximation

Consider all diagrams in Fig. 5.6. For large N, $1/N$ contributions are ignored, and the effective potential reads

$$\begin{aligned} V_{eff} = V_0 &+ \frac{1}{2}\sum\!\!\!\!\!\!\int_k \ln\left(\omega_n^2+\omega_{k\sigma}^2\right) + \frac{N-1}{2}\sum\!\!\!\!\!\!\int_k \ln\left(\omega_n^2+\omega_{k\pi}^2\right) \\ &- \frac{1}{2}\overline{M}_\sigma^2\sum\!\!\!\!\!\!\int_k \frac{1}{\omega_n^2+\omega_{k\sigma}^2} - \frac{N-1}{2}\overline{M}_\pi^2\sum\!\!\!\!\!\!\int_k \frac{1}{\omega_n^2+\omega_{k\pi}^2} \\ &+ \frac{N\lambda_B}{2}\left(\sum\!\!\!\!\!\!\int_k \frac{1}{\omega_n^2+\omega_{k\pi}^2}\right)^2 + \lambda_B\sum\!\!\!\!\!\!\int_k \frac{1}{\omega_n^2+\omega_{k\sigma}^2}\sum\!\!\!\!\!\!\int_k \frac{1}{\omega_n^2+\omega_{k\pi}^2}. \end{aligned} \tag{5.57}$$

Minimizing this potential as above, leads to Eqs. (5.53), (5.54) and (5.55). The large-N approximation leads to the same expressions for ϕ_0^2, M_σ^2 and M_π^2 as the Hartree approximation with $N >> 1$. Thus, Goldstone's theorem is satisfied in the large-N approximation.

5.3 The $O(4)$ linear sigma model in the Hartree approximation

The Euclidean Lagrangian of the $O(4)$ linear sigma model is obtained from Eq. (5.39) by inserting $N = 4$. In addition, a term $h\phi_\sigma$ is subtracted, giving

$$\mathcal{L}_E = \frac{1}{2}(\partial_\mu\phi_i)^2 + \frac{1}{2}m_B^2\vec{\phi}^2 + \frac{\lambda_B}{8}(\vec{\phi}^2)^2 - h\phi_\sigma. \tag{5.58}$$

In the real world, pions have small, but nonzero masses. The term $h\phi_\sigma$ is introduced to generate masses for the pions [5]. As discussed in section 4.2, the masses of the pions explicitly break the chiral symmetry. However, the pion masses are small compared to other hadrons, and the chiral symmetry can be considered as approximate. In the following sections, the chiral limit where $h = 0$ and the physical point where $h \neq 0$, are studied.

5.3.1 The chiral limit

The equations for M_σ^2, M_π^2 and ϕ_0^2 in the chiral limit are obtained by inserting $N = 4$ in Eqs. (5.46), (5.49) and (5.50). The following is found for the order parameter in the broken phase

$$\begin{aligned} \frac{\lambda_B}{2}\phi_0^2 = -m_B^2 &- \frac{3\lambda_B}{2}\sum\!\!\!\!\!\!\int_k \frac{1}{\omega_n^2+\omega_{k\sigma}^2} \\ &- \frac{3\lambda_B}{2}\sum\!\!\!\!\!\!\int_k \frac{1}{\omega_n^2+\omega_{k\pi}^2}. \end{aligned} \tag{5.59}$$

The sigma and pion masses are given by

$$\begin{aligned} M_\sigma^2 = m_B^2 + \frac{3\lambda_B}{2}\phi_0^2 + \frac{3\lambda_B}{2}\sum\!\!\!\!\!\!\int_k \frac{1}{\omega_n^2+\omega_{k\sigma}^2} \\ + \frac{3\lambda_B}{2}\sum\!\!\!\!\!\!\int_k \frac{1}{\omega_n^2+\omega_{k\pi}^2} \end{aligned} \tag{5.60}$$

and

$$\begin{aligned} M_\pi^2 = m_B^2 + \frac{\lambda_B}{2}\phi_0^2 + \frac{\lambda_B}{2}\sum\!\!\!\!\!\!\int_k \frac{1}{\omega_n^2+\omega_{k\sigma}^2} \\ + \frac{5\lambda_B}{2}\sum\!\!\!\!\!\!\int_k \frac{1}{\omega_n^2+\omega_{k\pi}^2}. \end{aligned} \tag{5.61}$$

The first two terms in Eqs. (5.60) and (5.61) are the tree-level masses of the sigma and pions, respectively. The last two terms are tadpole corrections of the sigma and pion fields. As was shown in the previous section, the gap equation in the case of one scalar field could be renormalized by defining the renormalized coupling constant as $\frac{1}{\lambda} = \frac{1}{\lambda_B} + \frac{1}{16\pi^2\epsilon}$ and the renormalized mass as $m^2 = \frac{\lambda}{\lambda_B}m_B^2$. In the following we show that defining $\frac{1}{\lambda} = \frac{1}{\lambda_B} + \frac{a}{16\pi^2\epsilon}$ where a is a constant of order unity, and $m^2 = \frac{\lambda}{\lambda_B}m_B^2$, does not work in the Hartree approximation. Using dimensional regularization, we obtain

$$\begin{aligned} M_\sigma^2 = m_B^2 + \frac{3\lambda_B}{2}\phi_0^2 + \frac{3\lambda_B}{2}\frac{M_\sigma^2}{(4\pi)^2}\left[-\frac{2}{\epsilon} - 1 + \gamma_E + \ln\left(\frac{M_\sigma^2}{4\pi\mu^2}\right)\right] \\ + \frac{3\lambda_B}{2}\frac{M_\pi^2}{(4\pi)^2}\left[-\frac{2}{\epsilon} - 1 + \gamma_E + \ln\left(\frac{M_\pi^2}{4\pi\mu^2}\right)\right] \\ + \frac{3\lambda_B}{2}\int\frac{d^3k}{(2\pi)^3}\frac{n_B(\omega_{k\sigma})}{\omega_{k\sigma}} + \frac{3\lambda_B}{2}\int\frac{d^3k}{(2\pi)^3}\frac{n_B(\omega_{k\pi})}{\omega_{k\pi}}, \end{aligned} \tag{5.62}$$

and

$$\begin{aligned} M_\pi^2 = m_B^2 + \frac{\lambda_B}{2}\phi_0^2 + \frac{\lambda_B}{2}\frac{M_\sigma^2}{(4\pi)^2}\left[-\frac{2}{\epsilon} - 1 + \gamma_E + \ln\left(\frac{M_\sigma^2}{4\pi\mu^2}\right)\right] \\ + \frac{5\lambda_B}{2}\frac{M_\pi^2}{(4\pi)^2}\left[-\frac{2}{\epsilon} - 1 + \gamma_E + \ln\left(\frac{M_\pi^2}{4\pi\mu^2}\right)\right] \\ + \frac{\lambda_B}{2}\int\frac{d^3k}{(2\pi)^3}\frac{n_B(\omega_{k\sigma})}{\omega_{k\sigma}} + \frac{5\lambda_B}{2}\int\frac{d^3k}{(2\pi)^3}\frac{n_B(\omega_{k\pi})}{\omega_{k\pi}}. \end{aligned} \tag{5.63}$$

Dividing Eq. (5.62) and Eq. (5.63) by λ_B and inserting $\frac{1}{\lambda} = \frac{1}{\lambda_B} + \frac{a}{16\pi^2\epsilon}$ gives

$$\begin{aligned}\frac{1}{\lambda}M_\sigma^2 - \frac{a}{16\pi^2\epsilon}M_\sigma^2 = \frac{1}{\lambda}m^2 + \frac{3}{2}\phi_0^2 - \frac{3M_\sigma^2}{16\pi^2\epsilon} - \frac{3M_\pi^2}{16\pi^2\epsilon} \\ + \frac{3}{2}\frac{M_\sigma^2}{(4\pi)^2}\left[-1+\gamma_E+\ln\left(\frac{M_\sigma^2}{4\pi\mu^2}\right)\right] \\ + \frac{3}{2}\frac{M_\pi^2}{(4\pi)^2}\left[-1+\gamma_E+\ln\left(\frac{M_\pi^2}{4\pi\mu^2}\right)\right] \\ + \frac{3}{2}\int\frac{d^3k}{(2\pi)^3}\frac{n_B(\omega_{k\sigma})}{\omega_{k\sigma}} + \frac{3}{2}\int\frac{d^3k}{(2\pi)^3}\frac{n_B(\omega_{k\pi})}{\omega_{k\pi}},\end{aligned} \tag{5.64}$$

and

$$\begin{aligned}\frac{1}{\lambda}M_\pi^2 - \frac{a}{16\pi^2\epsilon}M_\pi^2 = \frac{1}{\lambda}m^2 + \frac{1}{2}\phi_0^2 - \frac{M_\sigma^2}{16\pi^2\epsilon} - \frac{5M_\pi^2}{16\pi^2\epsilon} \\ + \frac{1}{2}\frac{M_\sigma^2}{(4\pi)^2}\left[-1+\gamma_E+\ln\left(\frac{M_\sigma^2}{4\pi\mu^2}\right)\right] \\ + \frac{5}{2}\frac{M_\pi^2}{(4\pi)^2}\left[-1+\gamma_E+\ln\left(\frac{M_\pi^2}{4\pi\mu^2}\right)\right] \\ + \frac{1}{2}\int\frac{d^3k}{(2\pi)^3}\frac{n_B(\omega_{k\sigma})}{\omega_{k\sigma}} + \frac{5}{2}\int\frac{d^3k}{(2\pi)^3}\frac{n_B(\omega_{k\pi})}{\omega_{k\pi}}.\end{aligned} \tag{5.65}$$

From Eqs. (5.64) and (5.65), renormalizing by absorbing the divergences in the coupling constant and mass can only be done if $M_\sigma^2 = M_\pi^2$, which gives $a = 6$. As mentioned above, this is undesirable since we know that the in the broken phase, the masses are not equal. The definition of the renormalized coupling constant and mass used above is not the proper way to renormalize since it gives only symmetric solutions.

In the following, the equations are renormalized by adding temperature dependent counterterms. This approach was also used by Lenaghan and Rischke in [22]. The use of such terms is discussed in section 5.5. Dimensional regularization and the MS scheme are used. The counterterms are chosen to cancel both the ϵ-pole proportional to M_σ^2 and that proportional to M_π^2. Each integral $\int\frac{d^3k}{(2\pi)^2}\frac{1}{2\omega_{kM}}$ requires a counterterm $\frac{2M^2}{16\pi^2\epsilon}$. The renormalized equations for M_σ^2 and M_π^2 are given by

$$\begin{aligned}M_\sigma^2 = m^2 + \frac{3\lambda}{2}\phi_0^2 + \frac{3\lambda}{2}\frac{M_\sigma^2}{(4\pi)^2}\left[-1+\gamma_E+\ln\left(\frac{M_\sigma^2}{4\pi\mu^2}\right)\right] \\ + \frac{3\lambda}{2}\frac{M_\pi^2}{(4\pi)^2}\left[-1+\gamma_E+\ln\left(\frac{M_\pi^2}{4\pi\mu^2}\right)\right] \\ + \frac{3\lambda}{2}\int\frac{d^3k}{(2\pi)^3}\frac{n_B(\omega_{k\sigma})}{\omega_{k\sigma}} + \frac{3\lambda}{2}\int\frac{d^3k}{(2\pi)^3}\frac{n_B(\omega_{k\pi})}{\omega_{k\pi}},\end{aligned} \tag{5.66}$$

and

$$\begin{aligned} M_\pi^2 = m^2 + \frac{\lambda}{2}\phi_0^2 + \frac{\lambda}{2}\frac{M_\sigma^2}{(4\pi)^2}\left[-1+\gamma_E+\ln\left(\frac{M_\sigma^2}{4\pi\mu^2}\right)\right] \\ + \frac{5\lambda}{2}\frac{M_\pi^2}{(4\pi)^2}\left[-1+\gamma_E+\ln\left(\frac{M_\pi^2}{4\pi\mu^2}\right)\right] \\ + \frac{\lambda}{2}\int\frac{d^3k}{(2\pi)^3}\frac{n_B(\omega_{k\sigma})}{\omega_{k\sigma}} + \frac{5\lambda}{2}\int\frac{d^3k}{(2\pi)^3}\frac{n_B(\omega_{k\pi})}{\omega_{k\pi}}. \end{aligned} \tag{5.67}$$

Adding Eq. (5.59) to Eq. (5.60) gives $M_\sigma^2 = \lambda_B\phi_0^2$ from the bare Lagrangian, and

$$M_\sigma^2 = \lambda\phi_0^2 \tag{5.68}$$

from the Lagrangian with counterterms. In the phase of broken symmetry, the expression for M_σ^2 thus reads

$$\begin{aligned} M_\sigma^2 = -2m^2 - 3\lambda\frac{M_\sigma^2}{(4\pi)^2}\left[-1+\gamma_E+\ln\left(\frac{M_\sigma^2}{4\pi\mu^2}\right)\right] \\ - 3\lambda\frac{M_\pi^2}{(4\pi)^2}\left[-1+\gamma_E+\ln\left(\frac{M_\pi^2}{4\pi\mu^2}\right)\right] \\ - 3\lambda\int\frac{d^3k}{(2\pi)^3}\frac{n_B(\omega_{k\sigma})}{\omega_{k\sigma}} - 3\lambda\int\frac{d^3k}{(2\pi)^3}\frac{n_B(\omega_{k\pi})}{\omega_{k\pi}}. \end{aligned} \tag{5.69}$$

Inserting Eq. (5.68) into Eq. (5.67) the expression for M_π^2 reads

$$\begin{aligned} M_\pi^2 = m^2 + \frac{M_\sigma^2}{2} + \frac{\lambda}{2}\frac{M_\sigma^2}{(4\pi)^2}\left[-1+\gamma_E+\ln\left(\frac{M_\sigma^2}{4\pi\mu^2}\right)\right] \\ + \frac{5\lambda}{2}\frac{M_\pi^2}{(4\pi)^2}\left[-1+\gamma_E+\ln\left(\frac{M_\pi^2}{4\pi\mu^2}\right)\right] \\ + \frac{\lambda}{2}\int\frac{d^3k}{(2\pi)^3}\frac{n_B(\omega_{k\sigma})}{\omega_{k\sigma}} + \frac{5\lambda}{2}\int\frac{d^3k}{(2\pi)^3}\frac{n_B(\omega_{k\pi})}{\omega_{k\pi}}. \end{aligned} \tag{5.70}$$

At $T = 0$ the equations for M_σ^2 and M_π^2 read

$$\begin{aligned} m_\sigma^2 = -2m^2 - 3\lambda\frac{m_\sigma^2}{(4\pi)^2}\left[-1+\gamma_E+\ln\left(\frac{m_\sigma^2}{4\pi\mu^2}\right)\right] \\ - 3\lambda\frac{m_\pi^2}{(4\pi)^2}\left[-1+\gamma_E+\ln\left(\frac{m_\pi^2}{4\pi\mu^2}\right)\right] \end{aligned} \tag{5.71}$$

and

$$\begin{aligned} m_\pi^2 = m^2 + \frac{m_\sigma^2}{2} + \frac{\lambda}{2}\frac{m_\sigma^2}{(4\pi)^2}\left[-1+\gamma_E+\ln\left(\frac{m_\sigma^2}{4\pi\mu^2}\right)\right] \\ + \frac{5\lambda}{2}\frac{m_\pi^2}{(4\pi)^2}\left[-1+\gamma_E+\ln\left(\frac{m_\pi^2}{4\pi\mu^2}\right)\right], \end{aligned} \tag{5.72}$$

respectively, where m_σ is the zero temperature sigma mass and m_π is the zero temperature pion mass. In the chiral limit, the pions are massless at zero temperature. Inserting $m_\pi = 0$ in Eqs. (5.71) and (5.72) leads to $\overline{m}^2 \equiv -2m^2 = m_\sigma^2$ and

$$4\pi\mu^2 = m_\sigma^2 e^{\gamma_E - 1}. \tag{5.73}$$

The zero temperature sigma mass is in the range $m_\sigma^2 = 400 - 1200$ MeV [18], and here the value $m_\sigma = 600$ MeV is chosen. $\phi_0 = f_\pi$ at $T = 0$, where $f_\pi = 93$ MeV is the pion decay constant [5]. From the minimum of the classical potential V_0, a value for the coupling constant can be found,

$$\lambda = -\frac{2m^2}{f_\pi^2} = \frac{m_\sigma^2}{f_\pi^2} \approx 41.6. \tag{5.74}$$

The following is obtained for M_σ^2 at finite temperature

$$\begin{aligned} M_\sigma^2 = m_\sigma^2 - 3\lambda\frac{M_\sigma^2}{(4\pi)^2}\left[-1+\gamma_E+\ln\left(\frac{M_\sigma^2}{m_\sigma^2 e^{\gamma_E-1}}\right)\right] \\ - 3\lambda\frac{M_\pi^2}{(4\pi)^2}\left[-1+\gamma_E+\ln\left(\frac{M_\pi^2}{m_\sigma^2 e^{\gamma_E-1}}\right)\right] \\ - 3\lambda\frac{T^2}{2\pi^2}\int_0^\infty du\,\frac{u^2}{\sqrt{u^2-\frac{M_\sigma^2}{T^2}}}\frac{1}{e^{\sqrt{u^2-\frac{M_\sigma^2}{T^2}}}-1} \\ - 3\lambda\frac{T^2}{2\pi^2}\int_0^\infty du\,\frac{u^2}{\sqrt{u^2-\frac{M_\pi^2}{T^2}}}\frac{1}{e^{\sqrt{u^2-\frac{M_\pi^2}{T^2}}}-1} \end{aligned} \tag{5.75}$$

and for M_π^2

$$
\begin{aligned}
M_\pi^2 = &-\frac{1}{2}m_\sigma^2 + \frac{M_\sigma^2}{2} + \frac{\lambda}{2}\frac{M_\sigma^2}{(4\pi)^2}\left[-1+\gamma_E+\ln\left(\frac{M_\sigma^2}{m_\sigma^2 e^{\gamma_E-1}}\right)\right] \\
&+ \frac{5\lambda}{2}\frac{M_\pi^2}{(4\pi)^2}\left[-1+\gamma_E+\ln\left(\frac{M_\pi^2}{m_\sigma^2 e^{\gamma_E-1}}\right)\right] \\
&+ \frac{\lambda}{2}\frac{T^2}{2\pi^2}\int_0^\infty du\,\frac{u^2}{\sqrt{u^2-\frac{M_\sigma^2}{T^2}}}\frac{1}{e^{\sqrt{u^2-\frac{M_\sigma^2}{T^2}}}-1} \\
&+ \frac{5\lambda}{2}\frac{T^2}{2\pi^2}\int_0^\infty du\,\frac{u^2}{\sqrt{u^2-\frac{M_\pi^2}{T^2}}}\frac{1}{e^{\sqrt{u^2-\frac{M_\pi^2}{T^2}}}-1}.
\end{aligned}
\tag{5.76}
$$

ϕ_0^2 is given by Eq. (5.68).

When $\phi_0 = 0$ the $O(4)$ symmetry is restored. By inserting $\phi_0 = 0$ into Eqs. (5.66) and (5.67) and subtracting the latter from the former, it is easy to see that $M_\sigma^2 = M_\pi^2 = M^2$ in this phase. The masses become degenerate. The renormalized expression for M^2 is given by

$$
\begin{aligned}
M^2 = &-\frac{1}{2}m_\sigma^2 + 3\lambda\frac{M^2}{(4\pi)^2}\left[-1+\gamma_E+\ln\left(\frac{M^2}{m_\sigma^2 e^{\gamma_E-1}}\right)\right] \\
&+ 3\lambda\frac{T^2}{2\pi^2}\int_0^\infty du\,\frac{u^2}{\sqrt{u^2-\frac{M^2}{T^2}}}\frac{1}{e^{\sqrt{u^2-\frac{M^2}{T^2}}}-1}.
\end{aligned}
\tag{5.77}
$$

To find a value of the lowest temperature at which $\phi_0 = 0$ is a minimum of the effective potential, $M = 0$ is inserted into Eq. (5.77). The following is obtained

$$
\frac{1}{2}m_\sigma^2 = \frac{\lambda T_{c1}^2}{4}, \tag{5.78}
$$

which gives

$$
T_{c1} = \sqrt{\frac{2m_\sigma^2}{\lambda}} \approx 131.6 \text{ MeV}. \tag{5.79}
$$

The results from solving Eqs. (5.75), (5.76) and (5.77) numerically are shown in Fig. 5.7. A plot ϕ_0 in shown in Fig. 5.8. For values of T between $T_{c1} \approx 131.6$ MeV and $T_{c2} \approx 235$ MeV in the renormalized case, and $T_{c1} \approx 131.6$ MeV and $T_{c2} \approx 190$ MeV in the nonrenormalized case, ϕ_0 has several values for the same temperature. There are two local minima and a local maximum of the potential [5]. At $T = T_{c1}$ ϕ_0 occurs as a local minimum of the effective potential, but the global minimum is $\phi_0 \neq 0$. At $T = T_{c2}$,

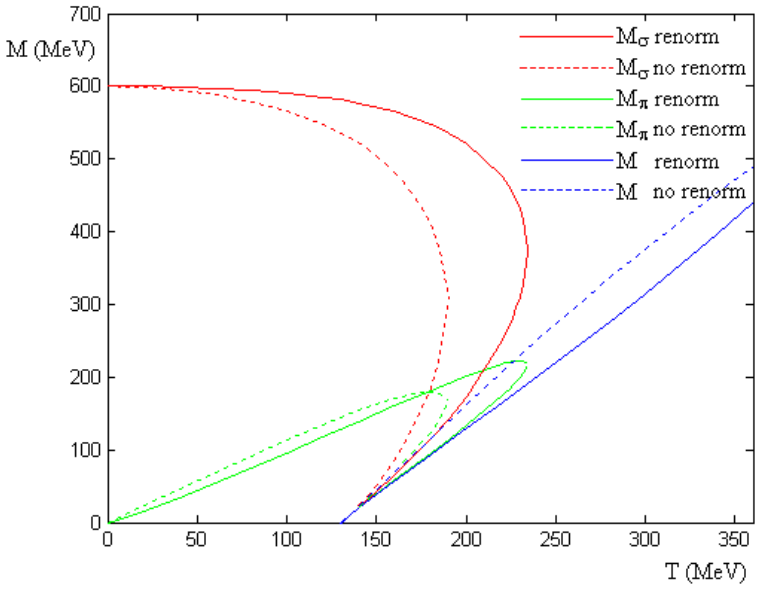

Figure 5.7: The sigma mass M_σ, pion mass M_π and the mass in the symmetric phase, M, as functions of temperature in the Hartree approximation. The renormalized masses (solid lines) are qualitatively the same as the nonrenormalized masses (dotted lines).

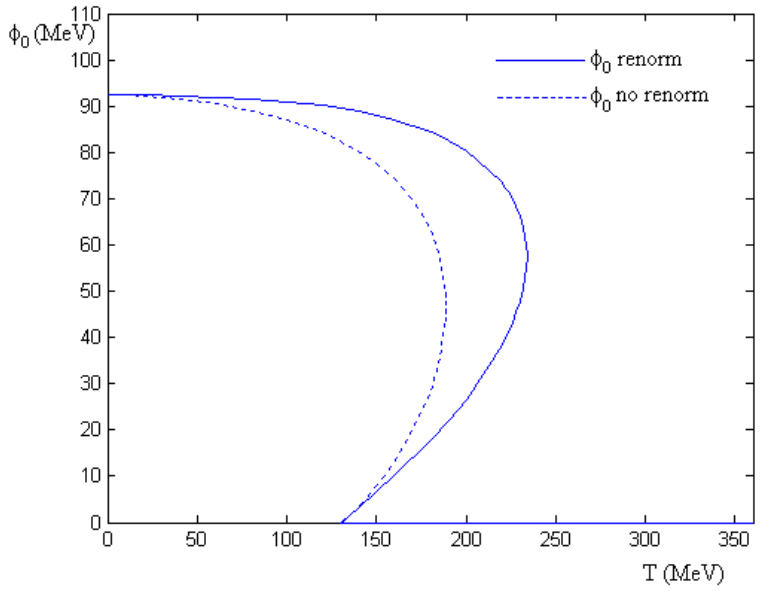

Figure 5.8: ϕ_0 as a function of temperature in the renormalized (solid line) case and in the nonrenormalized (dotted line) case. The order parameter is qualitatively the same in the two cases. ϕ_0 indicates that a first-order phase transition takes place in the Hartree approximation.

$\phi_0 = 0$ is the global minimum. At some temperature $T = T_c$ between T_{c1} and T_{c2}, the global minimum changes from being located at $\phi_0 \neq 0$ to being located at $\phi_0 = 0$. A first order phase transition takes place at $T = T_c$.

Renormalization does not qualitatively change the order parameter or the masses. T_{c1} is the same for the renormalized case and the nonrenormalized case, since when $M = 0$ the contribution from the temperature-independent term disappears. T_c and T_{c2} are different in the two cases. The temperature at which the phase transition occurs is larger in the renormalized case than in the case where the zero-temperature contributions have been omitted.

5.3.2 The physical point

The result of a nonzero value of h is that $\phi_0 = 0$ is no longer a minimum of the potential since $\frac{\partial V_{eff}}{\partial \phi_0} \rightarrow \frac{\partial V_{eff}}{\partial \phi_0} - h$. The equation for ϕ_0^2 in the broken phase reads

$$\begin{aligned} \frac{\lambda_B}{2}\phi_0^2 = \frac{h}{\phi_0} - m_B^2 - \frac{3\lambda_B}{2}\sum\!\!\!\!\!\!\int_k \frac{1}{\omega_n^2 + \omega_{k\sigma}^2} \\ - \frac{3\lambda_B}{2}\sum\!\!\!\!\!\!\int_k \frac{1}{\omega_n^2 + \omega_{k\pi}^2}, \end{aligned} \tag{5.80}$$

The equations for M_σ^2 and M_π^2 remain the same and are given by Eqs. (5.60) and (5.61). The renormalized equations are given by Eqs. (5.66) and (5.67) Adding Eq. (5.60) to Eq. (5.80) gives $h = \phi_0 \left[M_\sigma^2 - \lambda_B \phi_0^2\right]$, or from the Lagrangian with counterterms

$$h = \phi_0 \left[M_\sigma^2 - \lambda \phi_0^2\right]. \tag{5.81}$$

At zero temperature $\phi_0 = f_\pi$, $M_\sigma^2 = m_\sigma^2$ and $M_\pi^2 = m_\pi^2$. In this case the zero temperature pion mass is $m_\pi = 139.6$ MeV [18]. The zero temperature values of m_σ and ϕ_0 are $m_\sigma = 600$ MeV and $\overline{\phi}_0 = 93$ MeV as before. From Eq. (5.81) the following is obtained at zero temperature

$$\lambda = \frac{m_\sigma^2 - \frac{h}{f_\pi}}{f_\pi^2} \tag{5.82}$$

Subtracting Eq. (5.67) from Eq. (5.66) at zero temperature, λ can be written as

$$\lambda = \frac{m_\sigma^2 - m_\pi^2}{f_\pi^2 + \frac{m_\sigma^2}{(4\pi)^2}\left[-1 + \gamma_E + \ln\left(\frac{m_\sigma^2}{4\pi\mu^2}\right)\right] - \frac{m_\pi^2}{(4\pi)^2}\left[-1 + \gamma_E + \ln\left(\frac{m_\pi^2}{4\pi\mu^2}\right)\right]}. \tag{5.83}$$

For Eqs. (5.82) and (5.83) to be consistent, $m_\pi^2 = \frac{h}{f_\pi}$ and

$$\frac{m_\sigma^2}{(4\pi)^2}\left[-1+\gamma_E+\ln\left(\frac{m_\sigma^2}{4\pi\mu^2}\right)\right] = \frac{m_\pi^2}{(4\pi)^2}\left[-1+\gamma_E+\ln\left(\frac{m_\pi^2}{4\pi\mu^2}\right)\right], \quad (5.84)$$

giving

$$\lambda = \frac{m_\sigma^2 - m_\pi^2}{f_\pi^2}. \quad (5.85)$$

By rearranging the terms in Eq. (5.84), the following is obtained

$$\begin{aligned} & m_\sigma^2 \ln\left(\frac{m_\sigma^2}{4\pi\mu^2}\right) - m_\pi^2 \ln\left(\frac{m_\pi^2}{4\pi\mu^2}\right) \\ & = m_\sigma^2 \ln\left(\frac{600^2(\text{MeV})^2}{4\pi\mu^2}\right) - m_\pi^2 \ln\left(\frac{139.6^2(\text{MeV})^2}{4\pi\mu^2}\right) \\ & = m_\pi^2(\gamma_E - 1) - m_\sigma^2(\gamma_E - 1) \end{aligned} \quad (5.86)$$

giving

$$4\pi\mu^2 = e^{\frac{m_\sigma^2(\gamma_E-1) - m_\pi^2(\gamma_E-1) + m_\sigma^2 \ln 600^2 - m_\pi^2 \ln 139.5^2}{m_\sigma^2 - m_\pi^2}} (\text{MeV})^2. \quad (5.87)$$

An expression for the renormalized mass parameter m can be found from Eqs. (5.66) and (5.67) at zero temperature and reads

$$\begin{aligned} \overline{m}^2 \equiv -2m^2 = m_\sigma^2 - 3m_\pi^2 \\ + 6\lambda \frac{m_\pi^2}{(4\pi)^2}\left[-1+\gamma_E+\ln\left(\frac{m_\pi^2}{4\pi\mu^2}\right)\right]. \end{aligned} \quad (5.88)$$

From the values of the zero temperature parameters given above, the following is obtained; $4\pi\mu^2 = (527.9\text{ MeV})^2$, $\lambda = 39.37$, $h = (121.9\text{ MeV})^3$ and $\overline{m} = 460.1$ MeV.

The results from solving Eqs. (5.66), (5.67) and (5.81) numerically are shown in Figs. 5.9 and 5.10. At zero temperature, the sigma and pion effective masses appear as the observed masses. At high temperatures the sigma and pions have the same effective mass. They become degenerate when the thermal contributions to the effective masses dominate, since h is a constant and does not contribute when $T \to \infty$. ϕ_0 decreases with temperature and approaches zero smoothly at high temperatures. There is no phase transition in this case, but rather a smooth crossover. Qualitatively, renormalization does not change the results.

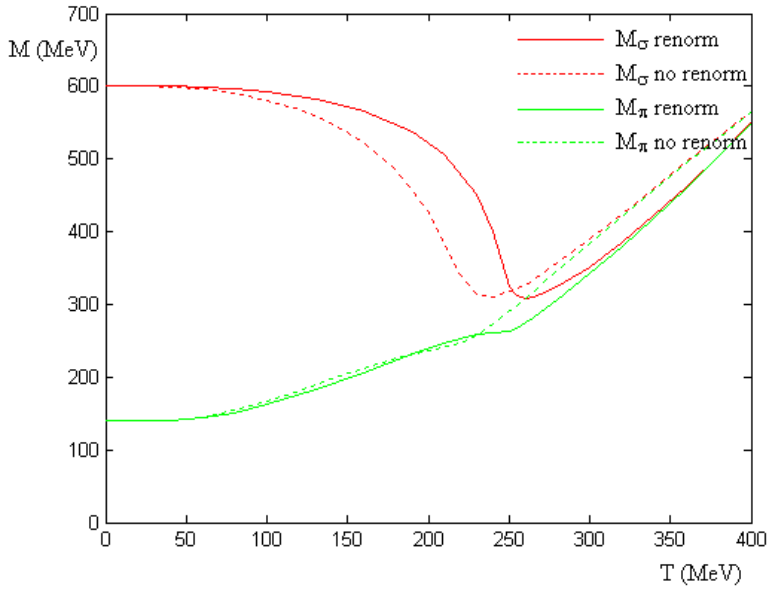

Figure 5.9: M_σ and M_π as functions of temperature in the case of explicitly broken symmetry. The renormalized masses (solid lines) and the non-renormalized masses (dotted lines) are not qualitatively different.

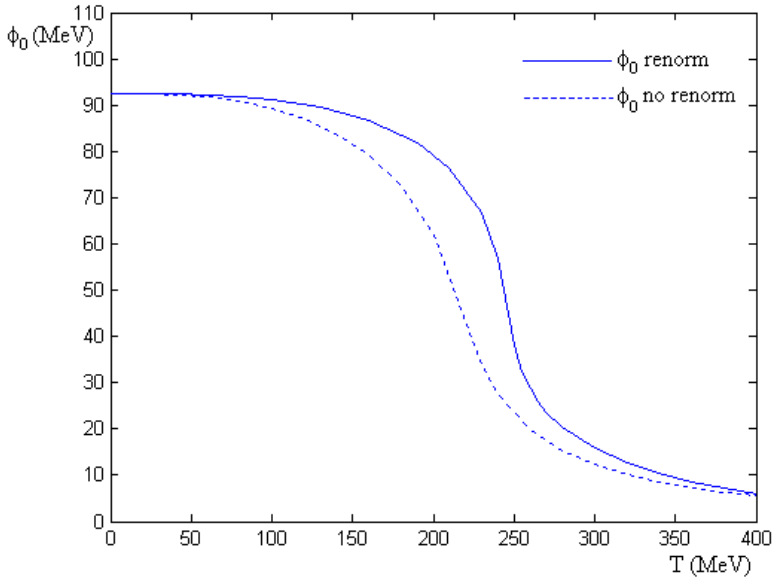

Figure 5.10: ϕ_0 as a function of temperature in the case of explicitly broken symmetry. The renormalized order parameter (solid line) is not qualitatively different from the nonrenormalized order parameter (dotted line). When the symmetry is explicitly broken, there is no phase transition, but rather a smooth crossover.

5.4 The $O(4)$ linear sigma model in the large-N approximation

Above we found that renormalizing the gap equations in the Hartree approximation by defining the renormalized coupling constant as $\frac{1}{\lambda} = \frac{1}{\lambda_B} + \frac{a}{16\pi^2\epsilon}$ and the renormalized mass as $m^2 = \frac{\lambda}{\lambda_B} m_B^2$, does not work. In the following section, it is shown that the above definitions of the renormalized coupling constant and mass can be used to renormalize the gap equations in the large-N approximation. Andersen used this approach in [20]. Both the chiral limit and the physical point will be studied.

5.4.1 The chiral limit

The equations for ϕ_0^2, M_σ^2 and M_π^2 in the large-N approximation in the broken phase are found by inserting $N = 4$ in Eqs. (5.53), (5.54) and (5.55). The following equation is obtained for the order parameter in the broken phase

$$\frac{\lambda_B}{2}\phi_0^2 = -m_B^2 - 2\lambda_B \sum\!\!\!\!\!\!\int_k \frac{1}{\omega_n^2 + \omega_{k\pi}^2}. \tag{5.89}$$

The equations for M_σ^2 and M_π^2 are given by

$$M_\sigma^2 = m_B^2 + \frac{3\lambda_B}{2}\phi_0^2 + 2\lambda_B \sum\!\!\!\!\!\!\int_k \frac{1}{\omega_n^2 + \omega_{k\pi}^2} \tag{5.90}$$

and

$$M_\pi^2 = m_B^2 + \frac{\lambda_B}{2}\phi_0^2 + 2\lambda_B \sum\!\!\!\!\!\!\int_k \frac{1}{\omega_n^2 + \omega_{k\pi}^2}. \tag{5.91}$$

As seen from Eqs. (5.89) and (5.91), $M_\pi^2 = 0$ in the broken phase. Using dimensional regularization, the expression for M_σ^2 can be written as

$$\begin{aligned} M_\sigma^2 &= m_B^2 + \frac{3\lambda_B}{2}\phi_0^2 + 2\lambda_B \frac{M_\pi^2}{(4\pi)^2}\left[-\frac{2}{\epsilon} - 1 + \gamma_E + \ln\left(\frac{M_\pi^2}{4\pi\mu^2}\right)\right] \\ &\quad + 2\lambda_B \int \frac{d^3k}{(2\pi)^3}\frac{n_B(\omega_{k\pi})}{\omega_{k\pi}} \\ &= m_B^2 + \frac{3\lambda_B}{2}\phi_0^2 + 2\lambda_B \int \frac{d^3k}{(2\pi)^3}\frac{n_B(k)}{k}. \end{aligned} \tag{5.92}$$

The integral in the last line in Eq. (5.92) has been calculated in section 3.9. It gives $\frac{T^2}{12}$. Dividing Eq. (5.92) by λ_B and using the expression we found in section 5.1 for the renormalized mass, $m^2 = \frac{\lambda}{\lambda_B} m_B^2$, gives

$$\frac{1}{\lambda_B}M_\sigma^2 = \frac{1}{\lambda}m^2 + \frac{3}{2}\phi_0^2 + \frac{T^2}{6}. \tag{5.93}$$

Adding Eq. (5.89) to Eq. (5.90), M_σ^2 can be related to the order parameter by

$$\lambda_B\phi_0^2 = M_\sigma^2. \tag{5.94}$$

By inserting this into Eq. (5.93) the following is obtained

$$\frac{\lambda}{2}\phi_0 = -m^2 - \frac{\lambda T^2}{6} \tag{5.95}$$

and

$$M_\sigma^2 = -2m^2 - \frac{\lambda T^2}{3}. \tag{5.96}$$

At $T = 0$, $\phi_0 = f_\pi$ and $M_\sigma^2 = m_\sigma^2$, which have the values $m_\sigma = 600$ MeV and $f_\pi = 93$ MeV as before. From Eq. (5.96) at zero temperature it is found that $\overline{m}^2 \equiv -2m^2 = m_\sigma^2$. As in the Hartree approximation, λ is calculated from the minimum of the classical potential V_0 and is given by $\lambda = 41.6$. In this case, however, it is not possible to find a value of $4\pi\mu^2$ from the zero-temperature parameters. Thus μ is a free parameter. The finite-temperature equation for M_σ^2 in the broken phase is given by

$$M_\sigma^2 = m_\sigma^2 - \frac{\lambda T^2}{3}, \tag{5.97}$$

and the order parameter in the broken phase is given by $\phi_0^2 = \frac{M_\sigma^2}{\lambda}$.

When $\phi_0^2 = 0$, Eqs. (5.90) and (5.91) gives $M_\sigma^2 = M_\pi^2 = M^2$. The masses become degenerate in the symmetric phase. The equation for M^2 is given by

$$M^2 = m_B^2 + 2\lambda_B \sum\!\!\!\!\!\!\int_k \frac{1}{\omega_n^2 + \omega_{kM}^2}, \tag{5.98}$$

Eq. (5.98) can be renormalized in the same way we renormalized Eq. (5.9). Using dimensional regularization the equation can be written as

$$M^2 = m_B^2 + 2\lambda_B \frac{M^2}{(4\pi)^2}\left[-\frac{2}{\epsilon} - 1 + \gamma_E + \ln\left(\frac{M^2}{4\pi\mu^2}\right)\right] + 2\lambda_B \int \frac{d^3k}{(2\pi)^3}\frac{n_B(\omega_{kM})}{\omega_{kM}}. \tag{5.99}$$

Dividing by λ_B and using the expressions $\frac{1}{\lambda} = \frac{1}{\lambda_B} + \frac{1}{4\pi^2\epsilon}$ and $m^2 = \frac{\lambda}{\lambda_B}m_B^2$ for the renormalized coupling constant and mass, respectively, the following renormalized equation for M^2 is obtained

$$M^2 = -\frac{1}{2}m_\sigma^2 + 2\lambda \frac{M^2}{(4\pi)^2}\left[-1 + \gamma_E + \ln\left(\frac{M^2}{4\pi\mu^2}\right)\right] + 2\lambda \int \frac{d^3k}{(2\pi)^3}\frac{n_B(\omega_{kM})}{\omega_{kM}}, \tag{5.100}$$

where we have used that $m^2 = -\frac{1}{2}m_\sigma$. Inserting $M^2 = 0$ in Eq. (5.100) gives

$$\frac{1}{2}m_\sigma^2 = \lambda\frac{T_c^2}{6}. \tag{5.101}$$

Thus, the value for the critical temperature is

$$T_c = \sqrt{\frac{3m_\sigma^2}{\lambda}} \approx 161 \text{ MeV}. \tag{5.102}$$

The results from solving Eq. (5.100) numerically are shown in Fig. 5.11, together with the masses in the broken phase. A plot of ϕ_0 is shown in Fig. 5.12. Here, the renormalization parameter μ is given the value $\mu = 1$ GeV. This is the value of the symmetry breaking scale, given by $\Lambda \sim 4\pi f_\pi \sim 1$ GeV. The $O(4)$ linear sigma model is a low-energy effective theory and the only particles involved are the sigma and pion mesons with masses smaller than Λ.

In this approximation Goldstone's theorem is satisfied since the pions are massless in the broken phase. At high temperatures the masses become degenerate due to the thermal contributions. The plot of ϕ_0 indicates a second-order phase transition as it vanishes continuously at T_c.

In the large-N approximation the only divergence in the expression for M_σ is proportional to M_π. Since $M_\pi = 0$ in the broken phase, the results from renormalizing are the same as simply dropping the temperature-independent term. This is seen in Fig. 5.11. In the symmetric case, the masses are qualitatively the same in the renormalized case and the non-renormalized case, but in the renormalized case the masses depend on the choice of μ. Renormalization does not affect the order parameter.

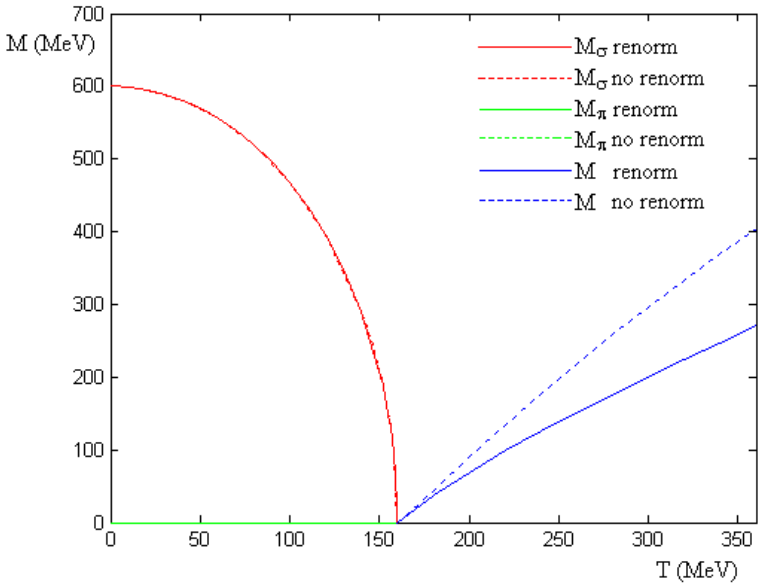

Figure 5.11: The sigma mass M_σ, pion mass M_π, and the mass, M, in the symmetric phase as functions of temperature. In the broken phase, there is no difference between the renormalized (solid line) and the non-renormalized (dotted lines) cases. In the phase of restored symmetry, the renormalized mass depends on the choice of μ.

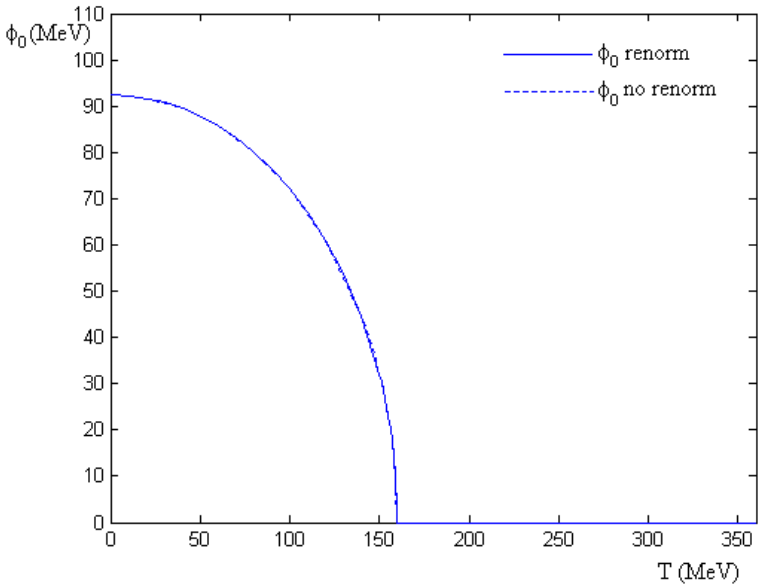

Figure 5.12: ϕ_0 as a function of temperature. There is no difference between the renormalized and the nonrenormalized cases. The order parameter indicates a second-order phase transition.

5.4.2 The physical point

By subtracting a term $h\phi_\sigma$ from the Lagrangian, the $\phi_0 = 0$ solution no longer exists. Instead, the equation for ϕ_0^2 in the broken phase reads

$$\frac{\lambda_B}{2}\phi_0^2 = \frac{h}{\phi_0} - m_B^2 - 2\lambda_B \sum\!\!\!\!\!\!\int_k \frac{1}{\omega_n^2 + \omega_{k\pi}^2}. \tag{5.103}$$

The equations for M_σ^2 and M_π^2 are given by Eqs. (5.90) and (5.91), respectively. Subtracting Eq. (5.91) from Eq. (5.90) gives

$$M_\sigma^2 - M_\pi^2 = \lambda_B \phi_0^2. \tag{5.104}$$

Eq. (5.91) can be renormalized by using dimensional regularization and inserting $\frac{1}{\lambda} = \frac{1}{\lambda_B} + \frac{1}{4\pi^2\epsilon}$ and $m^2 = \frac{\lambda}{\lambda_B} m_B^2$. The renormalized equation for M_π^2 reads

$$\begin{aligned} M_\pi^2 = m^2 &+ \frac{\lambda}{2}\phi_0^2 + 2\lambda \frac{M_\pi^2}{(4\pi)^2}\left[-1 + \gamma_E + \ln\left(\frac{M_\pi^2}{4\pi\mu^2}\right)\right] \\ &+ 2\lambda \int \frac{d^3k}{(2\pi)^3}\frac{n_B(\omega_{k\pi})}{\omega_{k\pi}}. \end{aligned} \tag{5.105}$$

Eq. (5.104) holds in any renormalization scheme. If the left-hand side is a renormalized expression, so is the right-hand side. This gives the following renormalized equation for M_σ^2

$$\begin{aligned} M_\sigma^2 &= M_\pi^2 + \lambda\phi_0^2 \\ &= m^2 + \frac{3\lambda}{2}\phi_0^2 + 2\lambda \frac{M_\pi^2}{(4\pi)^2}\left[-1 + \gamma_E + \ln\left(\frac{M_\pi^2}{4\pi\mu^2}\right)\right] \\ &+ 2\lambda \int \frac{d^3k}{(2\pi)^3}\frac{n_B(\omega_{k\pi})}{\omega_{k\pi}}. \end{aligned} \tag{5.106}$$

From Eqs. (5.91) and (5.103) the order parameter can be related to M_π by

$$\phi_0 = \frac{h}{M_\pi^2}. \tag{5.107}$$

At zero temperature, $\phi_0 = f_\pi$, $M_\sigma^2 = m_\sigma^2$ and $M_\pi^2 = m_\pi^2$. As in the explicitly broken symmetry case in the Hartree approximation $m_\pi = 139.6$ MeV, $h = m_\pi^2 f_\pi = (121.9 \text{ MeV})^3$ and $\lambda = \frac{m_\sigma^2 - m_\pi^2}{f_\pi^2} = 39.37$. The pion decay constant and zero-temperature sigma mass are given by $f_\pi = 93$ MeV and

$m_\sigma = 600$ MeV, as before. μ is a free parameter as in the chiral limit in the large-N approximation, and is again chosen to be $\mu = 1$ GeV. An expression for m^2 is found from Eqs. (5.105) and (5.106) at zero temperature and is given by

$$\begin{aligned} \overline{m}^2 &\equiv -2m^2 \\ &= m_\sigma^2 - 3m_\pi^2 \\ &+ 4\lambda \frac{m_\pi^2}{(4\pi)^2}\left[-1 + \gamma_E + \ln\left(\frac{m_\pi^2}{4\pi\mu^2}\right)\right] \\ &= (409.4 \text{ MeV})^2 . \end{aligned} \tag{5.108}$$

The results from solving Eqs. (5.105), (5.106) and (5.107) numerically are shown in Figs. 5.13 and 5.14. As in the explicitly broken case in the Hartree approximation, the pion and sigma masses start at their observed values at zero temperature. At high temperatures they become degenerate due to the contribution from the thermal bath. As mentioned in the explicitly broken case in the Hartree approximation, this happens because h is independent of temperature and does not matter when $T \to \infty$. There is no phase transition, but a smooth crossover. Renormalization does not qualitatively change the results.

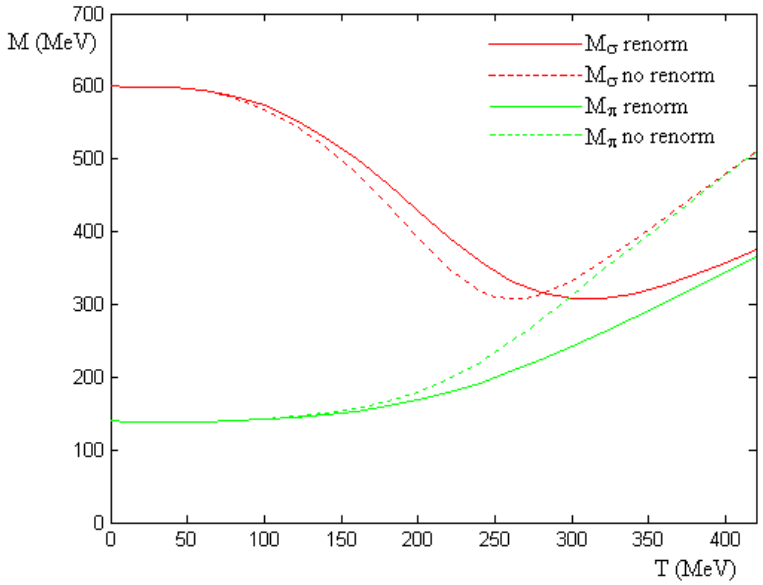

Figure 5.13: M_σ and M_π as functions of temperature in the case of explicitly broken symmetry. The renormalized masses (solid lines) does not differ qualitatively from the nonrenormalized masses (dotted lines).

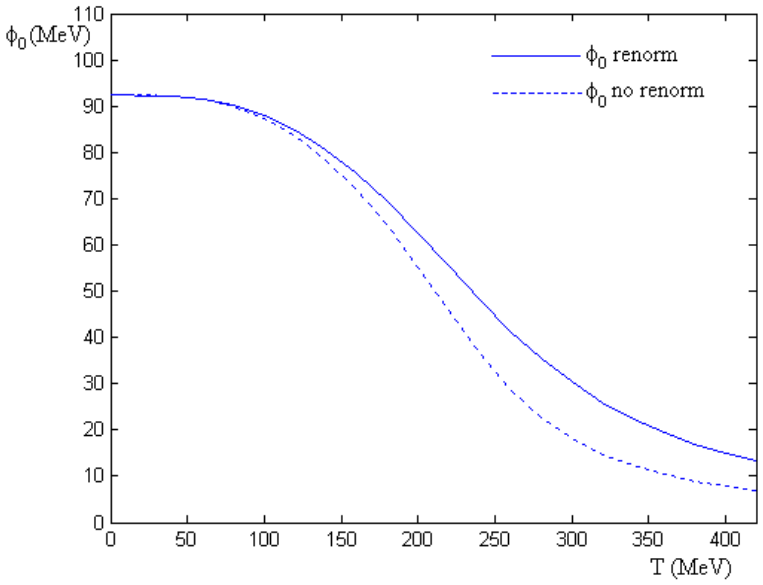

Figure 5.14: ϕ_0 as a function of temperature. The order parameter is not qualitatively different in the renormalized (solid line) and nonrenormalized (dotted line) cases. There is no phase transition when the symmetry is explicitly broken, but rather a smooth crossover.

5.5 Results and discussion of the Hartree and large-N approximations

Above, the $O(4)$ linear sigma model has been studied in the Hartree and large-N approximations, both with and without an explicitly symmetry breaking term $h\phi_\sigma$. The term $h\phi_\sigma$ generates mass for the low temperature pions [5]. The gap equations are renormalized, and the results are compared with the case where the zero-temperature contributions have been omitted. Both approximations restore chiral symmetry at high temperatures, as expected. The results agree with those obtained by other authors, e.g. [5, 22].

When $h = 0$ the Hartree approximation predicts a first-order phase transition. At temperature T_c, $\phi_0 \neq 0$ and $\phi_0 = 0$ change role as the global minimum of the potential. At T_c there are thus two values of the order parameter ϕ_0 giving the same minimum, which signals a first-order phase transition. In the large-N approximation for $h = 0$, the order parameter approaches zero continuously for $T < T_c$ and is zero for $T \geq T_c$. In this approximation the phase transition takes place at $T_c = 161$ MeV. The large-N approximation predicts a second-order phase transition. Lattice calculations and other effective models suggest that the chiral phase transition when considering two massless quarks, is of second order [5]. Thus, the large-N approximation seems to be in agreement with other models concerning the

order of the phase transition.

In the Hartree approximation, the pions in the broken phase are not massless except at $T = 0$, where $m_\pi = 0$ was chosen. Thus, Goldstone's theorem is violated, and no Goldstone bosons occur in the broken phase. Throughout this thesis we have used $\hbar = 1$. Restoring $\hbar$ gives $\mathcal{L} \to \frac{1}{\hbar}\mathcal{L}$. The propagator is the inverse of the differential operator in the quadratic terms occurring in $\frac{1}{\hbar}\mathcal{L}$. Thus, each line I contains a factor of $\hbar$. Each vertex V contains a factor $\frac{1}{\hbar}$. This gives the power P in $\hbar$ as $P = I - V$. The number of loops L is the number of internal momentum integrations, corresponding to the number of internal lines minus the number of vertices due to the momentum conserving δ-functions there. Including the overall momentum conservation of the graph at one of the vertices, gives $L = I - V + 1 = P + 1$. Thus, counting the power of $\hbar$ counts the number of loops and a loop expansion is essentially an expansion in powers of the Lagrangian. This feature is important for theories containing some symmetry, such as the $O(4)$ linear sigma model. Individual graphs of such theories do not necessarily obey the symmetry, but the sum of all graphs containing the same number of loops represents the symmetry [23]. For a fixed number of loops n, the symmetry of the Lagrangian is respected if all diagrams containing n loops are included. In the Hartree approximation, only the double-bubble diagram is included in the calculations, and the sunset diagram is not considered even though is has as many loops as the double-bubble. The Hartree approximation is not consistent in the number of loops. Thus the symmetry of the Lagrangian is not respected, leading to violation of Goldstone's theorem [2]. The Hartree approximation includes some, but not all next-to-leading order contributions in $\frac{1}{N}$, and is thus not consistent in $\frac{1}{N}$ either.

In the broken phase in the large-N approximation, the pions are massless and Goldstone's theorem is satisfied. All diagrams with two-loops are included, although only the double-bubble diagrams survive the $N \to \infty$ limit. The sunset diagram is not just simply dropped as in the Hartree approximation, it disappears when the $\frac{1}{N}$ terms are neglected.

When $h \neq 0$, the $O(4)$ symmetry is explicitly broken down to $O(3)$. In this case there is no phase transition, but rather a smooth crossover. The pion and sigma masses start at the experimental values at zero temperature. The masses become degenerate at high temperatures since at high temperatures the thermal contributions dominate. When $h = 0$ the phase transition is of first order in the Hartree approximation and of second order in the large-N approximation. This is seen in Fig. 5.15, as the first-order phase transition at $h = 0$ leaves the order parameter ϕ_0 at $h \neq 0$ steeper in the Hartree approximation compared to the large-N approximation. The case of nonzero h gives a better description of the real world, since pions have nonzero masses and are considered as pseudo-Goldstone bosons.

As was seen in section 5.3, the gap equations in the Hartree approximation cannot be renormalized by defining $\frac{1}{\lambda} = \frac{1}{\lambda_B} + \frac{a}{16\pi^2\epsilon}$ and $m^2 = \frac{\lambda}{\lambda_B} m_B^2$,

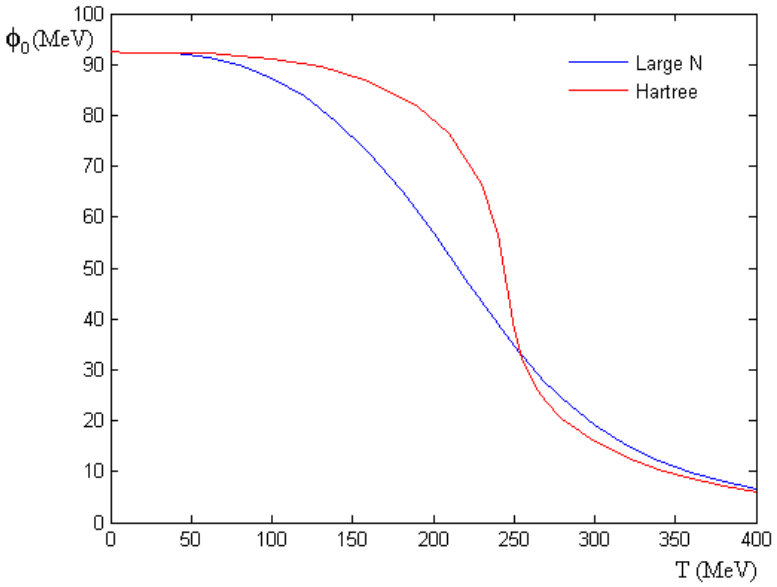

Figure 5.15: The order parameter in Hartree and large N approximation when $h \neq 0$. The first-order phase transition which is predicted in the Hartree approximation when $h = 0$ leaves the order parameter at $h \neq 0$ steeper than in the large-N approximation.

because it required $M_\sigma = M_\pi$ for all values of ϕ_0. The equations in the Hartree approximation are renormalized by adding temperature-dependent counterterms. However, counterterms should in general not depend on temperature, as the counterterms depend on ϵ as $\frac{1}{\epsilon}$. This is in contradiction with the physical picture where short distance physics cannot be affected by the physics in the infrared [16]. In addition to the inconsistencies mentioned above, the Hartree approximation suffers from renormalization problems.

Renormalization by absorbing the divergence in the coupling constant and mass does work in the large-N approximation. This approximation does not suffer from the renormalization problems which the Hartree approximations suffers from, and can be renormalized with temperature-independent counterterms.

Compared to the case where the zero-temperature contributions are not included in the calculations, renormalization does not qualitatively change the results. In the broken phase in the large-N approximation, the renormalization does not affect the results at all. The reason for this is that $M_\pi = 0$ for all temperatures in the broken phase. As the temperature-independent integral in the equation for M_σ is proportional to M_π after using dimensional regularization, this contribution disappears. This is thus the same as simply dropping the temperature-independent contribution. In this approximation,

μ is a free parameter, and in the phase of restored symmetry, the masses of the sigma and pions depend on the choice of μ. In the Hartree approximation, the renormalization parameter μ is fixed in order for the equations to be consistent with zero-temperature parameters. The figures throughout this section show that renormalization quantitatively changes the results in the Hartree approximation more than in the large-N approximation.

6 SUMMARY

In section 3.10 it was seen that the finite-temperature scalar $\lambda\phi^4$-theory suffers from IR divergences. These divergences arise because the bosons acquire thermal mass when they propagate through the thermal bath. The free propagator $\frac{1}{\omega_n^2+\omega_k^2}$ should be replaced by the effective propagator $\frac{1}{\omega_n^2+\omega_k^2+M^2}$, which includes the thermal mass M. The problems with IR divergences lead to a breakdown of ordinary perturbation theory, and a resummation of an infinite set of Feynman diagrams, daisy diagrams, is needed. The effective propagator represents the resummation of daisy diagrams. In the high temperature limit, where the temperature is much larger than the zero temperature mass, thermal fluctuations contribute to the mass as $\sqrt{\lambda}T$ at one loop.

The contribution to the mass from thermal fluctuations is also important when studying phase transitions. As seen in section 5.1, the symmetry of the $\lambda\phi^4$-theory is spontaneously broken at zero temperature when the parameter $m_B^2 < 0$. As the temperature increases, the thermal fluctuations contribute increasingly to the mass. At some critical temperature the thermal contributions dominate and the symmetry is restored.

A series of phase transitions is believed to have taken place in the early Universe. The QCD phase transition is one of them. Deconfinement of quarks and gluons and restoration of chiral symmetry are related to the QCD phase transition. The $O(4)$ linear sigma model can be used as an effective theory for QCD at low temperatures. It describes the physics of mesons and makes it possible to study the chiral phase transition. The model displays many important aspects of the phase transition. In section 5, the $O(4)$ linear sigma model was considered in both Hartree and large-N approximations. The self-consistent equations for the sigma and pion masses were renormalized. As was seen, the divergent terms depended on the temperature through the effective mass M, as the divergences occured as $\sim \frac{M^2}{\epsilon}$. Using temperature-dependent counterterms is not a good way to renormalize. The large-N approximation could however be renormalized by defining the renormalized coupling constant $\frac{1}{\lambda} = \frac{1}{\lambda_B} + \frac{1}{4\pi^2\epsilon}$ and the renormalized mass $m^2 = \frac{\lambda}{\lambda_B}m_B^2$. This approach did not work in the Hartree approximation, and the gap equations in this approximation was renormalized by using temperature-dependent counterterms. In addition to the renormalization problems, the results obtained in the Hartree approximation are not consistent with the results obtained in other models as it predicts a first-order phase transition. Goldstone's theorem is violated in this approximation. The large-N approximation agree with other models, as it predicts a phase transition of second order. Goldstone's theorem is satisfied in this approximation.

Including a term in the Lagrangian which represents the mass of pions,

there is no phase transition but rather a smooth crossover. Pions are interpreted as pseudo-Goldstone bosons with small, but nonzero mass. This case gives a better description of the real world.

The linear sigma model is only an approximation to the underlying theory, which is QCD, but studying the phase transition in this model might help in the understanding of the QCD phase transition in the early Universe.

References

[1] M. Le Bellac. *Thermal Field Theory.* Cambridge University Press, 2000.

[2] J.I. Kapusta. *Finite-Temperature Field Theory.* Cambridge University Press, 1989.

[3] M. Guidry. *Gauge Field Theories. An introduction with applications.* John Wiley and sons, Inc., 1991.

[4] A. Das. *Finite temperature field theory.* World Scientific Publishing Co. Pte. Ltd., 1997.

[5] N. Petropoulos. Linear sigma model at finite temperature. *arXiv:hep-ph/0402136v1*, 2004.

[6] T. Matsubara. A new approach to quantum-statistical mechanics. *Prog. Theor. Phys., Vol 14, No. 4*, 1955.

[7] F. Mandl and G. Shaw. *Quantum field theory.* John Wiley and sons, Inc., 2005.

[8] M. Stone. *The physics of quantum fields.* Springer-Verlag New York, Inc., 2000.

[9] M. E. Peskin and D. V. Schroeder. *An introduction to quantum field theory.* Westview Press, 1995.

[10] J. Lindeberg and Y. Öhrn. *Propagators in Quantum chemistry.* John Wiley and sons, Inc., 2004.

[11] E. Kreyszig. *Advanced engineering mathematics.* John Wiley and sons, Inc., 1999.

[12] J.-P. Blaizot and E. Iancu. *QCD Perspectives on Hot and Dense Matter.* Kluwer Academic Publishers, 2002.

[13] V. Stepin. *Theoretical knowledge.* Springer, 2005.

[14] H. Kleinert and V. Schulte-Frohlinde. *Critical properties of ϕ^4 theories.* World Scientific Publishing Co. Ptc. Ltd., 2001.

[15] G. 'tHooft. Dimensional regularization and the renormalization group. *Nuclear Physics B61, 455-468*, 1973.

[16] A. Jakovac and Zs. Szep. Renormalization and resummation in finite temperature field theories. *Phys.Rev. D71 (2005) 105001*, 2004.

[17] T. Mannel. *Effective Field Theories in Flavour Physics.* Springer, 2004.

[18] S. Eidelman et al. *Particle Physics Booklet.* Particle Data Group, 2004.

[19] P. Coles and F. Lucchin. *Cosmology: The origin and evolution of cosmic structure.* John Wiley and Sons, 2002.

[20] J.O. Andersen. Pion and kaon condensation at finite temperature and density. *Phys. Rev. D75, 065011 (2007)*, 2007.

[21] J.M. Cornwall, R. Jackiw, and E. Tomboulis. Effective action for composite operators. *Phys. Rev. D10, 2428-2445 (1974)*, 1974.

[22] J.T. Lenaghan and D.H. Rischke. The *O(N)* model at finite temperature: Renormalization of gap equations in hartree and large-n approximations. *J.Phys. G26 (2000) 431-450*, 2000.

[23] L.S. Brown. *Quantum field theory.* Cambridge University Press, 1992.